UNIVERSIDAD
DE MÁLAGA

Departamento Ingeniería Mecánica, Térmica y de Fluidos

Escuela de Ingenierías Industriales

TESIS DOCTORAL

Thermal-hydraulic and optical modeling of solar Direct Steam Generation systems based on Parabolic-Trough Collectors

Juan José Serrano Aguilera

Programa de Doctorado en Ingeniería Mecatrónica

Directores:

Dra. Loreto Valenzuela Gutiérrez
Dr. Luis Parras Anguita

Tesis presentada para la obtención del título de Doctor Ingeniero Industrial,

Universidad de Málaga, 2017

UNIVERSIDAD
DE MÁLAGA

AUTOR: Juan José Serrano Aguilera

http://orcid.org/0000-0003-4341-3967

Por la presente, la **Dra. Loreto Valenzuela Gutiérrez**, responsable del Grupo de Media Concentración de la Plataforma Solar de Almería y el **Dr. Luis Parras Anguita**, Profesor Contratado Doctor del área de Mecánica de Fluidos de la Universidad de Málaga.

Certificamos:

Que la presente Tesis Doctoral, titulada "*Thermal-hydraulic and optical modeling of solar Direct Steam Generation systems based on Parabolic-Trough Collectors*", ha sido realizada por **D. Juan José Serrano Aguilera** bajo nuestra dirección y supervisión. Dicho trabajo ha sido avalado por compendio de publicaciones, reuniendo a nuestro juicio los requisitos necesarios para que su autor opte al grado de Doctor. Por tanto, consideran que esta Tesis es apta para su defensa ante tribunal en la Universidad de Málaga.

En Málaga a 24 de Julio de 2017.

Fdo.:

Fdo.:

Dra. Loreto Valenzuela Gutiérrez
Responsable del Grupo de Media
Concentración
Plataforma Solar de Almería (CIEMAT)

Dr. Luis Parras Anguita
Profesor Contratado Doctor
Universidad de Málaga

Filosófico es el preguntar, y poético el hallazgo.

María Zambrano

A mi madre, por enseñarme a leer y escribir.

A mi padre, por saber transmitirme la curiosidad y el placer de aprender.

A Cristina, por acompañarme y ser mi alegría durante media vida.

A mi tío Antonio y a mi abuela, por ser el mejor ejemplo de fortaleza y dignidad.

A los que todavía no pierden las esperanzas de que desde esta tierra se pueda hacer ciencia e innovar en condiciones dignas, para que algún día podamos volver a ser lo que fuimos.

Acknowledgements

First of all, I would like to express my gratitude for the assistance provided by my main PhD supervisor Dr. Loreto Valenzuela and for the advice and comments she has made in the elaboration of the papers and this thesis. I am also grateful to her for giving me the opportunity to perform this thesis for the last four years.

I would like to extend my gratitude to some members of the Fluid Mechanics Department at the University of Málaga. Special thanks to Dr. Luis Parras for accepting being my PhD supervisor, for his intuition and his ability to point me always to the right direction when answers are required. I also wish to acknowledge the generosity and support provided by Dr. Carlos del Pino.

I owe my deepest gratitude to Professor Annalisa Manera, from the University of Michigan-Ann Arbor, for what she has taught me about TH. I am so grateful for having the opportunity of doing my internship at the Nuclear Engineering and Radiological Sciences Department (NERS). The time I spent in Michigan has been one of the most remarkable experiences in my life. I have fond memories of all the partners and colleagues I met in the Experimental and Computational Multiphase Flow Lab in Ann Arbor.

Also, I hold Vasilis, Irene, Norberto and Cristina in high regard for being 'mi familia' during my stay in Ann Arbor. Thanks as well to Alyssa for being a wonderful and accommodating roommate.

Many thanks to those delightful friends I have met at Plataforma Solar de Almería: Carmen Montesinos for his charismatic laugh and kindness, to my officemate Alejandro for sharing a common sense of humor and to Rafa, Sergio, Mary Elaine, Aureli, Thorsten, Mabel, Laura, Diego, Eneko, David, Joan de Déu, Javier and all the people from the 2 p.m.

shift for the great moments we have enjoyed during the lunch break. I deeply appreciate the effort carried out by some staff members like Rafael Góngora or Jorge García Tejeo who keep doing a great job and are always willing to lend a helping hand despite the existing difficulties.

Finally, I am using this opportunity to express my gratitude to my family for supporting me during all these years of hard study and work. Their help has been of key importance at certain moments.

Publications in this Thesis

International Journals (main topic of the thesis)

- Serrano-Aguilera, J.J., Valenzuela, L. and Parras, L. (2014). Thermal 3D model for Direct Solar Steam Generation under superheated conditions, *Applied Energy* **132**(1): 370 - 382.

- Serrano-Aguilera, J.J., Valenzuela, L. and Fernández-Reche, J. (2016). Inverse Monte Carlo Ray-Tracing method (IMCRT) applied to line-focus reflectors, *Solar Energy* **124**(1): 184 - 197.

- Serrano-Aguilera, J.J., Valenzuela, L. and Fernández-Reche, J. (2016). Modified geometry of line-focus collectors with round absorbers by means of the inverse MCRT method, *Solar Energy* **139**(1): 608 - 621.

- Serrano-Aguilera, J.J., Valenzuela, L. and Parras, L. (2017). Thermal hydraulic RELAP5 model for a solar direct steam generation system based on parabolic troughs collectors operating in once-through mode, *Energy,* **133**(1): 796 - 807.

International Journals (other topics)

- Serrano-Aguilera, J.J., Parras, L., del Pino, C. and Rubio-Hernandez, F.J. (2016). Rheo-PIV of Aerosil® R816/polypropylene glycol suspensions, *Journal of Non-Newtonian Fluid Mechanics* **232**(1): 22 - 32.

- Serrano-Aguilera, J.J., García-Ortiz, J.H., Gallardo-Claros, A., Parras, L. and del Pino, C. (2016). Experimental characterization of wingtip vortices in the near field using smoke flow visualizations, *Exp Fluids* **57**: 137.

International Conferences

- Serrano-Aguilera, J.J., Valenzuela, L. and and Fernández-Reche, J. Inverse MCRT method for obtaining solar concentrators with quasi planar flux distribution, Energy Procedia 69 (2015): 208 – 2017. Oral Communication in *SolarPACES 2014*, Beijing (China), September 2014.

- Gallardo-Claros, A., Serrano-Aguilera, J.J, Parras, L. and del Pino, C. Experimental observations of trailing vortices at moderate Reynolds numbers, Oral Communication in *10th European Fluid Mechanics Conference (EFMC10)*, Copenhagen (Denmark), September 2014.

- Domíguez-Vázquez, A., García-Ortiz, J.H, Serrano-Aguilera, J.J., Parras, L. and del Pino, C. Influence of Reynolds number on theoretical models for trailing vortices, Oral Communication in *Bifurcations and Instabilities in Fluid Dynamics, BIFD 2015*, Paris (France), July 2015.

- Serrano-Aguilera, J.J. and Valenzuela, L. Transient validation of RELAP5 model with the DISS facility in once through operation mode, Oral Communication in *International Conference on Concentrating Solar Power and Chemical Energy Systems, SolarPACES 2015*, Cape Town (South Africa), October 2015.

- Pulido, D., Serrano-Aguilera, J.J. and Valenzuela, L and Fernández-García A. Optimizing design of a linear Fresnel reflector for process heat supply, Oral Communication in *11th ISES EuroSun Conference*, Palma (Spain), October 2016.

Reports

- Biencinto, M., González, L., Serrano J.J., Valenzuela, L. and Vuillerme, V. Report on thermo-hydraulic behaviour of line-focus solar fields with direct steam generation, European Project *STAGE-STE*: Scientific and Technological Alliance for Guaranteeing the European Excellence in Concentrating Solar Thermal Energy (Grant Agreement no.: 609837), Deliverable 11.4, November 2016.

Contents

i

List of Figures

List of Tables

Nomenclature

Abbreviations

2D	two dimensions	IMCRT	Inverse Monte Carlo Ray Tracing
3D	three dimensions		
ARDISS	Advanced Receiver for Direct Solar Steam	KJC	Kramer Junction Company
		LCOE	Levelized Cost of Electricity
ATS	Advanced Trough System	LCR	Local Concentration Ratio
BOP	Balance of Plant	MAE	Mean Absolute Error
CCD	Charge-Coupled Device	MENA	Middle East and North Africa
CFD	Computational Fluid Dynamics	NMAE	Normalized Mean Absolute Error
CIEMAT	Centro de Investigaciones Energéticas, Medioambientales y Tecnológicas	NREL	National Renewable Energy Laboratory
CS	Cross Section	NRMSE	Normalized Root-Mean-Square Error
CSP	Concentrated Solar Power		
CSR	Circumsolar Ratio	PSA	Plataforma Solar de Almería
DISS	DIrect Solar Steam	PTC	Parabolic-Trough Collector
DLR	Deutsches Zentrum für Luft und Raumfahrt	RD	Royal Decree
		RELAP	Reactor Excursion and Leak Analysis Program
DNI	Direct Normal Irradiance		
DSG	Direct Steam Generation	RMSE	Root-Mean-Square Error
FIT	Feed-in-Tariff	R&D	Research and Development
FYP	Five-Year Plan	SCA	Solar Collector Assembly
GDP	Global Domestic Product	SEGS	Solar Electricity Generating system
HCE	Heat Collector Element		
HEM	Homogeneous Equilibrium Model	SVD	Single Value Decomposition
		TMY	Typical Meteorological Year
HIPRESS	High Pressure Experiments on Solar Steam	US	United States
		UVAC	Universal Vacuum Collector

Roman symbols

A_{99}	defocusing performance chart area above 99%	$\vec{n}$	normal vector to the mirror surface
C_0	distribution parameter (-)	$\vec{v}$	unitary vector
F	cumulative distribution (-)	a	fitting parameter of heat loss correlation (W m^{-1} K^{-1})
F^{-1}	inverse of cumulative distribution function (-)	b	fitting parameter of heat loss correlation (W m^{-1} K^{-4})
G	mass flux (kg m^{-2} s^{-1})		
L_w	reflector half width (m)	$d_{T\odot}$	Sun-Earth distance (m)
Q	source term of power (W m^{-3})	f_c	focal distance (m)
$R_\odot$	Sun radius (m)	g	gravity acceleration (m s^{-2})
T	temperature (K)	h	specific enthalpy (J kg^{-1})
$\dot{m}$	mass flow rate (kg s^{-1})	p	pressure (Pa)
$\hat{\mathbf{X}}$	sequence of uniformly distributed random numbers	q_{HL}	heat losses (W m^{-1})
		t	time (s)
$\hat{x}$	steam quality (-)	u_{df}	drift velocity (m s^{-1})
$\hat{z}$	local coordinate laid along the width of a flat absorber (m)	v	phase velocity (m s^{-1})
		z	axial variable (m)

Greek symbols

$< \alpha >$	amplitude of oscillations of void fraction (-)	ϕ	relative intensity of sunshape (-)
		ϕ_{rim}	rim angle (deg)
Δ	variation of variable	ρ	density (kg m^{-3})
α	void fraction (-)	σ	standard deviation of the gaussian distribution (rad)
χ	circumsolar ratio (-)		
δ	radial angle projected on the cross-sectional plane (rad)	θ	radial angle in spherical coordinates or angle that circles round absorbers (rad)
η	efficiency (-)		
γ	Buie's sunshape variable (-)	θ_{tilt}	tilt of pipe (rad)
γ	intercept factor (-)	φ	azimuthal angle in spherical coordinates (rad)
κ	Buie's sunshape variable (-)		
$\hat{\theta}$	Sequence of angles (rad)	ξ	conic eccentricity (-)
μ	mean value of the gaussian distribution (rad)	ζ	relative amplitude of the tube bend (-)

Subscripts

∞	ambient conditions	m	mixture
$conv$	convection	max	maximum
e	electric	mod	model
er	relative to the gaussian distribution modeling errors of mirror surface	n	normal to mirror surface
		out	outlet
		r	reflected ray
exp	experimental	$refl$	reflector
f	fluid	s	absorber wall
$fric$	friction	sky	to the sky
g	glass cover or gas phase	$srad$	solar radiation
i	incident ray	ss	relative to the sunshape
in	inlet	th	thermal
l	liquid phase	$thrad$	thermal radiation

Abstract

CSP systems based on Parabolic-Trough Collectors (PTCs) account for a representative share of the global solar thermal capacity installed. As a result of the experience gained in the SEGS plants, most of the existing PTC power plants use synthetic oil as heat transfer fluid. However, water can be alternatively used as heat transfer fluid, where both single and two-phase flow are present in the system. This technology is called Direct Steam Generation (DSG) and it presents some remarkable advantages in terms of system overall efficiency and plant cost reduction. Nevertheless, some complexities inherent to two-phase flow have to be addressed to succeed in the future deployment of commercial DSG power plants. Control strategies of such systems need to deal with some transient phenomena that have to be studied in detail. The development of numerical codes to model this type of systems is of key importance to put new insights into them, without having to invest significant resources in experimental studies in the first stage of the development of future plants. Both, the thermal-hydraulic and optical modeling are of relevance.

Conventional parabolic-trough reflectors concentrate solar radiation on absorber tubes following a characteristic pattern with a non-homogeneous distribution in the angular direction. It means that the bottom half of the absorber tube receives much more flux than the upper half. Under specific two-phase flow patterns (e.g. stratified flow) the refrigeration of the absorber tube is not homogeneous and thermal bending may take place. This problem can also be reported in single-phase flow conditions (e.g. superheated steam), where a significant thermal gradient at the cross-sectional plane of the absorber tube can be critical. A new technique called Inverse Monte Carlo Ray Tracing (IMCRT) method is proposed in this thesis. It aims to design new reflector geometries so that a more homogeneous distribution of concentrated solar radiation on the absorber tube can be accomplished. In line with this, new reflector geometries have been proposed with the same aperture width as the LS-3 design for the

UNIVERSIDAD
DE MÁLAGA

same absorber design, where quasi-constant flux distribution is achieved within a specific angular range. Other types of objective profiles have also been tested (i.e. triangular). Not only the round absorber tube has been studied, but as a matter of example, the potential of the IMCRT method has also been applied to flat absorbers. In the light of results, it has been shown that a wide variety of objective profiles can be attained for specific purposes.

A thermal model of a linear receiver has also been performed with the aim of describing the heat transfer mechanisms between all the elements on it. Heat diffusion in the absorber tube wall as well as the glass cover has been modeled in three dimensions, whereas the fluid domain (superheated steam) has been simplified according to a 1D approach. Results have been validated with experimental data from the DISS facility located at Plataforma Solar de Almería. Besides, a detailed thermal-hydraulic study has also been carried out by means of the commercial code RELAP5. This code is based on a transient two-fluid model where both, single-phase and two-phase flow regions can be simulated. The thermal behavior of the absorber tube can also be approximated by means of the standard capabilities of RELAP5. A full and detailed model of the DISS facility has been performed where the connection pipes between adjacent collectors have been included. This model has been validated with experimental data obtained from full day tests getting a good agreement. According to the results, the 1D approach followed by RELAP5 is able to reproduce transient phenomena which usually take place in common operation conditions. In addition, heat losses have been experimentally characterized in the same facility. A new correlation, which takes into account heat losses of receivers after two years and a half of operation, is proposed. It has been included in the aforementioned model, therefore. Thermal-hydraulic codes also make it possible to study severe slugging in connection pipes. For that purpose, a particular connection pipe alongside their two adjacent collectors have been simulated to figure out in which range of operation conditions severe slugging occurs at a pressure of 0.5 MPa.

Summary
(extended abstract)

Full deployment of renewable energy at a global scale, is one of the alternatives to face new challenges like global warming, which is a real threat with major implications. In this context, **the prospects of Concentrated Solar Power (CSP) are of key importance to guarantee a sustainable post-carbon economy based on a balanced energy mix**. Among the main advantages, CSP allows thermal storage, which in turns guarantees a better dispatchability so that renewable energy accounts for a significant share of the global energy production.

Despite the current high Levelized Cost of Electricity (LCOE) associated to CSP, the short-term economic criteria should not be the only factor determining future policies. Current pricing of fossil fuels do not take into account the incurred costs due to pollution and other public expenses. Actually, $5.3 trillion were spent in fuel subsidies in 2015, which implies that market prices of fossil fuels do not represent their real costs. Within the current free market context, the diminished public sector and its inability to make policies in favor of the general interest, hinders the deployment of an ambitious public strategy to reduce the LCOE of CSP thanks to the economy of scale. Among the most relevant CSP developers, it can be highlighted the role played by the European Union through Spanish and German companies in conjunction with some public research centers and the funds provided by the European Commission. Solar thermal was supposed to play a relevant role in the Desertec concept, although it did not succeed due to political reasons. The United States (US) launched the Sunshot Initiative and Chile, where a remarkable amount of CSP power is being installed in the north of the country (Atacama), is another key investor. Furthermore, according to the plans delivered by the Chinese government through the last five-year plan (13th FYP) deployment of CSP is still likely to happen in the near future. All these factors, suggest that CSP is a technology that could supply energy at an affordable price provided that new breakthroughs are made.

The total CSP electric power installed by the end of 2015 was 4.8 GW$_e$. It was significantly lower than the photovoltaic (227 GW$_e$) or wind power (433 GW$_e$) installed in that time. **Most of the operating CSP power corresponds to Parabolic-Trough Collectors (PTCs)**, which is the most mature technology up to the moment. They basically consist of linear-focusing collectors using a cylindrical absorber as a receiver, whose central axis is placed along the focal line. It is surrounded by a glass cover in such a way that air is removed from the gap between them. As a result, convective heat losses can be considerably reduced. The reflector is formed by a set of facets shaped as a parabola with a characteristic focal distance and width. The Heat Transfer Fluid (HTF) flows inside the absorber receiving part of the energy in the form of thermal energy, whereas a single-axis tracking mechanism is used to move the whole collector following the sun position during the day. Among all the available commercial PTC designs the LS-3 geometry is one of the most extended models, from which different Solar Collector Assemblies (SCA) have been developed (e.g. *Euro-Trough*). In this design, the focal distance is 1.71 m whereas the aperture width is 5.76 m. However, there exists other commercial designs with larger widths, such as the SenerTrough2 with an aperture width of 6.87 m. The general trend consists of increasing the width of parabolic reflectors in new commercial plants to reduce costs.

The initial development of the Parabolic-Trough Collector (PTCs) technology has taken place since the second half of the XIX century, so that several prototypes were developed in Europe, the US and the Soviet Union. However, it was not until the 1980s when the American-Israeli company LUZ International Ltd. made significant steps forwards designing and installing the SEGS plants in California. This set of nine commercial plants consisted of different types PTCs using thermal oil as Heat Transfer Fluid (HTF). More specifically, 3 different designs were developed. The last model (LS-3) is one of the key references used to design most of the collector models installed in current commercial PTC plants, as it has been previously mentioned. After the experience gained in the installation and operation of the SEGS plants, the reliability and the ability to generate electricity was proved. Substantial improvements were made concerning the receiver design (e.g. the Solel UVAC absorber) and durability. Operation and maintenance procedures were optimized as well as new concepts of interconnections between adjacent collectors were created based on rotary joints. Maintenance and characterization of mirrors reflectance were also improved. The Spanish CSP industry took over the deployment of PTC technology in Europe from 2008 to 2013. Relying on a favorable legislation and a profitable remuneration scheme, a total of 45 PTC power plants were installed in this country

(44 of them were 50 MW$_e$ plants). The change of government in 2011 and the effects of the emerging economic crisis changed the entire existing legal framework and the last plant was connected to the grid in November 2013. Since then, no new PTC plants have been projected or installed in Spain. The industry turned into a more international market, where bigger power plants are now under construction or in operation in South Africa, MENA region and the US. Recent facilities, keep using collector designs with a similar aperture width to those used in the SEGS plants, but with longer assemblies. The same can said for the use of synthetic oil as HTF, which is the most extended option up until now.

Some applicable technical challenges have to be addressed in order to guarantee a sustained increase in the installed capacity of this technology. Most of the **research effort should focus on some relevant issues to enable a noticeable reduction of the LCOE**. It is essential to improve the durability and reliability of receivers to expand the lifespan of PTC plants, and improvements in the collector designs are also needed. At the same time, the **study of new reflector geometries**, as well as looking for **innovative heat transfer fluids** are of key importance. **Direct Steam Generation (DSG) is in line with this goal**. It implies a number of relevant advantages: The overall plant efficiency is higher because the superheated steam exiting the solar field can drive directly the turbine, avoiding some of the heat exchangers required in current plants using thermal oil. The subsequent simplification of the system is evident, and the cost reduction can be more than 5% of the total cost of the plant. There also exist safety and environmental implications because thermal oil leakage or spillage can contaminate the ground. Furthermore, oil leaks may trigger a fire at operation conditions. In addition, DSG systems rely on latent heat transfer within the two-phase flow region, despite the complexities due to such type of flow, the heat transfer rate is a noticeable advantage in this region at constant temperature (as long as pressure is kept stable) respect to single phase flow. At the same time, the freezing point of conventional thermal oil requires a warming system when the ambient temperature is low enough at night.

The first step in DSG based on a linear focus system was taken at the beginning of the XX century in Egypt, where a PTC system was used for irrigation purposes. However, it was not until the 1980s, when the company LUZ International Ltd. made significant breakthroughs by means of the ATS project. It was compiled of several stages. The first one installed a lab scale test loop using electrical heaters to heat up water instead of the concentrated solar radiation by reflectors. However, in the second stage a parallel loop of tilted LS-3 collectors were installed. An ambitious

third stage aimed to install a full scale experimental facility in the Negev desert, but the company went bankrupt in 1991 and the project could not be completed. Later projects developed further lab-scale prototypes in order to give new insights into two-phase flow characterization. This was the case of the HIPRESS project equipped with a set of X-ray sensors to characterize the two-phase flow patterns and to measure the void fraction. Both the HIPRESS alongside the GUDE projects gathered massive experimental information about several factors such as pipe diameter effects, pressure influence on flow regime, thermal gradients on absorber walls and interphase behavior. All the information was of relevance for the projects accomplished later.

The DISS (DIrect Solar Steam) project was launched 1996 with the objective of installing a full scale experimental facility at Plataforma Solar de Almería (PSA). The first phase of this project was finished in 1998 and eventually due to budget limits, it was only formed by a single-loop system of eleven horizontal LS-3 collectors with all the auxiliary subsystems required. It was designed to work in three different operation modes: once-through, recirculation and injection. The first model of absorber tubes installed was made of A335 carbon steel and they were manufactured by the company Solel. Different cross-sectional thermocouples were installed at different axial locations so as to know about the temperature field in the absorber tube wall. A second phase of the DISS project was launched in the end of 2001 by which an ambitious test campaign was planned and performed accumulating lots of hours of operation and systems improvements were also accomplished. The INDITEP project started in 2002 and two *EuroTrough* (ET-100) solar collectors were added at the inlet of the solar collector row installed at the DISS pilot plant and the corresponding experimental campaign was carried out. Finally, the last upgrade of the facility took place by means of the DUKE project (from 2011 to 2014). Three additional collectors were installed (model SL4600+), two of them in the pre-heating section and one in the superheating section. Likewise, all absorber tubes were replaced by brand-new SCHOTT PTR-70-DSG with a thinner pipe wall made of A316 stainless steel. All the experimental data collected since the beginning of the DISS project is a valuable database compiled of times series of fluid and absorber wall temperature, pressure and other valuable data useful for the validation of models developed for solar DSG. This is the case of this thesis.

In recent years, two commercial DSG plants have been installed. The 5 MW_e plant Thai Solar One (TSE-1) is a DSG facility located in Thailand formed by PTCs (SL4600) whose turbine is fed with superheated steam at 30 bar. It operates following the recirculation mode concept. A second 30 MW_e DSG plant using the

Linear Fresnel technology is currently operating in Spain. Despite not being based on PTCs, problems related to the two-phase flow complexities are also of interest in that plant.

In spite of the goals achieved up until now, all research efforts and technological attempts to accomplish definitive commercial deployment of DSG have to continue. All the scientific and technical knowledge gained points out the prospects and potential advances of this developing technology respect to current commercial systems based on thermal oil. More research is needed to implement new simulation strategies in order to optimize DSG systems, but also to assess the efficiency of future commercial plants and to design them. Suitable simulation tools are also effective to carry out reliability studies where critical scenarios are of interest to analyze systems response. In line with this, both the optical and thermal-hydraulic issues matter. **The scope of the present thesis deals with ray tracing algorithms made to know about the concentrated radiation distribution on absorbers as well as to design new geometries of reflectors. At the same time, thermal models are performed in order to study the heat transfer mechanisms in single-phase and two-phase flow conditions.**

The **use of optical models is of key importance in the design of any CSP system**. The first step requires a realistic distribution of the direction of rays generated by the Sun. This is the purpose of the sunshape profile. As a result of the Sun-Earth distance and its diameter, a mean angular extent of the Sun seen from the Earth can be worked out (whose half angle is 4.65 mrad). The different models of sunshape describe how the intensity of radiation generated by the Sun decays as long as this angle increases. A stochastic approach is used to generate a bunch of rays whose direction is according to this distribution (i.e. Monte Carlo Ray Tracing algorithms). Rays path is modeled as straight lines, and reflection is described by means of the specular reflection law, where some non-specular effects can be included using stochastic methods as well. The Gaussian distribution with null mean value is generally used for that purpose. 3D ray tracing algorithms, model the rays trajectory taking into account all the space dimensions. It is a suitable option when a detailed description of radiation is required on the absorber tube, including the axial coordinate. However, it requires noticeable computing resources. If linear-focusing systems are under study (e.g. PTC), and it is only required to know about the flux distribution of the concentrated solar radiation around the cross-sectional plane of the absorber tube, a 2D approach can be used. To accomplish that, some non-trivial considerations have to be assumed. It is necessary to project the sunshape and the

Gaussian distributions on the cross-sectional plane. Special attention has to be paid if the angle of incidence is not null, because some further adaptations are needed.

The implementation of **an efficient ray tracing algorithm** is important **to design and optimize alternative reflector geometries**. In line with this, both **a 3D and a 2D ray tracing in-house algorithms have been implemented to get the concentrated flux profile on the absorber of PTCs**. The 3D algorithm has been used to work out the concentrated flux distribution on a full absorber tube of a LS-3 collector (**paper I**), whereas the 2D algorithm has been validated with results from Tonatiuh software for a LS-3 reflector concentrating solar radiation onto a flat absorber (**paper II**). The 2D algorithm has been used to validate the new reflector geometries proposed in this work.

The Inverse Monte Carlo Ray Tracing (IMCRT) method is a new procedure conceived in the course of this thesis, whose purpose is to calculate the reflector geometry so that a given concentrated flux profile is obtained onto a linear absorber. Nevertheless, the underlying idea of the method can be used to design analogous methods for point-focus concentrators. Given a specific absorber geometry and the desired flux distribution on it (objective profile), the IMCRT method provides a numerical description of the required reflector in function of a free parameter related to the rim angle. The first stage of the IMCRT method calculates a first approach to the solution simplifying the Sun as a point source. However, due to the Sun extent, solar rays reach the reflector following different directions within the solar cone. This fact means that the reflector geometry provided by the first stage is sometimes significantly different with respect to the reflector needed to get the objective profile. The goal of the second stage is to tweak the geometry supplied by the first stage to get a final flux profile as close as possible to the objective one. It is worth to mention that it is not always possible to accomplish certain objective profiles.

Results prove that the IMCRT method is able to get reflector geometries to get quasi-constant and triangular objective profiles onto flat absorbers (as shown in **paper II**). The selection of such simple geometry of absorber eases the method explanation and enables an initial evaluation of its capabilities. The quasi-planar objective profile is of practical interest because it aims to distribute homogeneously concentrated radiation within a strip on the center of the flat absorber. The first stage solution significantly differs from the objective profile. The second stage is able to refine the reflector geometry in order to get a plateau region in the flux profile but with a slightly gradual decay in the profile tails. In the case of aiming to get a triangular profile, the results

of the second stage accurately reproduce the objective profile. The final reflector geometries calculated by the IMCRT method are not unique. This fact makes it necessary to select optimum solutions in function of some optimization variables that are good indicators of the collector cost: the focal distance (related to the cost of the brackets holding the absorber) and the reflector arc length (indicator of the amount of material needed to manufacture mirrors and its weight). Accordingly, the proposed reflector designs have been selected based on cost-effectiveness criteria as well as the intercept factor, which is a good indicator of the geometric performance of the reflector curve. In addition, the reflector curve has to be smooth enough so that its manufacture process is feasible. The conclusions drawn after completing **paper II** indicate that when the objective profile is smooth enough, the second stage succeeds in getting a final flux profile close enough to the objective one. The development of the IMCRT method for flat absorbers can be useful for concentrated photovoltaic applications, where the concentrated radiation distribution on photovoltaic cells should be as homogeneous as possible.

Paper III consists of the application if the IMCRT method for cylindrical absorbers (absorber tubes like those existing in commercial PTC plants). Similarly to **paper II**, quasi-planar and triangular objectives profiles are considered where the glass cover refraction is taken into account. The method performs well for the triangular objective profile case. However, some problems arise concerning the quasi-constant objective profile. As in the flat absorber case, sharp profile tails cannot be addressed. This case is even more critical than in the flat absorber case, because profile tails receive concentrated radiation from the outer region of the reflector, which is further than the central region of the reflector (beneath the absorber). Three design points are calculated to show how a trade-off solution can be selected according to the reflector design requirements. Besides, a new type of diagram called defocusing performance chart is presented within the framework of this thesis. The goal of this graph is to describe how the intercept factor decreases as the absorber tube center shifts from the focal point in the cross-sectional plane. A graphical comparison between different reflector geometries can be provided in order to analyze how vulnerable new reflector geometries are to undesired displacements of the absorber due to bending. In order to quantify this vulnerability, the dimensionless area of the chart region where the intercept factor is higher than 0.99 can be used. The inconvenience of some reflector geometries obtained by the IMCRT method is that they are more vulnerable to downwards displacements in comparison with the LS-3 (or *EuroTrough*) geometry. This issue is directly related to the width of the objective profile. The wider it is,

the sharper decay of the intercept factor is with downwards displacements of the absorber.

It is important to mention that all the examples and solutions provided by the IMCRT method in papers **II** and **III**, correspond to ideal conditions where specular reflection and null angle of incidence have been considered. It does not mean that these factors cannot be taken into account in future applications of this tool. The use of this method can be extended to a wide variety of problems and conditions of operation. The examples and solutions provided in this work are just intended to be an initial explanation of how the method proceeds and the kind of solutions that can be found.

Modeling of heat transfer mechanisms taking place in PTCs is part of the scope of this thesis. **Paper I** deals with the numerical model of a single absorber tube (4.06 m long). It calculates the 3D temperature field within the wall of the absorber tube and the glass cover in conjunction with a 1D description the temperature of the single-phase fluid (superheated steam) in steady-state. The heat equation (Laplace's equation in steady-state) is solved in cylindrical coordinates in both solid domains by means of the finite differences method. More specifically, a second order, central finite differences scheme is used to approximate the second order derivates to guarantee that all terms have the same truncation order. Likewise, an iterative method is used to solve the corresponding system after the discretization of the partial differential equations is performed. The IAPWS-IF97 standard formulation is used to compute the water-steam thermodynamic properties.

Boundary conditions are compiled of the distribution of concentrated solar radiation that is previously calculated by a 3D MCRT algorithm and the corresponding heat transfer terms between the different parts of the receiver domain and the surrounding air, where Fourier's law is applied in solid domains borders. Heat transfer between the inner absorber tube surface and the fluid is modeled by means of the Gnielinski correlation, which is valid for the transitional and turbulent flow regime. Since air is removed from the gap between the absorber tube and the glass cover to avoid convective losses, thermal radiation is the main mechanism accounting for most of the heat transferred through the vacuum annulus (note that free molecular convection has been neglected). Assuming that the borosilicate glass cover is opaque to thermal radiation, terms corresponding to thermal radiative exchange are defined in three dimensions where the axial evolution of temperature has also been regarded. It means that the computing cost required to calculate all the view factors is not negligible. An internal generation term (source term) is included in the heat equation of the glass

cover in order to model the absorption of concentrated solar radiation passing through it. The corresponding attenuation coefficient has been obtained from experimental measurements.

The temperature distribution of the fluid domain is calculated from the incoming heat from the absorber wall and the axial pressure drop. For that purpose, the Colebrook-White equation has been approximated by the Goudar-Sonnad solution. The relative roughness of the inner surface of the absorber tube has been experimentally characterized by means of confocal and interferometry techniques (3D microscope) from absorber samples collected from the DISS facility.

A mesh test has been performed to justify the number of elements in each coordinate to guarantee results independence from the mesh size. The thermal model has been validated using experimental data collected from the DISS test facility so that the absolute operation pressure ranges from 3 to 10 MPa under different fluid inlet temperatures. In addition, the mass flow rate covers a representative range of the operation conditions. The temperature distribution in the absorber wall is also validated at a specific cross-section of the absorber tube where eight thermocouples are inserted. In light of results, the model accurately predicts the angular distribution of temperature around the absorber tube and provides a realistic estimation of the overall heat losses in the receiver. However, the experimental heat losses are slightly higher than those calculated by the model. Some of the premises taken in the model could be the reason for that. It is also concluded that the assumed approach consisting of coupling a 3D description of the solid domain along with a 1D description of the fluid domain is a good approximation, at least in single-phase flow conditions and steady-state. The fact of avoiding the resolution of the Navier-Stokes equations in three dimensions (CFD) makes the proposed approach a suitable option to model full scale plants when an accurate description of the temperature field on the solid domain is required.

Paper IV deals with the **simulation of a DSG system formed by a complete loop of PTCs**. Unlike in **paper I**, here it is necessary to **implement a thermal hydraulic model that describes the entire two-phase flow region along with single phase-flow sections** (i.e. subcooled water at the loop beginning and superheated steam at the outlet). Nuclear industry has broad experience in the 1D modeling of two-phase flow, due to the fact that most of cores in commercial nuclear plants are cooled with water (especially in boiling water reactors). RELAP5 (Reactor Excursion and Leak Analysis Program) is a six-equations code that models independ-

ently each phase (also known as two-fluid model). It is based on thoroughly validated correlations and flow maps gathering massive experimental data. In addition, thermal behavior of the absorber tube can be approximated using heat structures, which is the name given by RELAP5 to solid domains attached to fluid nodes. Despite the existing Homogeneous-Equilibrium-Models (HEM) widely used in the literature, they cannot accurately predict relative displacements between phases (slip ratio is equal to one) and other phenomena related to the interface geometry. Although some intermediate approaches like models based on drift flux correlations are available (e.g. FLOCAL), the present work aims to validate RELAP5 for solar thermal purposes implementing a detailed model of the DISS test facility.

According to the standard capabilities of RELAP5, it is not possible to model the absorber tube with a three dimensional discretization. In contrast, only radial and axial discretization are allowed by default options in RELAP5. This is actually a limitation to reproduce accurately the temperature field around the absorber tube, because one particularity of absorber tubes in PTC is that the incoming flux is not homogeneously distributed around it. However, an approximation can be used to model the whole absorber tube attaching several heat structures to the same fluid node. Consequently 6 heat structures are attached to each fluid node (same number as the number of thermocouples inserted in the absorber tube wall of the experimental setup). Unlike in the thermal model detailed in **paper I**, glass cover and vacuum annulus are not included, so their effect on the heat losses of the absorber tube have to be taken into consideration by means of an experimental correlation. For that purpose, a new correlation for heat losses is obtained from recent tests carried out at the DISS facility with SCHOTT PTR-70-DSG receivers installed in 2013. The correlation is valid to represent heat losses of such receivers already-installed in the solar field after at least two years of operation. Besides, passive sections of the hydraulic circuit forming the collector loop have also been included. This is the case of connection pipes, which are compiled of insulated tubes forming a sequence of vertical and horizontal segments which have an effect on the transient behavior of the system and the axial evolution of local pressure and void fraction.

RELAP5 model has been validated from transient tests carried out at the DISS test facility where whole operation days were carried out. Common working conditions or events likely to happen like clouds shadow, changes in the mass flow rate or sudden defocusing of any collector are present in the experimental time series along with start up and turn off procedures. A total of 6 cases have been simulated in order to check the model accuracy. This comparison is based on

fluid temperature and pressure measurements taken along the system as well as on the wall temperature of the absorber tube. Further details supplied by the code are also displayed, e.g. the void fraction. It can be concluded that RELAP5 is able to reproduce transient phenomena such as the subsequent oscillations after a sudden drop of direct solar radiation due to clouds or other equivalent events. Furthermore, the maximum temperature difference in the angular distribution of temperature is well approximated by the approach assumed, where the tendency of such variable in time is attained. An additional **transient analysis has been accomplished to study severe slugging phenomena in connection pipes (paper IV)**. Due to gravitational effects in vertical sections, relative velocity between both phases may arise. Two adjacent collector are considered with the corresponding connection pipe between them. Despite having steady inlet conditions, sustained oscillations in the mass flow rate may take place at the outlet of the connection pipe. The present thesis shows that RELAP5 is capable of reproducing such oscillations given specific conditions of pressure, steam quality of the two-phase mixture and mass flow rate at the inlet. A total of 374 simulations have been carried out in order to compile a chart to highlight conditions under which these sustained oscillations take place at an inlet pressure of 0.5 MPa. The space-averaged void fraction in the riser has been taken as one of the reference variables, whose oscillation amplitude have been characterized. Single Value Decomposition (SVD) has also been applied to the time-space distribution of the void fraction (first mode) in order to characterize the frequency of such oscillations.

Some relevant conclusions can be drawn in light of the results obtained. Firstly, the implementation of an in-house Monte Carlo Ray Tracing (MCRT) code in three dimensions has made it possible to study in detail the distribution of concentrated solar radiation on the absorber tubes of parabolic-trough collectors (PTCs). This ad-hoc code for PTCs can be run faster than general purpose RT codes, taking advantage of the element-wise arithmetic operations in Matlab®. A 2D MCRT code, which is significantly faster than 3D version, has also been implemented after projecting the sunshape profile onto the cross-sectional plane of the absorber. This 2D code has been a key tool to check that the geometries provided by the Inverse MCRT (IMCRT) method are valid. It means that the IMCRT method is a potential tool for designing new reflectors with more homogeneous flux on the absorber tubes. In addition, the results obtained by the thermal model in **paper I**, show that the approach consisting of coupling a 3D domain for the solid parts of the receiver along with a 1D model for the fluid domain performs well (at least in steady-state). Besides, RELAP5 has been

proved to be a suitable tool for transient simulation of a single-loop DSG system (DISS test facility) and it is considered as a potential option to carry out further studies regarding systems formed by several loops in parallel.

This thesis has been developed within the framework of the project GEDIVA (Ref. ENE2011-24777) through a FPI PhD scholarship funded by the Spanish government (Ref. BES-2012-056876) and the DETECSOL project (Ref. ENE2014-56079-R). Most of research work has been carried out in the Solar Concentrating Systems Unit at Plataforma Solar de Almería, division of the Centro de Investigaciones Energéticas, Medioambientales y Tecnológicas (CIEMAT).

The results obtained in this thesis and the conclusions drawn are expected to be useful to future designs of systems based on line-focusing collectors and for implementing efficient modeling tools for full scale DSG solar plants.

Resumen
(extended abstract in Spanish)

El despliegue de las energías renovables a escala global constituye una de las alternativas para hacer frente a nuevos retos como el cambio climático, que es una amenaza con implicaciones considerables. En este contexto, **las opciones ofrecidas por de la Energía Solar de Concentración** (CSP, del inglés *Concentrated Solar Power*) **son de una importancia clave para poder garantizar una transición sostenible a una economía sin el uso de combustible fósiles basada en un *mix* energético equilibrado**. Entre sus principales ventajas, la CSP permite almacenamiento térmico, lo que garantiza un suministro más adaptable a la distribución temporal de la demanda. De esta forma, las energías renovables podrían representar una fracción significativa de la producción energética global.

A pesar del elevado coste nivelado de la electricidad (LCOE, del inglés *Levelized Cost of Electricity*) asociado a la CSP, las políticas energéticas del futuro no sólo deberían obedecer a criterios pensados a corto plazo. El precio actual de los combustibles fósiles no tiene en cuenta los costes asociados a la contaminación y otros gastos públicos vinculados al uso de estas fuentes de energía. De hecho, en 2015 se han gastado 5.3 trillones de dólares en subsidios a los combustibles fósiles. En el actual contexto de libre mercado, el debilitado sector público y su incapacidad para hacer políticas en favor del interés general, dificulta el desarrollo de una estrategia ambiciosa para reducir el LCOE de la CSP a partir de la economía de escala. Entre los países con un papel más activo en el desarrollo de la tecnología CSP, destacan la Unión Europea a través de empresas y centros de investigación públicos españoles y alemanes gracias a la financiación prestada por la Comisión Europea. La energía solar térmica iba a tener un peso relevante en el proyecto Desertec, aunque fuera descartado por motivos políticos. En Estados Unidos se lanzó la iniciativa *Sunshot* y en Chile se prevé instalar una potencia termosolar destacable en el norte del país (Atacama). Además, de acuerdo con el décimo tercer plan quinquenal anunciado por el Gobierno

chino, se espera ampliar de forma considerable la potencia termosolar instalada en dicho país. Todos estos factores indican que la CSP es una tecnología con posibilidad de proporcionar energía a un precio asumible siempre que se consigan ciertos avances.

La potencia termosolar global instalada al final del año 2015 era de 4.8 GW$_e$. Es significativamente menor que la potencia fotovoltaica instalada (227 GW$_e$) o eólica (433 GW$_e$) en esas mismas fechas. **La mayoría de la potencia termosolar instalada corresponde a la tecnología de colectores cilindroparabólicos** (PTC del inglés *Parabolic-Trough Collector*). Esto demuestra la madurez tecnológica lograda por esta tecnología hasta el momento. Estos sistemas consisten básicamente en captadores[1] de foco lineal que usan un tubo absorbedor con forma cilíndrica como receptor, de forma que su eje axial coincide con la línea focal del concentrador. El tubo absorbedor está cubierto por un tubo exterior de vidrio de tal forma que el aire entre ellos se extrae para reducir considerablemente las pérdidas térmicas por convección. El reflector está formado por un conjunto de facetas conformando una parábola con una anchura y distancia focal características. El fluido caloportador (HTF del inglés *Heat Transfer Fluid*) circula dentro del tubo absorbedor recibiendo en forma de calor parte de la energía captada, mientras que el mecanismo de orientación de un solo eje se usa para mover todo el captador siguiendo la posición del sol durante el día. De entre todos los diseños comerciales de PTCs, el diseño LS-3 es uno de los modelos más extendidos, a partir cuyas dimensiones se ha desarrollado la estructura de captadores más usadas (por ejemplo, el modelo *EuroTrough*). En este diseño la distancia focal del reflector es de 1.71 m mientras que su ancho de apertura es de 5.76 m. No obstante, existen otras alternativas comerciales con mayor anchura como es el caso del captador Sener-Trough2 con una anchura de 6.87 m. Por tanto, la tendencia general en la industria persigue el incremento de estas dimensiones en los captadores de plantas comerciales para reducir costes.

El desarrollo inicial de la tecnología de concentradores cilindroparabólicos se ha desarrollado desde la segunda mitad del siglo XIX, de forma que se realizaron varios prototipos en Europa, los Estados Unidos y la Unión Soviética, pero no fue hasta la década de los 80 cuando la compañía americano-israelí LUZ International Ltd. logró avances significativos con el diseño e instalación de las plantas SEGS en California. Un conjunto de nueve plantas comerciales estaban formadas por varios tipos de PTCs que usaban aceite térmico como HTF. Concretamente, 3 modelos de captadores fueron desarrollados. Tal como se ha indicado previamente, el último modelo (LS-3) es una

---

[1]Terminología en español acorde con la norma UNE 206009 (AENOR; 2013).

de las referencias más usadas para posteriores modelos de captadores que han sido empleados en numerosas plantas comerciales. Después de la experiencia adquirida en la instalación y operación de las plantas SEGS, se comprobó la fiabilidad y capacidad para producir electricidad. Se lograron mejoras relevantes respecto al diseño y durabilidad de los receptores (por ejemplo el absorbedor UVAC de Solel). Se optimizaron los procedimientos de operación y mantenimiento, así como el desarrollo de nuevos tipos de interconexiones entre captadores basados en juntas rotativas. El mantenimiento de los espejos así como la caracterización de la reflectancia de los mismos fue mejorada. Tras las plantas SEGS, la industria termosolar española tomó el testigo del despliegue de la tecnología PTC en Europa desde 2008 hasta 2013. A partir de un marco legislativo favorable y un mecanismo de retribuciones ventajoso, se construyeron un total de 45 plantas termosolares con concentradores cilindroparabólicos en este país (44 de ellas eran de una potencia de 50 MW_e). El cambio de Gobierno en 2011 y los efectos de la incipiente crisis económica desembocaron en un cambio drástico del marco legal de forma que la última planta termosolar se conectó a red en España en noviembre de 2013. Desde entonces, no se han proyectado o instalado nuevas plantas con PTCs en España. La industria española tuvo que adaptarse y expandirse en un contexto internacional, donde nuevas plantas están bajo construcción u operación en Sudáfrica, Oriente Medio y el norte de África y los Estados Unidos. La mayoría de las centrales termosolares actuales siguen empleando diseños de captadores con una anchura similar a las empleadas en las plantas SEGS pero con longitudes mayores. Algo similar ocurre con el aceite térmico usado como fluido caloportador, que sigue siendo la opción más extendida hasta el momento.

Algunos retos tecnológicos están todavía pendientes de ser abordados para garantizar el crecimiento sostenible de la capacidad instalada de esta tecnología. **La mayoría de los esfuerzos en investigación se deben enfocar hacia determinados aspectos que pueden conducir a una reducción significativa del LCOE.** Es imprescindible mejorar la durabilidad y fiabilidad de los receptores para aumentar la vida útil de las plantas, así como mejorar el diseño de los captadores cilindroparabólicos. Al mismo tiempo, **el estudio de nuevas geometrías de reflectores es crucial**, como también la búsqueda de **nuevos fluidos caloportadores**. **La generación directa de vapor** (DSG del inglés *Direct Steam Generation*) **está dentro de este objetivo**. Esta nueva tecnología implica numerosas ventajas: el incremento del rendimiento global del sistema ya que el vapor sobrecalentado producido a la salida del campo solar puede alimentar directamente la turbina, evitando el uso de intercambiadores de calor empleados en las plantas actuales con aceite térmico. La

simplificación del sistema que esto conlleva es evidente y la reducción en los costes puede ser superior al 5 % del coste total de la planta. También existen razones de seguridad y ambientales ya que posibles fugas o derrames del aceite térmico pueden contaminar el suelo. Además, las fugas de aceite en condiciones de operación pueden desencadenar un incendio. A todo esto se añade que los sistemas DSG se basan en transferencia de calor latente en la región de flujo bifásico. A pesar de la complejidad que este tipo de flujo implica, el coeficiente de transferencia de calor es notablemente mejor donde la temperatura es constante siempre que la presión se mantenga estable. Al mismo tiempo, el punto de congelación de los aceites convencionales usados hasta la fecha pueden necesitar de un sistema de calentamiento si la temperatura es lo suficientemente baja por la noche.

El primer paso dado en el desarrollo de un sistema DSG de foco lineal tuvo lugar al comienzo del siglo XX en Egipto, donde una planta con PTCs se empleó para propulsar un sistema de riego. Sin embargo, no fue hasta los años 80, cuando la compañía LUZ International Ltd. logró avances significativos gracias al proyecto ATS, que estuvo organizado en varias fases. La primera de ellas consistió en la instalación de un circuito de ensayo a escala de laboratorio usando resistencias eléctricas para calentar el agua, en vez de la radiación solar concentrada por espejos. Sin embargo, fue en la segunda fase cuando se instaló otro circuito en paralelo al anterior con captadores LS-3 inclinados. A través de un ambicioso plan concebido para la tercera fase, se esperaba construir una instalación experimental completa en el desierto del Neguev, pero la compañía se declaró en quiebra en 1991 y el proyecto no pudo concluirse. Proyectos posteriores desarrollaron nuevos prototipos a escala de laboratorio con la intención de estudiar y caracterizar el flujo bifásico. Este fue el caso del proyecto HIPRESS, que estaba equipado con un conjunto de sensores de rayos X para caracterizar patrones de flujo bifásico y medir la fracción de vacío (*void fraction*). El proyecto HIPRESS junto con el proyecto GUDE lograron una destacable cantidad de información experimental relativa a varios factores como los efectos del diámetro de tubería, la influencia de la presión en el régimen de flujo, los gradientes térmicos en la pared de los absorbedores y el comportamiento de la interfase. Toda la información recopilada fue útil en proyectos posteriores.

El proyecto DISS (del inglés *DIrect Solar Steam*) comenzó en 1996 con el objetivo de instalar un sistema experimental completo en la Plataforma Solar de Almería (PSA). La primera fase de este proyecto finalizó en 1998 y finalmente a causa de limitaciones presupuestarias, se compuso sólo de una sola fila de once captadores horizontales LS-3 con todos los subsistemas auxiliares necesarios. Se diseñó para trabajar en tres

modos de operación diferentes: paso único (*once-through*), recirculación e inyección. El primer tipo de tubo absorbedor instalado estaba fabricado en acero al carbono A335 por la empresa Solel. Se instalaron también varios termopares en diferentes secciones del tubo para conocer la distribución de temperaturas en su pared. En una segunda fase del proyecto DISS acometida desde 2001 se desarrolló una ambiciosa campaña de ensayos acumulando numerosas horas de operación. Por su parte, el proyecto INDITEP, comenzó en 2002 añadiendo dos captadores modelo *EuroTrough* en la entrada de la fila de captadores y llevando a cabo la correspondiente campaña de ensayos. Finalmente, la última ampliación de la instalación fue acometida en el proyecto DUKE desde 2011 hasta 2014. Tres captadores más fueron incorporados (modelo SL4600+), dos de ellos en la entrada de la instalación y uno en la sección de vapor sobrecalentado. Además, todos los receptores fueron reemplazados por otro nuevo modelo (SCHOTT PTR-70-DSG) con una pared de tubo más delgada hecha de acero inoxidable A316. Como conclusión, toda la información experimental recopilada desde el comienzo del proyecto DISS constituye una base de datos útil (temperatura y presión de fluido así como temperatura de pared) para la validación de futuros modelos sobre sistemas DSG.

En lo últimos años, dos plantas comerciales basadas en DSG han sido instaladas. Se trata de la central termosolar de 5 MW$_e$ Thai Solar One (TSE-1) localizada en Tailandia, formada por captadores SL4600 cuya turbina es alimentada por vapor sobrecalentado a 30 bar. Esta instalación opera en modo de recirculación. Una segunda planta de 30 MW$_e$ que usa la tecnología de concentradores de foco lineal Fresnel está actualmente operando en España. A pesar de no emplear PTCs, su operación también presenta ciertas complejidades relacionadas con el flujo bifásico.

Aunque se ha avanzado, los esfuerzos en investigación y la apuesta tecnológica tiene que continuar para lograr el despliegue definitivo de la tecnología DSG. Todo el conocimiento técnico y científico adquirido señala el potencial de esta tecnología respecto a los sistemas actuales basados en aceite térmico. Es necesaria más investigación no sólo para implementar nuevas estrategias de simulación con la finalidad de optimizar los sistemas DSG, sino también para evaluar la eficiencia de las futuras centrales y acometer su diseño. Las herramientas de simulación adecuadas son eficaces a la hora de realizar estudios donde se impongan casos críticos para analizar su respuesta. De acuerdo con lo anterior, tanto los temas de modelado óptico como termo-hidráulico son importantes. **El alcance de esta tesis trata sobre algoritmos de trazado de rayos implementados para estudiar la distribución de radiación concentrada sobre los tubos absorbedores así como el diseño de nuevas geometrías de**

reflectores. Del mismo modo, se han implementado modelos térmicos para estudiar los mecanismos de transferencia de calor tanto en flujo monofásico como bifásico.

El **uso de modelos ópticos es de especial relevancia para el diseño de cualquier sistema CSP**. El primer paso requiere una distribución realista de la dirección de rayos generados por el Sol (*sunshape*). Como resultados de la distancia entre la Tierra y el Sol y el diámetro de éste último, el Sol es visto desde la Tierra como un disco que subtiende un ángulo de 4.65 mrad. Los diferentes modelos de *sunshape* describen como la intensidad de la radiación generada por el Sol disminuye a la vez que el ángulo radial aumenta. Se emplea un enfoque estocástico para generar un conjunto de rayos cuya dirección obedece a esta distribución (en esto consiste el trazado de rayos por métodos de Monte Carlo, MCRT del inglés *Monte Carlo Ray Tracing*). El camino que siguen los rayos es modelado como líneas rectas mientras que la reflexión se describe mediante la ley de reflexión especular, donde algunos efectos no especulares pueden incluirse mediante una distribución gaussiana con valor medio nulo. Los algoritmos de trazado de rayos en 3D modelan el camino seguido por los rayos en las tres dimensiones espaciales. Es una opción apropiada cuando se necesita una descripción adecuada de la distribución de la radiación concentrada en el tubo absorbedor (incluyendo la coordenada axial). Sin embargo, esto requiere un coste computacional considerable. Si el objeto del estudio es un sistema de foco lineal, y sólo se requiere información sobre la distribución de flujo en una sección transversal representativa del tubo absorbedor, puede emplearse un algoritmo de trazado de rayos en 2D. Para que esto sea posible, hay que asumir varias consideraciones que no son triviales. Entre otras tareas, es necesario proyectar tanto el *sunshape* como la distribución gaussiana en el plano transversal, además de incluir otros cambios si el ángulo de incidencia no es nulo.

La implementación de un algoritmo de trazado de rayos eficiente es clave para el diseño y optimización de geometrías de reflectores alternativas. Es por esto por lo que en este trabajo se han desarrollado algoritmos propios de trazado de rayos en 2D y 3D para conocer el flujo sobre los tubos absorbedores de PTCs. El algoritmo 3D se ha usado para calcular la distribución de flujo concentrado en toda la superficie de un tubo absorbedor de un captador LS-3 (**artículo I**), mientras que el algoritmo 2D ha sido validado a partir del software Tonatiuh para un reflector (LS-3) concentrando radiación solar sobre un absorbedor plano (**artículo II**). Este algoritmo 2D ha sido finalmente empleado para validar las nuevas geometrías de reflectores propuestas en este trabajo.

Resumen

El método inverso de trazado de rayos por Monte Carlo (IMCRT del inglés *Inverse Monte Carlo Ray Tracing*) es un nuevo procedimiento concebido durante el trabajo realizado en esta tesis, cuyo propósito es calcular la geometría de reflectores de forma que se pueda obtener un determinado perfil objetivo de flujo concentrado sobre un absorbedor de foco lineal. No obstante, la idea subyacente en este nuevo método puede adaptarse a otro método análogo para concentradores de foco puntual. Dada una geometría específica de absorbedor de foco lineal, así como la distribución de flujo deseada sobre éste (conocida también como perfil objetivo), el método IMCRT proporciona una descripción numérica del reflector necesario para obtener ese perfil de flujo en función de un parámetro libre que está vinculado al ángulo de rodeo (*rim angle*). La primera etapa del método IMCRT calcula una primera aproximación a la solución considerando el Sol como una fuente de radiación puntual. Sin embargo, debido a la extensión del Sol, los rayos alcanzan el reflector siguiendo una dirección acotada dentro del cono solar. Este hecho implica que la geometría proporcionada por la primera etapa del método puede ser diferente al reflector que realmente se necesita para obtener el perfil objetivo. El objetivo de la segunda etapa es refinar la geometría de reflector proporcionada por la primera etapa, para obtener un perfil de radiación tan próximo como sea posible al perfil objetivo. Conviene indicar que no siempre es posible conseguir ciertos perfiles objetivos.

Los resultados muestran que el método IMCRT es capaz de obtener geometrías de reflectores para lograr perfiles objetivos casi constantes y triangulares sobre absorbedores planos (**artículo II**). La opción por esta geometría de absorbedor tan simple se debe a la facilidad que ofrece para una explicación inicial del método así como evaluar su potencial. El perfil constante es de interés práctico ya que su finalidad es distribuir homogéneamente la radiación concentrada dentro de una banda localizada en el centro del absorbedor plano. La solución proporcionada por la primera etapa del método difiere significativamente del perfil objetivo, mientras que en la segunda etapa se refina la geometría del reflector para obtener una distribución constante en el centro del perfil de radiación con unos extremos donde el flujo de radiación decae gradualmente. En el caso de buscar obtener un perfil triangular, los resultados de la segunda etapa consiguen reproducir fielmente el perfil objetivo. Las soluciones propuestas por el método IMCRT no son únicas, lo que implica tener que seleccionar la opción adecuada en función de variables de optimización, que son buenos indicadores del coste del reflector: distancia focal (relacionada con el coste de los soportes del tubo absorbedor) y la longitud de arco del reflector (relacionada con la cantidad de material necesaria para construir el espejo). Por lo tanto, los diseños de reflector

propuestos han sido seleccionados acorde a criterios de coste así como el factor de interceptación, que es un buen indicador del rendimiento geométrico. A esto se añade que las geometrías propuestas deben ser lo suficientemente suaves para que sea posible fabricarlas. Después de finalizar el **artículo II** se concluye que cuando el perfil objetivo es lo suficientemente suave, la segunda etapa del método logra reproducir el perfil objetivo. Por su parte, la aplicación del método IMCRT a absorbedores planos, puede ser útil en sistemas fotovoltaicos de concentración, donde la distribución de radiación sobre la célula fotovoltaica debe ser lo más homogénea posible.

El **artículo III** consiste en aplicar el método IMCRT a receptores cilíndricos (tubos absorbedores como los que existen en las plantas comerciales). De la misma forma que en el **artículo II**, en el III se busca conseguir un perfil casi constante y otro triangular sobre el absorbedor donde se tiene en cuenta la refracción de la cobertura de vidrio. El método ofrece resultados satisfactorios para el perfil triangular, sin embargo, la obtención del perfil constante ofrece algunos problemas. Tal como ocurre en el caso del absorbedor plano, no se puede lograr un perfil final con bordes verticales, siendo ahora incluso un problema más crítico. Esto ocurre, debido a que la radiación contenida en la cola del perfil procede de regiones exteriores del reflector, que están más lejos del absorbedor que la zona central del reflector. Se ha trabajado sobre tres puntos de diseño para mostrar cómo se puede alcanzar una solución de compromiso conforme a los requisitos de diseño. Además, en esta tesis se propone un nuevo tipo de diagrama llamado diagrama de rendimiento de desenfoque (*defocusing performance chart*). El propósito de este diagrama es mostrar como decrece el factor de interceptación cuando el tubo absorbedor se mueve de su posición de diseño en el plano transversal. Es posible comparar gráficamente la vulnerabilidad de diferentes geometrías de reflectores frente al desplazamiento accidental por la torsión que pueda sufrir el tubo absorbedor. Con la finalidad de cuantificar esta vulnerabilidad, se define el parámetro (A_{99}) que indica el área adimensionalizada del diagrama donde el factor de interceptación es mayor de 0.99. El inconveniente que presentan algunas de las geometrías propuestas por el método IMCRT es que son más vulnerables a desplazamientos hacia abajo de absorbedor en comparación con el reflector del modelo LS-3 (o *EuroTrough*), problema especialmente crítico cuando el perfil objetivo es muy ancho.

Es importante señalar que todos los ejemplos y soluciones proporcionadas por el método IMCRT en los artículos **II** y **III** corresponden a condiciones ideales, donde se ha considerado reflexión especular y un ángulo de incidencia nulo. Esto no quiere decir que estos factores no puedan ser tenidos en cuenta en aplicaciones futuras de este método, que puede extenderse a una amplia variedad de problemas y condiciones

de operación. Los ejemplos y soluciones mostradas en este trabajo solo pretenden ser una muestra inicial de cómo funciona el método y los tipos de soluciones que pueden hallarse.

El modelado de los mecanismos de transferencia de calor que tienen lugar en un PTC forma también parte del objetivo de esta tesis. El **artículo I** trata sobre el modelo numérico de un solo tubo absorbedor con 4.06 m de longitud, donde se calcula el campo 3D de temperaturas en la pared del mismo y la cobertura de vidrio junto con una descripción unidimensional del fluido (monofásico, vapor sobrecalentado) en estado estacionario. Se ha resuelto la ecuación del calor (ecuación de Laplace en estado estacionario) en coordenadas cilíndricas en ambos dominios sólidos por medio del método de diferencias finitas. Concretamente, se ha empelado un esquema centrado de segundo orden para discretizar las derivadas parciales de segundo orden garantizando que todos los términos tienen un error de truncado del mismo orden, al igual que se ha utilizado un esquema iterativo para resolver el sistema de ecuaciones algebraico obtenido. Para evaluar la propiedades termodinámicas del agua se ha recurrido a la librería estándar IAPWS-IF97.

Las condiciones de contorno comprenden la distribución de radiación solar concentrada, que ha sido previamente calculada por el algoritmo de trazado de rayos en 3D, así como los diferentes términos de transferencia de calor entre las diferentes partes que componen el receptor y el ambiente. La transferencia térmica entre la cara interior del tubo absorbedor y el fluido se ha modelado mediante la correlación de Gnielinski, que es válida tanto para flujo turbulento como para el régimen de transición. Debido al vacío que existe en el hueco entre el tubo absorbedor y la cobertura de vidrio para evitar pérdidas por convección, la radiación térmica es el mecanismo de transferencia dominante a través del anillo de vacío (es necesario indicar en este punto que la convección molecular libre no ha sido considerada). Asumiendo que la cobertura de vidrio (borosilicato) es opaca a la radiación térmica, los términos correspondientes de intercambio de calor por radiación se definen en tres dimensiones donde también se incorpora la evolución axial de la temperatura. Esto significa que el coste computacional para calcular los factores de forma no es despreciable. Un término fuente ha sido también incluido en la ecuación del calor de la cobertura de vidrio para modelar la absorción la radiación solar que la cruza, donde el coeficiente de atenuación ha sido determinado experimentalmente.

La distribución de temperatura en el dominio fluido se ha calculado a partir del flujo de calor entrante por la cara interior del tubo absorbedor y la caída de presión axial.

Para ello, la ecuación de Colebrook-White ha sido aproximada mediante la solución de Goudar-Sonnad. Por su parte, la rugosidad relativa de la cara interior del tubo absorbedor ha sido determinada experimentalmente por medio de microscopía 3D a partir de una muestra extraída de la instalación DISS.

Se ha realizado un test de mallado para justificar el número de elementos y garantizar la independencia de los resultados respecto al nivel de discretización. El modelo térmico se ha validado mediante datos experimentales obtenidos en la instalación DISS con presiones de operación entre 3 y 10 MPa bajo diferentes temperaturas del fluido a la entrada. Además, los valores de caudal ensayados cubren un rango representativo de condiciones de operación. Del mismo modo, la distribución de temperatura en la pared del tubo absorbedor ha sido comprobada en secciones transversales específicas donde se localizaban los ocho termopares insertados en la pared del tubo. De acuerdo con los resultados, el modelo reproduce adecuadamente la distribución angular de temperatura alrededor del mismo y proporciona una estimación realista de las pérdidas térmicas del receptor. No obstante, las pérdidas térmicas experimentales son ligeramente superiores a las proporcionadas por el modelo. Algunas de las aproximaciones asumidas en el modelo pueden ser la razón de estas discrepancias. También se puede concluir que acoplar el modelo térmico 3D para los dominios sólidos junto con una descripción 1D del fluido, proporciona una buena aproximación del proceso, al menos en condiciones estacionarias con flujo monofásico. Esta aproximación evita tener que resolver las ecuaciones de Navier-Stokes en 3D (CFD) lo que hace que esta herramienta pueda ser adecuada para modelar plantas PTC completas cuando se necesite una descripción realista del campo de temperaturas en el tubo absorbedor.

El **artículo IV** trata sobre la simulación de un sistema DSG formado por una fila completa de PTCs. A diferencia del **artículo I**, es necesario implementar un modelo termo-hidráulico que describa tanto la región de flujo bifásico como las de flujo monofásico (esto es, agua subenfriada a la entrada y vapor sobrecalentado a la salida). La industria nuclear cuenta con una amplia experiencia en el modelado 1D de flujo bifásico, debido a que la mayoría de los reactores de centrales nucleares comerciales se refrigeran con agua, como es el caso de las centrales de agua en ebullición. RELAP5 (del inglés *Reactor Excursion and Leak Analysis Program*) es un código de 6 ecuaciones que modela independientemente cada fase (también conocido como modelo de dos fluidos). Se basa en un conjunto de correlaciones ampliamente validadas y mapas de flujo que reúnen una cantidad ingente de información experimental. A esto se añade que el comportamiento térmico del tubo absorbedor puede aproximarse usando estructuras de calor, que es el nombre dado por RELAP5 a los dominios sólidos

en contacto con nodos de fluido. A pesar de la existencia de modelos de equilibrio homogéneo (HEM, del inglés *Homogeneous-Equilibrium-Models*) de uso común en la bibliografía, estos modelos no pueden reproducir los desplazamientos relativos entre ambas fases ni otros fenómenos relacionados con la geometría de la interfase. Aunque existen aproximaciones intermedias como es el caso de modelos basados en una correlación de tipo *drift-flux* (por ejemplo el código FLOCAL), este trabajo pretende validar RELAP5 para aplicaciones solares implementando un modelo detallado de la instalación experimental DISS.

A partir de las opciones estándar de RELAP5, no es posible modelar el tubo en 3D, donde sólo la discretización axial y radial es posible. Esto supone una limitación para reproducir fielmente el campo de temperaturas alrededor del tubo absorbedor. Este aspecto es especialmente relevante ya que una de las particularidades de los tubos absorbedores en sistemas PTC es que el flujo concentrado incidente no es homogéneo alrededor de la coordenada angular. Sin embargo, se puede emplear una aproximación que consiste en adjuntar varias estructuras de calor al mismo nodo de fluido. De esta forma, se han adjuntado 6 estructuras de calor a cada nodo de fluido (mismo número que termopares insertados en las pared de los tubos actuales de la instalación experimental). A diferencia del modelo térmico descrito en el **artículo I**, ni la cobertura de vidrio ni el anillo de vacío se han incorporado. En su lugar, una correlación experimental describe sus efectos. Con esta finalidad, se ha obtenido una nueva correlación de pérdidas a partir de ensayos experimentales recientes llevados a cabo en la instalación DISS con receptores modelo SCHOTT PTR-70-DSG instalados en 2013. Esta correlación es válida para representar las pérdidas térmicas de estos receptores ya instalados en el campo solar después de al menos dos años de operación. Además, las secciones pasivas del circuito termo-hidráulico que forma la fila de captadores han sido incluidas. Este es el caso de las interconexiones entre captadores, que están formadas por una serie de segmentos verticales y horizontales que tienen un efecto en la dinámica del sistema y la evolución axial de la presión y la fracción de vacío.

El modelo en RELAP5 ha sido validado a partir de ensayos transitorios realizados en la planta experimental DISS, donde se han llevado a cabo jornadas completas de operación. Estos ensayos incluyen condiciones de operación estacionarias y también transitorias, como paso de nubes, cambios de caudal o desenfoques bruscos de algunos captadores incluyendo los procedimiento de arranque y apagado de planta. Se han simulado un total de 6 casos para comprobar los resultados del modelo. Esta comprobación se ha basado en las medidas de temperatura y presión del fluido tomadas a lo largo del sistema así como la temperatura de pared de los tubos absorbedores.

Se puede concluir que RELAP5 puede reproducir fenómenos transitorios tales como las oscilaciones posteriores a un descenso brusco de la radiación solar directa debido al paso de nubes. Además, la diferencia máxima en la distribución angular de temperatura en la pared de los tubos puede ser aproximada a partir de la estrategia adoptada, donde se consigue reproducir la variación temporal de dicha variable. También se ha realizado un estudio del fenómeno conocido como *severe slugging* en las interconexiones (**artículo IV**). Debido a los efectos de la aceleración gravitatoria en las secciones verticales, puede originarse un desplazamiento relativo entre las fases. Para ello, se han considerado dos captadores contiguos junto con la interconexión que los une. A pesar de imponer condiciones de flujo estacionarias a la entrada del primer colector, pueden aparecer oscilaciones sostenidas en el caudal de salida del segundo. Esta tesis muestra que RELAP5 puede reproducir estas oscilaciones dadas unas condiciones concretas de presión, título de vapor y caudal a la entrada. Un total de 374 simulaciones se han llevado a cabo para reunir un diagrama con el que determinar las condiciones bajo las que aparecen estas oscilaciones con una presión de entrada de 0.5 MPa. Se ha caracterizado la amplitud en las oscilaciones de la fracción de vacío promediada a los largo de la última sección vertical (*riser*), al igual que también se ha aplicado el método de descomposición en valores singulares (SVD, del inglés *Single Value Decomposition*) para caracterizar las oscilaciones a partir de la distribución espacio-temporal de la citada fracción de vacío en la interconexión.

Se pueden extraer algunas conclusiones relevantes a partir de los resultados. En primer lugar, la implementación de un código propio de trazado de rayos por técnicas de Monte Carlo (MCRT) en 3D ha permitido estudiar al detalle la distribución de radiación solar concentrada en los tubos absorbedores de un PTC. Este código a medida para PTCs puede ejecutarse más rápido que los códigos de propósito general, beneficiándose de las operaciones elemento a elemento en Matlab®. Por otra parte, se ha implementado el código MCRT en 2D, que es sustancialmente más rápido que la versión en 3D, tras proyectar el *sunshape* sobre el plano transversal del absorbedor. Esta herramienta 2D ha sido clave para comprobar que las geometrías propuestas por el método IMCRT son válidas. Esto significa que el método IMCRT es una herramienta útil para diseñar nuevas geometrías de reflectores con distribución de flujo más homogéneo sobre tubos absorbedores. Además, los resultados obtenidos por el modelo térmico en el **artículo I**, muestran que el enfoque basado en acoplar un dominio 3D para las partes sólidas del receptor junto con un modelo unidimensional para el dominio fluido es válido al menos en régimen estacionario. Por otra parte, se ha mostrado que RELAP5 es una herramienta adecuada para simular en régimen

transitorio un lazo único de un sistema DSG (instalación experimental DISS) y puede considerarse una herramienta con potencial para futuros estudios sobre sistemas con filas en paralelo.

Esta tesis se ha desarrollado dentro del proyecto GEDIVA (Ref. ENE2011-24777), a través de la beca doctoral FPI financiada por el Gobierno español (Ref. BES-2012-056876), y del proyecto DETECSOL (Ref. ENE2014-56079-R). La mayor parte del trabajo de investigación ha sido llevada a cabo en la Unidad de Sistemas de Concentración Solar en la Plataforma Solar de Almería, división del Centro de Investigaciones Energéticas, Medioambientales y Tecnológicas (CIEMAT).

Se espera que las conclusiones y los resultados alcanzados en esta tesis sean útiles para futuros diseños de plantas solares basadas en captadores de foco lineal y para implementar herramientas de modelado eficiente en plantas DSG a escala completa.

1 INTRODUCTION

1.1 Deployment and prospects of Concentrated Solar Power

The future of solar thermal energy at an industrial scale depends on economic and political factors; likewise technical breakthroughs in such technology are expected. According to the international energy market, which is based on unplanned economy policies, a cost reduction in the electricity price produced by the solar thermal industry is necessary to be fully competitive under current market rules. However, economic criteria are not the only factors to be taken into consideration. Social and environmental issues are also relevant. Global warming is an actual threat with major implications (VijayaVenkataRaman et al.; 2012; Haer et al.; 2013; Williams; 2007) and future energy policies should turn into a sustainable alternative.

Current pricing of fossil fuels do not take into account the incurred costs due to pollution and other public expenses (e.g. foreign affairs, strategic policies) required to provide a steady supply in western countries. In line with this, worldwide fossil fuel subsidies were about \$4.9 trillion in 2013. Global warming accounts for 22 % of these subsidies, likewise local air pollution is the main factor (46 %). It means that environmental issues accounts for most of the expenses associated with fossil fuel consumption (see Fig. 1.1). In recent years it has shown an upward trend, so that the total amount of subsidies in 2015 was about \$5.3 trillion (6.5% of global GDP) (Coady et al.; 2017). This situation can be explained by the diminished public sector
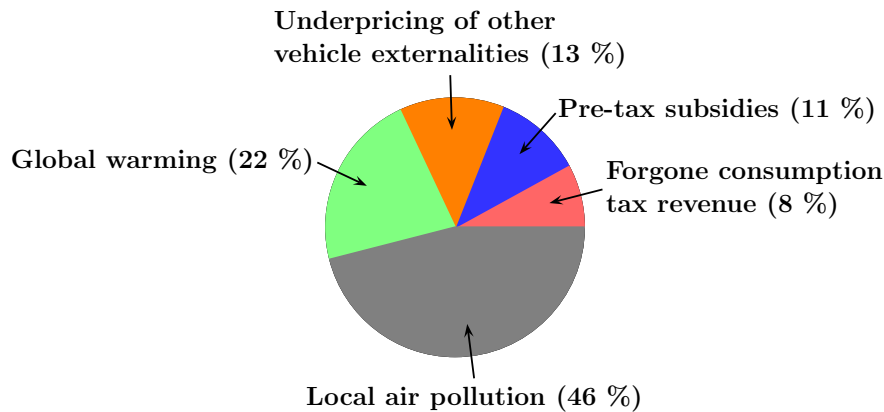
Figure 1.1: Break-down of post-tax fossil fuel subsidies into different components by 2013 (Coady et al.; 2017).

and its inability to make policies in favor of the general interest, which sometimes are opposed by the private sector agenda. The current economic crisis poses an additional dilemma to policy makers, because an increase in the price of fossil fuels as a consequence of phasing out such subsidies will negatively affect competitiveness and short-term economic growth. However, as commented by Wang and Li (2015), the plunge in the oil global prices that took place in 2015 gives a new opportunity to remove fossil fuel subsidies. Countries counting on a significant public sector have more leeway and tools to correct their energy policy. State-level financial incentives play a major role in the deployment of solar technologies (Sarzynski et al.; 2012). This is the case in China where for example, an ambitious plan ($ 30 billion) of subsidies and bank loans at lower rates provided by the government (or state-owned banks) to promote the photovoltaic industry, led to a drastic cost reduction in the sector (Vieira-de-Souza and Gilmanova Cavalcante; 2016). As a consequence, China became the top exporter of photovoltaic panels worldwide. Such strategic decision gave China an additional industrial market involving at least 2000 companies (Zhang et al.; 2013).

It is pretty obvious that initiatives for a new post-carbon economy are not coming from the private market itself. If decisions are made exclusively according to the levelized cost of electricity (LCOE), and short-term perspective prevails over environmental and social principles, no solutions will be found to climate change. Any attempt to address this issue should evaluate the real costs (based on a long-term basis) of fossil fuels and other non-renewable energy sources.

In this transition, the less polluting of the current conventional energy resources

have to be supplemented along with several types of renewable energy. The intermittent nature of renewable resources requires a balanced mix of wind, solar photovoltaic and concentrated solar power (CSP), among others. This combination is the only way to guarantee a good dispatchability so that renewable energy accounts for a significant share of the global energy production. As detailed in Table 1.1, CSP is still the most expensive technology in terms of LCOE. This drawback can be partially explained by the lack of determined and ambitious public R&D projects with the aim of boosting the CSP industry worldwide. In addition, the existing efforts have not been promoted globally and it is difficult to set an accepted method of placing a real value on the benefits provided by the thermal storage. Future cost reduction are closely related to the economy of scale and it fully depends on its deployment, but as commented by Vieira-de-Souza and Gilmanova Cavalcante (2016), policy uncertainty is hindering prospects of growth.

The EU is one of the most committed regions to the development of solar technologies. For example, CSP was supported by $45 million from the member states governments plus $7 million from the EU sources in 2007 (Bosetti et al.; 2012). As a matter of fact, the German CSP industry is well positioned in the international market, whereas Spanish companies are involved as general contractors (Vallentin and Viebahn; 2010). The United States also plays a relevant role in CSP deployment (Mehos et al.; 2017). The SunShot Initiative is expected to reduce the CSP LCOE to $c6/kWh by 2020 without federal incentives. However, later studies showed that this objective was not fully realistic (Ho et al.; 2014). Besides, the US Department of Energy allocated $10 million for new CSP research projects: *DoE initiative aims to advance US solar industry* (2014). China is becoming a central investor. The target of the 12th five-year-plan (FYP) of 1 GW_e of installed capacity was not achieved though. The 13th FYP (2016-2020) set a more ambitious roadmap for CSP development. According to an initial draft of the plan, it was expected to achieve the goal of 10 GW_e by 2020. As indicated by Vieira-de-Souza and Gilmanova Cavalcante (2016), the agreement between the government and projects developers was based on a Feed-in-Tariff (FIT) scheme ($c22/kWh). However, the final 13th FYP announced by the Chinese government halved this goal to 5 GW_e. A first batch of 1.349 GW_e is being finished by 2018, so an additional capacity of 3.681 GW_e is to be installed by 2020. CSP only accounts for a small share of the total solar power capacity planned (110 GW_e) (Wu; 2016). Northern Chile has outstanding solar radiation conditions. In addition, their mining industry, which is mainly located in the same part of the country, requires a huge amount of thermal energy. Despite the fact that most of

Table 1.1: LCOE estimates per technology and country/region ($c/kWh). Table extracted from the review by Vieira-de-Souza and Gilmanova Cavalcante (2016).

Technology	China	USA	Europe
CSP	19-46	20-49	20-49
Photovoltaic	7.9-14.9	11-23	10-25
On-shore wind	4.9-9.3	6.1-13.6	7.1-11.7
Hydro	3	9	10
Coal	3.5-3.9	7	12-17

the projects use photovoltaics, some interesting CSP plants are under construction (e.g. Maria Elena Solar Power Plant with a total power of 400 MW_e) (Grágeda et al.; 2016). In general terms, by October 2015, 110 MW_e of CSP power was under construction and an additional 980 MW_e had been approved (Starke et al.; 2016). The Republic of South Africa is also a country with excellent solar capacity, having excellent solar radiation conditions (Nakumuryango and Inglesi-Lotz; 2016). According to Pollet et al. (2015), 5 CSP projects have been awarded under the South Africa's renewable energy independent power producer procurement programme with a total power of 400 MW_e.

Despite of the current LCOE of CSP, such technology shows some advantages. Thermal energy storage systems are able to shift the electricity production to several hours past sunset. This enables better dispatchability respect to other renewable technologies (e.g. photovoltaics). However, CSP requires a higher initial investment than photovoltaics (Bosetti et al.; 2012). It is also important to mention that areas with high solar radiation, generally correspond to regions with a lower human development index, where any investment related to this technology enhances a balanced growth from the geographical and social perspective. Solar industry deployment implies economic and social growth (Caldés et al.; 2009) due to the fact that the solar industry provides more jobs than other technologies based on fossil fuels (Çetin and Eğrican; 2011; Soria et al.; 2015; Kost et al.; 2012) and the need for local suppliers.

According to the 2016 Global Status Report on Renewables delivered by REN21 (*Renewables 2016 Global Status Report*; 2016), the total CSP electric power installed by the end of 2015 is 4.8 GW_e. This power is not significant in comparison to the installed power of other renewable technologies: Solar photovoltaic is 227 GW_e whereas wind power is about 433 GW_e worldwide. The new CSP facilities are mainly a mix of parabolic trough and tower technologies including thermal storage.

In light of the available information it can be concluded that further deployment of CSP depends on political decisions that are being made in the next years. Despite the existence of mature CSP technologies, which have already been implemented at industrial scale, the global installed power should be higher so that the benefits of the economy of scale can lead to a lower LCOE. The role of developing economies is central in the prospects of CSP.

1.2   Parabolic-Trough Collectors

Parabolic-trough collectors (PTCs) are a particular type of linear-focusing solar concentrators classified as medium temperature system. Two main parts in the collector are responsible for the transmission and conversion of solar radiation into thermal energy. As depicted in Fig. 1.2, the reflector geometry is defined by the equation of parabola, where the focal distance f_c is defined as the distance between the focal point and the closest reflector point. The half width of the collector L_w defines the aperture area, whereas the rim angle ϕ_{rim} expresses the relation between focal distance and collector width. According to the specular reflection law, all sun rays reaching the reflector whose direction is parallel to the focal distance are reflected into the focal point. The Sun is not a point source of light though. From the collector point of view, the sun can be simplified as a solar disk with an half angular extent of 4.65 mrad. This fact limits the concentration ratio along with the non-specular reflection (or scattering effect) which takes place in the reflection phenomena due to imperfections on the mirror surface.

The absorber tube is the element where solar radiation is converted into thermal energy and transferred to the heat transfer fluid (HTF). In most systems, the absorber consists of a cylinder whose center is located at the focal point. The fluid (single phase or two-phase mixture) circulates inside the absorber pipe increasing its enthalpy. The absorber outer surface has a selective coating to improve optical properties. This selective coating has a high absorptance for radiation in the solar energy spectrum, and low emittance in the infrared region of spectrum in order to reduce thermal radiative losses. Most of the selective coatings are made of nickel-chrome or cermets from which absortance higher than 95% and emittance lower than 10% at 400° C can be achieved.

The absorber is covered by a glass cover generally made of borosilicate (e.g.
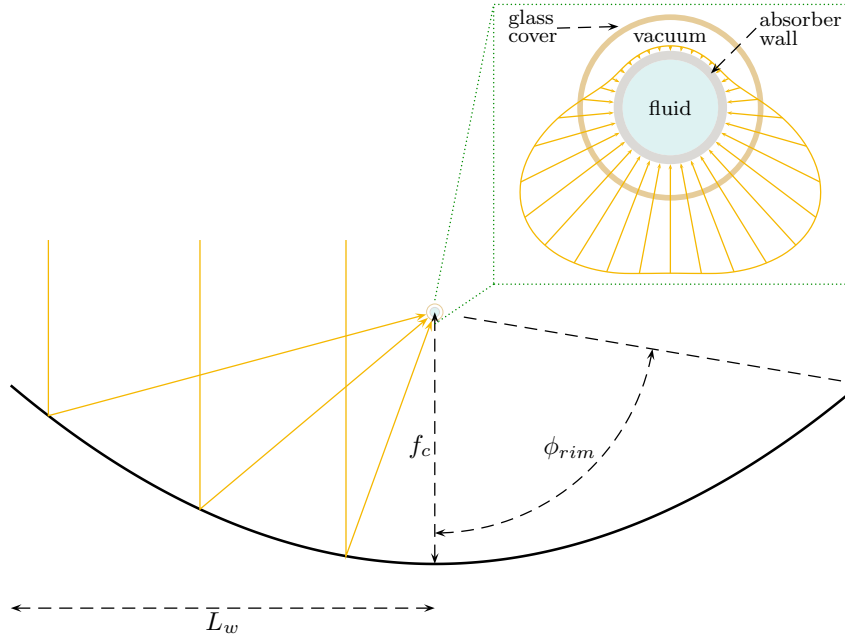
Figure 1.2: Diagram of a Parabolic-Trough Collector.

Pyrex ®) to protect selective coating. The air in the gap between the absorber and the glass cover is removed, so that a vacuum annulus can reduce convective losses due to the high temperature reached at the outer surface of the absorber. An additional anti-reflective treatment is applied to the glass cover to avoid reflective losses. Bellows are required for the glass-to-metal junction and to compensate the thermal expansion of the steel absorber. The vacuum is sealed by a glass-to-metal welding between the expansion bellow and the glass cover. This welding is one of the most critical parts of the receiver increasing significantly its cost.

The concentrated radiation impinging onto the absorber is not homogeneously distributed around it. For a PTC with its aperture plane looking at the zenith, the bottom half of the absorber tube receives most of the solar concentrated radiation where two characteristics peaks of radiation can be found (see Fig. 1.2). The upper half hardly receives concentrated radiation so that thermal gradients may appear in the absorber wall. As a result, flow conditions should be suitable in order to guarantee at least a minimum heat transfer between the absorber wall and the fluid.

Commercial PTCs use a single-axis tracking system to follow the sun position during the day. Despite the fact that dual-axis systems able to achieve an optimal tracking exist, they are not as cost competitive as the single-axis option for full scale plants. The rotation axis is generally north-south or east-west. The former

provides the maximum amount of energy collected on a yearly basis, whereas the latter gets a better distribution of the thermal energy collected throughout the year, with less difference between winter and summer. With the aim of optimizing the total thermal energy production, commercial power plants usually follow the north-south orientation. In case of small collectors (e.g. *Acurex* design), an electric tracking actuator is the best option, whereas a hydraulic actuator is the suitable alternative for wider designs needing higher torque, e.g. *EuroTrough* (Fernández-García et al.; 2010). A mechanical structure is required to hold the mirrors. Depending on the collector size, the reflector may not be formed by a single mirror but by several facets assembled on a frame. The structural strength of the collector affects its length and the number of tracking units which has to be reduced in order to optimize the system cost. Table 1.2 gathers the most common designs of Solar Collector Assemblies (SCA) from the commercial perspective and research interest. The historical trend seeks to get longer collectors in order to reduce the number of drives and connection pipes between adjacent collectors. Note that this type of connection is responsible for additional head loss and instabilities in case of two-phase flow.

Table 1.2: Most relevant commercial designs of parabolic trough collectors. Information obtained from several sources. Among others: (Dagan et al.; 1992), (Fernández and Acuñas; 2012) and (Fernández-García et al.; 2010).

Model	f_c (m)	$2L_w$ (m)	ϕ_{rim} (deg)	SCA Length (m)	absorber outer diameter (mm)
Acurex 3011	0.53	2.13	90	36.7	31.8
LS-1	0.68	2.55	85	50.2	40
LS-2	1.40	5	80	47.1	70
LS-3	1.71	5.76	80	99	70
LS-4C (experimental)	1.91	10.5	110	49	114
EuroTrough 100	1.71	5.76	80	100	70
EuroTrough 150	1.71	5.76	80	150	70
SenerTrough	1.70	6	80	150	70
SenerTrough 2	2	6.87	81.3	150	80
HelioTrough	1.71	6.78	89.5	191	90
SkyTrough	1.71	6	82.5	115	80
Solarlite SL 4600	1.2	4.6	87.6	120	70

1.3 Development of Parabolic-Trough Collectors

Experimental research on concentrated solar power is reported to have started in the second half of the XIX century. Several prototypes were developed in Europe and the US with the aim of converting solar energy into mechanical power or for water distilling purposes. As detailed by Pytilinski (1978), some of these experimental facilities used mirrors similar to the current parabolic-trough collectors (e.g. A. Pifre

in France, 1880). Efforts continued in the first half of the XX century, mainly in the US and the Soviet Union. This is the case of the Andalusian engineer, Dr. Federico Molero, who between 1941 and 1946 developed not a line-focus but a point-focus concentration system to produce steam for process heat supply in Uzbekistan (The Deseret News; 1946). In the second half of the century, several systems for irrigation purposes were implemented. For instance, a system with 622.4 m^2 using parabolic-trough collectors was installed in New Mexico (US). It used a Rankine cycle operating at a peak temperature of 436 K.

It was not until the 1980s, when the American-Israeli company LUZ International Ltd., broke ground in the parabolic trough technology at an industrial scale. The first facility (SEGS I, Solar Electricity Generating System) came online in 1985 in the Mojave Desert (California) with a net power of 13.8 MW$_e$ (Skumanich; 2011). A total of 9 plants (SEGS I – SEGS IX) were eventually constructed in the same region at 3 different locations using synthetic oil (Therminol) as heat transfer fluid (HTF). Only the first SEGS plant had storage units which were out of order after being damaged by fire in 1999. The rest of the SEGS plants consisted of hybrid systems with natural gas to produce energy without solar radiation. The learning curve allowed an increase in the power of the subsequent plants leading to costs reduction until the last plant (SEGS IX) came online in 1990 (80 MW$_e$). Three different models of collectors were designed and manufactured. The first one (LUZ LS-1) was used in the two first SEGS plants. The next design (LUZ LS-2) had a larger area (235 m^2) and it was installed in 6 plants (SEGS III – SEGS VII). Finally, the definitive design (LUZ LS-3) was 99 m long with 5.7 m of aperture width (equivalent to 545 m^2). This last design was tested in the last two power plants (SEGS VII SEGS IX) so that most of the collector's models in current commercial PTC plants resemble it in terms of dimensions.

The purpose of constructing and operating the SEGS plants was to prove reliability and the ability of PTCs to generate electricity. The efficiency of the whole system was tested and several designs of absorbers have been checked (Baharoon et al.; 2015). As a consequence of the plunge in oil prices in previous decades, the regression in renewables energy policy starting with the Reagan administration (Skumanich; 2011) along with the withdrawal of the tax credits, LUZ was declared bankrupt in 1991. The plants were sold to a group of investors and they have been kept in operation with a total power of 354 MW$_e$ (net capacity) since (Cohen and Frier; n.d.; Cohen et al.; 1999). The five 30-MW$_e$ plants (SEGS III SEGS VII) located at Kramer Junction (California), were acquired and operated by Kramer Junction Company (KJC).

As detailed by Price and Kearney (2003), technology developments were kept in progress in the 1990s. A noticeable reduction of the LCOE was reached thanks to the improvements made and the experience gained. Step forwards were taken concerning different elements on the system:

- Improvements were made in the absorber tube, also called heat collector element (HCE). After several years, 15 % of absorber tubes in SEGS plants operated by KJC, had lost vacuum or had their glass cover broken. As a first solution, the glass cover was replaced in those whose envelope was broken. The emittance of the selective coating on the absorber is another aspect that concerns heat losses. In line with this, the company Solel Solar Systems developed the new Solel UVAC absorber, using a new cermet coating with an emittance of approximately 50% below the former absorber. In 1997, this new type of absorber was beginning to replace the previous ones. This breakthrough implied a significant reduction in the cost of electricity by lowering thermal losses by 20%. Likewise, reliability and durability of absorber improved.

- Operation and maintenance costs (O&M) were reduced: Mirror washing techniques improved, absorber tube failures were reduced and advances in the control and information systems were achieved.

- Interconnections between collectors were redesigned. The former connections were made up of corrugated steel, covered with insulation. Reliability of the flex hoses was minimal, and sometimes, catastrophic failure would lead to spills and fires (Price and Kearney; 2003). Rotating-ball-joint-type assemblies replaced the former flexible hoses. As a consequence of that, the hydraulic pressure drop was reduced by approximately 50% due to the inner corrugations of the previous hoses.

- Mirror reflectance: A new reflectometer was developed. The new device allowed gathering data points six times faster. This information was crucial for arranging rounds of cleaning.

- Pumps circulating the heat transfer fluid experienced sealing problems (e.g. SEGS V plant). After trying several repairs, a new seal was installed and changes in the pumps suction pressure were made. Substantial progress in the pumps reliability was achieved.

After the aforementioned projects developed in the US, no important break-

throughs were made in the early 2000s. All the know-how gathered in the SEGS plants would be useful for the future deployment of such technology in Spain. This country was the next hub in the deployment of CSP, particularly in the case of PTC technology. It was in the period from 2008 to 2013 when the CSP installed capacity growth was by 50% on average per year, so that in the end of this period, Spain accounted for 67% of the cumulative installed capacity worldwide (Martín et al.; 2015).

A new package of legislation was gradually approved in Spain. It was in line with the European goal of covering 12% of the European Union's gross inland energy consumption with renewable energies by 2010 (European Comission; 1997). Substantial changes in the economic and legal framework started from the Royal Decree (RD) 436/2004 (RD 436/2004 of 12 March; 2004). The entry into effect of this RD, introduced alternative remuneration policies for CSP plant selling electricity to the grid. It was based on the average electricity tariff, so that remuneration consisted up to 300% of it for the first 25 years. Hybrid production was allowed (natural gas or propane) provided that fuel consumption did not exceed 15% of production and several modifications of this RD were applied until it was repealed by the following RD 661/2007 in May 2007 (RD 661/2007 of 25 May; 2007). This new RD was in effect during the period of the boom of CSP sector. Two alternatives were available: regulated tariff[1] or the negotiated pool price plus a premium. According to this new legislation, the remuneration was reduced to 80% of its initial value after 25 years of operation (Martín et al.; 2015). However, the PTC technology deployment that took place in Spain from 2008, was possible because of this framework. Andasol I, which was the first parabolic trough power plant in Europe (NREL; 2015), came into operation on 26 November 2008. This 50 MW_e power plant was the first in the world with a 2-tank indirect thermal storage system, which is able to maintain the energy production for 7.5 hours after sunset. According to the RD 661/2007 those power plants eligible for the aforementioned tariff should have a capacity lower than 50 MW_e. This is the reason which explains why most of the PTC plants installed in Spain are of 50 MW_e (see table 1.3). From early 2009 until mid-2013, commercial deployment of PTC technology experienced growth in Spain which was not ever seen before in the CSP industry. The change of government in the end of 2011 implied a drastic change in the legal and economic framework though. A new package of laws were entered into effect in 2012 cancelling the former feed-in-tariff (FIT) scheme for new plants and reducing the remuneration for the existing ones. The special tariff was removed for the fraction of electricity generated with fossil fuels (Law 661/2012 of 27 December;

---

[1]The regulated tariff was 26.9375 c€/kWh for the first 25 years and 21.5498 c€/kWh after that.

Table 1.3: Commercial PTC power plants in operation (2016) in Spain. Information obtained from several sources: Review by Baharoon et al. (2015), NREL projects database (NREL Database; 2016), CSP Global tracker (CSP Today; 2017), Protermosolar (Protermosolar; 2017) and CSP World (2017).

Project	Power (MWe)	Location	Start Production	Storage (hours)	Hybrid
Andasol-1	50	Aldeire (Granada)	Nov. 2008	7.5	-
Solnova 1	50	Sanlúcar la Mayor (Sevilla)	Jan. 2009	-	-
Solnova 3	50	Sanlúcar la Mayor (Sevilla)	Jan. 2009	-	-
Ibersol	50	Puertollano (Ciudad Real)	Jan. 2009	-	-
Solnova 4	50	Sanlúcar la Mayor (Sevilla)	Jan. 2009	-	-
Andasol-2	50	La Calahorra (Granada)	Jun. 2009	7.5	-
La Risca	50	Alvardo (Badajoz)	Jun. 2009	-	-
Extresol-1	50	Torre de Miguel Sesmero (Badajoz)	Jan. 2010	7.5	-
Extresol-2	50	Torre de Miguel Sesmero (Badajoz)	Feb. 2010	7.5	-
La Florida	50	Badajoz	Jun. 2010	7.5	-
Majadas I	50	Majadas de Tiétar (Cáceres)	Oct. 2010	-	-
Palma del Río II	50	Palma del Río (Córdoba)	Dec. 2010	-	-
Manchasol-1	50	Alcázar de San Juan (Ciudad Real)	Jan. 2011	7.5	-
La Dehesa	50	La Garrovilla (Badajoz)	Feb. 2011	7.5	-
Manchasol-2	50	Alcázar de San Juan (Ciudad Real)	Apr. 2011	7.5	-
Palma del Río I	50	Palma del Río (Córdoba)	Jul. 2011	-	-
Andasol-3	50	Aldeire (Granada)	Aug. 2011	7.5	-
Helioenergy 1	50	Écija (Sevilla)	Sep. 2011	-	-
Lebrija I	50	Lebrija (Sevilla)	Dec. 2011	-	-
Arcosol 50	50	San José del Valle (Cádiz)	Dec. 2011	7.5	-
Termesol 50	50	San José del Valle (Cádiz)	Dec. 2011	7.5	-
Helioenergy 2	50	Écija (Sevilla)	Jan. 2012	-	-
ASTE 1A	50	Alcázar de San Juan (Ciudad Real)	Jan. 2012	8	-
ASTE 1B	50	Alcázar de San Juan (Ciudad Real)	Jan. 2012	8	-
Solacor 1	50	El Carpio (Córdoba)	Feb. 2012	-	-
Solacor 2	50	El Carpio (Córdoba)	Mar. 2012	-	-
Morón	50	Morón de la Frontera (Sevilla)	May. 2012	-	-
Helios 1	50	Puerto Lápice (Ciudad Real)	Jun. 2012	-	-
Solaben 3	50	Logrosán (Cáceres)	Jun. 2012	-	-
Guzmán	50	Palma del Río (Córdoba)	Jul. 2012	-	-
Helios 2	50	Puerto Lápice (Ciudad Real)	Aug. 2012	-	-
Orellana	50	Orellana (Badajoz)	Aug. 2012	-	-
Extresol-3	50	Torre de Miguel Sesmero (Badajoz)	Aug. 2012	7.5	-
Olivenza 1	50	Olivenza (Badajoz)	Sep. 2012	-	-
Solaben 2	50	Logrosán (Cáceres)	Oct. 2012	-	-
La Africana	50	Posadas (Córdoba)	Nov. 2012	7.5	-
Astexol II	50	Olivenza (Badajoz)	Nov. 2012	8	-
Borges Termosolar	25	Les Borges Blanques (Lleida)	Dec. 2012	7.5	Biomass
Termosol 1	50	Navalvillar de Pela (Badajoz)	Mar. 2013	9	-
Termosol 2	50	Navalvillar de Pela (Badajoz)	Mar. 2013	9	-
Enerstar	50	Villena (Alicante)	Jul. 2013	-	-
Casablanca	50	Talarrubias (Badajoz)	Jul. 2013	7.5	-
Solaben 1	50	Logrosán (Cáceres)	Aug. 2013	-	-
Solaben 6	50	Logrosán (Cáceres)	Aug. 2013	-	-
Arenales	50	Morón de la Frontera (Sevilla)	Nov. 2013	7	-

2012) and new taxes were added to the fuel employed to warm the heat transfer fluid (HTF) to avoid freezing at night[2]. Further legislation was approved in 2013, but the most relevant reform was published in July (RD 9/2013 of 12 July; 2013) through which the former regulated tariff was replaced by a compensation plus the electricity pool price. This compensation is particular to each technology and depends on the investment and operational cost corresponding to the facility. Due to the retroactive nature of the law, this new legal framework also concerned the former PTC plants. According to table 1.3, the last PTC power plant came online in November 2013 after 2 years of construction. Due to the economic and legal uncertainty in Spain, no new commercial PTC plants have been built since then and two 50 MW$_e$ PTC projects were dismissed. In such a short period of time (2009-2013) 45 commercial PTC plants were installed in Spain with a total capacity of 2.2 GW$_e$. Most of them are located in the south of the country (Andalusia, Extremadura and Castilla-La Mancha) and all of them are currently operating (2017).

Table 1.4: Worldwide projects of parabolic trough collectors in operation or construction (2017) equal or bigger than 100 MW$_e$. Information obtained from several sources: Review by NREL projects database (NREL Database; 2016) and CSP Global tracker (CSP Today; 2017).

Project	Power (MWe)	Location	Start Production	Storage (hours)	Hybrid
Ashalim	110	Ashalim (Israel)	2018 (Scheduled)	4.5	-
Genesis	125+125	California (US)	Mar. 2014	-	-
Mojave Solar Project	140+140	California (US)	Dec. 2014	-	-
Solana	140+140	Arizona (US)	Oct. 2013	6	Nat. Gas
Noor I	170	Ouarzazate (Morocco)	Dec. 2013	3	-
Noor II	200	Ouarzazate (Morocco)	2017 (Scheduled)	7	-
Noor III	150	Ouarzazate (Morocco)	2017 (Scheduled)	8	-
KaXu Solar One	100	Poffader (South Africa)	2015	2.5	-
Ilanga I	100	Upington (South Africa)	2017 (Scheduled)	4.5	-
Shams I	100	Madinat Zayed (UAE)	Mar. 2013	-	Nat. Gas

After the halt in the Spanish CSP market the deployment of this technology became more international. Some Spanish companies moved their industrial activity abroad. Likewise they took advantage of the accumulated know-how to promote the deployment of CSP technology in different countries where the industry was not established yet. As listed in table 1.4, the biggest projects of PTC plants are in the southwest of the US, MENA and South Africa, although further projects are in development or announced mainly in China, Chile and Africa. In most of these projects the European industry plays a major role.

By mid-2015, sixty three solar thermal power plants using parabolic-trough col-

---

[2]Note that the freezing point of the HTF used in Andasol-1 (Dowtherm A) is about 12°C.

lector (PTCs) were fully operational (Zarza-Moya; 2017). This is the most mature technology in terms of commercial deployment due to the fact that most of the installed CSP power corresponds to PTC plants. As mention by Chaanaoui et al. (2016), the installed PTC capacity by 2016 exceeds 3.5 GW_e whereas an additional capacity of 1.2 GW_e was under construction in that moment. The main objective of research in this industry aims to increase the efficiency of PTC systems, reduce installation, operation and maintenance cost as well as increase the lifespan of such systems (ESTELA; 2012). Based on the LCOE in 2011[3], a reduction of 45% in the LCOE is affordable by 2020. To achieve this goal, the research priorities are:

- Improving the reliability and durability of the absorbers in order to reach higher temperatures.

- Researching on innovative heat transfer fluids suitable for temperatures of at least 500 °C without risk of environmental impact (e.g. water, air, CO_2 and N_2).

- Making improvements in the collector designs, such as wider collectors to take advantage of the scale-up effect and alternatives to simplify the manufacturing process.

- Getting simpler and autonomous drive units as well as wireless DAQ systems and actuators.

Despite being a mature and a proven technology, future of the parabolic trough technology depends on technical and political factors. A significant reduction in the LCOE is required. It fully depends on the aforementioned breakthroughs. Policy makers should also take into account the social and economic benefits of renewable energies. In line with this, political will is required in order to guarantee a sustained funding for research.

---

[3]According to ESTELA (2012), the estimated LCOE in 2011 was 21 c€/kWh for a 50 MW_e PTC plant without thermal storage and 19 c€/kWh for a plant of the same power with 7.5 hours of storage.

1.4   Direct Steam Generation: A new step forward in PTC technology

The use of water as heat transfer fluid has already been proved in other CSP technologies. For example, central tower receivers such as the commercial Ivanpah Solar Power Facility (Ho et al.; 2015), where solar radiation is focused on steam receivers tube-type, which are located on the top of a solar tower system in order to produce steam that feeds directly the turbine. Direct Steam Generation (DSG) can also be regarded in the context of linear focus systems, where subcooled water enters into the solar field and phase change takes place on it. Superheated steam at the outlet can directly feed the power block without any intermediate heat exchanger.

Thermal oil has been thoroughly used in PTC commercial plants. In addition, lifespan of thermal oil and its thermal properties have improved since the start of the PTC technology. Lifespan of current thermal oils can last even longer than the CSP facility provided that suitable operating conditions are kept and maintenance tasks are performed correctly. As reported by Zarza-Moya (2017), modern plants use oil with a maximum working temperature of 398°C which is considerably higher than the maximum fluid temperature in the first SEGS plants (310°C). This is a fundamental factor in the overall plant efficiency, because the higher the temperature of the superheated steam is, the more efficient the thermodynamic cycle of the turbine is. However, the use of thermal oil implies inherent drawbacks that justify the attention paid to DSG. The upper limit in the superheated steam temperature supplied to the power block is not only due to the thermal properties of the oil but also due to the need of heat exchangers (or steam generator). A temperature difference is required in order to transfer heat from the oil (primary circuit) into the secondary circuit (water-steam). It means that the temperature of the steam feeding the turbine is noticeably lower than the oil temperature at the solar field outlet, a fact that in turn penalizes the overall efficiency of the system. In addition, the cost of the steam generator alongside the cost of the thermal oil, is not negligible in respect to the total cost of a commercial plant (more than 5% in a 50 MW$_\text{e}$ plant). This share is increased by the auxiliary systems required for oil maintenance and the fact that 4% of thermal oil has to be replaced annually (Zarza Moya; 2004).

The use of thermal oil implies environmental risks. In case of leakage or spillage, underneath ground can be contaminated. Measures to prevent it and decontamination

procedures have an effect on the operation costs. Furthermore, safety implications exists. Oil leaks may trigger a fire due to the fact that the thermal oil fire point is below the operation fluid temperature[4]. As a matter of fact, a fire took place in December 2009 in one of the Andasol plants.

Heat transfer mechanism is another issue that matters. The use of thermal oil implies single phase flow so that heat transferred to the fluid is in terms of sensible heat. Heat transfer coefficient in such case is considerably lower than when fluid phase change takes place (i.e. Direct Steam Generation). Having higher heat capacity (latent heat) and a high heat transfer rate during evaporation is a remarkable advantage. However, instability of flow and pressure due to the rapid variation of the mass content of the receiver tubes during transient conditions in two-phase flow may imply some complex issues. The freezing point of thermal oil is an additional critical aspect for PTC plants located where ambient temperature is low at night. Costs pertaining to the warming systems required to keep the fluid above the freezing temperature is another drawback.

As a consequence of all the previous drawbacks, Direct Steam Generation was regarded as an alternative with realistic prospects since the beginning of the $20th$ century.

1.4.1   Historical background of DSG

After carrying out preliminary tests in Pennsylvania, the North American engineer Frank Shuman, installed the first commercial DSG plant in 1912 (Pytilinski; 1978). It was located in a farming area in Meadi (Egypt) and it was planned for irrigation purposes. The collector design used at the time was similar to the current PTC designs. As displayed in Fig. 1.3 their aperture width was 4.27 m and they were 62.17 m long oriented north-south. The facility had a total aperture area of 1275 m^2 and it was compiled of five collectors arranged in parallel rows formed by a set of flat mirrors. The absorber was a 8.9 cm-diameter zinc pipe inside a trapezoidal chamber. The system was designed for supplying saturated steam at 0.1 MPa and it was based on a quite innovative automatic tracking device using a thermostat. The first test was a complete disaster because the absorber material melted down. As a consequence of the insufficient heat transfer in the zinc absorber, the temperature reached was very high. Former absorbers had to be replaced by steel pipes and finally, the plant

---

[4]Note that the fire point of Dowtherm A (used in Andasol plants) is about 118°C.

(a) General view of the facility
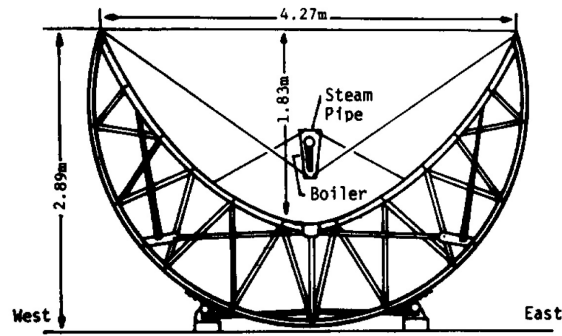
(b) Collector design

Figure 1.3: First DSG solar plant in Maedi (Egypt) extracted from Pytilinski (1978).

started operation in July 1913 with a maximum power of 60 HP. The high price of coal at the time, made this type of plants worthwhile and its deployment could have been attained provided that World War I had not broken out (Zarza Moya; 2004).

No significant breakthroughs were made until the 1980s, when the company LUZ International Ltd. launched the **ATS** (Advanced Trough System) project. DSG was intended to be a cheaper alternative to the HTF technology that the company was developing in the SEGS plants. According to LUZ, a cost reduction of 20% could be achieved. Ajona and Zarza (1994) agreed with the company and they estimated a reduction in the electricity cost of up to 30%. Previous studies in the US and Israel concerning two-phase flow, set the scientific background (Murphy and May; 1982; Taitel and Dukler; 1976; Barnea; 1987) to prove the feasibility of direct steam production in tilted pipes. However, technical viability of DSG at full scale facilities had not been proved yet. This explains why in 1988 LUZ launched the ATS project which initially comprised four phases. The first one consisted of a lab-scale test loop installed in the company's facility located in Jerusalem (Israel). Its evaporating section was formed by 8 pipes (10 m long) tilted 8°. Electrical heaters were installed around them to simulate thermal effects of concentrated solar radiation. The last two pipes could go beyond saturation conditions, so that the loop could produce superheated steam. No sensors to characterize two-phase flow pattern were installed, but pressure drop and temperature distribution were experimentally characterized in order to validate the previous models. An acceptable agreement was achieved in steady-state conditions. Neither information about transients nor temperature field in the absorber wall was published. The positive conclusions drawn by LUZ encouraged the company to keep making progress with the second phase of the project. It started in 1990 and real LS-3 PTC collectors were installed in parallel with the electrically-

heated pipes form the first phase (see Fig. 1.4b). Unlike conventional collectors, absorber tubes were fixed[5] so that the mirrors had to rotate around it. LS-3 collectors were tilted 8° as well and some modifications had to be made inside the absorber tubes so that the area of the flow cross-section was equal to the area in the first row. Despite cutting-edge characteristics of this facility, no relevant results were published.
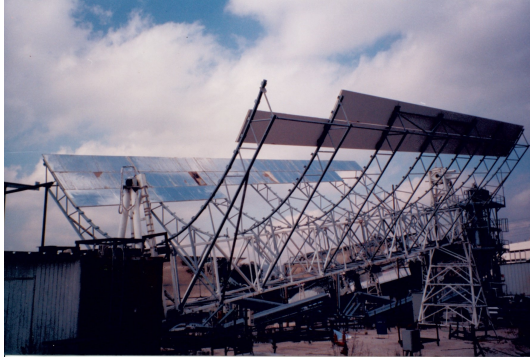
(a) Frame of the LS-4 collector prototype: 10.5 m of aperture width (Jerusalem)

(b) Two parallel rows: Second stage of the ATS Project (Jerusalem)

(c) Sde Boker facility: third stage of the ATS Project

(d) Sde Boker facility: third stage of the ATS Project

Figure 1.4: Photographs of the ATS Project (Israel)

The third phase was intended to be a more ambitious step forward. The construction of a new facility in the Ben-Gurion National Solar Energy Center (Negev desert, Israel) started in 1990. The plant layout consisted of two parallel rows of eight collectors which were each 12 m long with an aperture width of 5.76 m (see. Figs. 1.4c and 1.4d). Besides, a superheating section compiled of a single row of 4 collectors was fed by a steam separator. The finalization of this facility would have implied significant breakthroughs in this DSG technology, but as it has been previously mentioned, LUZ International went bankrupt in 1991. The project was cancelled. Before

---

[5]Technology of rotary couplings (also called ball joints) were not fully developed yet for working at high pressure.

the end of the ATS project, the fourth phase intended to develop the LS-4 collector whose aperture width was 10.5 m (see. Fig. 1.4a). This design was eventually not launched to the market.

After some years without activity, the Israeli Ministry of Energy awarded a joint contract to the Ben-Gurion National Center in cooperation with Solel to complete DSG plans by LUZ. Subsequent efforts were made but DSG was eventually dismissed as a consequence of problems to maintain the vacuum level due to hydrogen generation in the vacuum annulus of receivers by LUZ[6].

The **HIPRESS** (High Pressure Experiments on Solar Steam) facility gave new insights into the heat transfer mechanisms and flow conditions inside the absorber tubes in the two-phase flow region with up to 14 MPa of pressure. This lab-scale facility was installed at ZSW (Stuttgart, Germany) in 1992 and as in the first set-up developed by LUZ, the evaporator was surrounded by electrical heaters to simulate real temperature distribution in the evaporator (12 m long). Mixture quality at saturated conditions could be set at the inlet and as a result, a thorough two-phase flow map could be obtained. The most remarkable fact was that an X-ray device formed by 5 individual sensors could describe the flow pattern at a specific cross section of the evaporator.

A new concept of DSG was also studied in the **GUDE** project (1992-1995) for the integration of a solar field in a combined cycle power plant. It was promoted by SIEMENS KWU in collaboration with DLR (German Aerospace Center), ZSW and the Technical University of Munich. Several experimental studies were carried out to check the feasibility of the injection mode, a new control strategy in which liquid water is injected in the evaporator so that the output conditions can be controlled. The influence of several factors such as pipe diameter, pressure, injection mass flow rate and distances between injectors were characterized at lab scale. The **HIPRESS** facility was also used in this project and massive information about thermal gradients in the absorber pipe was provided as well as the accurate characterization of flow patterns and the interphase behavior.

Innovative designs of heat collector elements for DSG were analyzed in the **AR-DISS** (Advanced Receiver for Direct Solar Steam) project (Ajona et al.; 1997). The potential benefits of using secondary concentrators were highlighted by previous stud-

---

[6]Some of the information provided as well as some photographs displayed in Fig. 1.4 are courtesy of Professor David Faiman (Professor Emeritus at Ben-Gurion National Solar Energy Center).
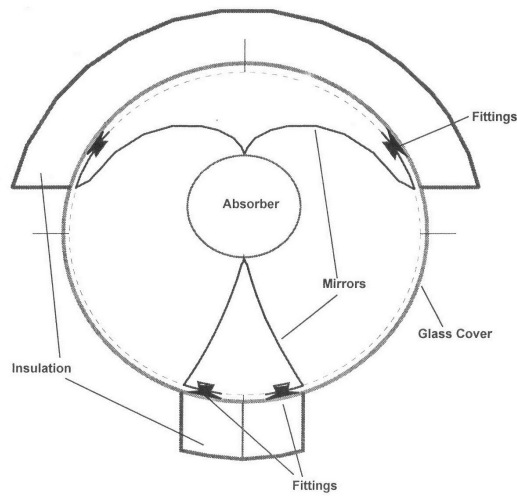
(a) Cross-sectional view of the receiver (Ajona and González; 1996)

(b) ARDISS receiver installed on the Heliomann 3/32 solar tracker

Figure 1.5: Experimental stage of the ARDISS project at PSA.

ies (Collares-Pereira et al.; 1991). Thermal losses can be attenuated by reducing the absorber diameter, and the risk of two-phase flow stratification can be diminished. This would optimize the overall system efficiency and improve the two-phase flow stability. Two test campaigns were performed. The first step took place at CIEMAT (Madrid), where the secondary reflector was manufactured, characterized and assessed. An ad-hoc test bench was designed to evaluate thermal losses. Conclusions drawn remarked some advantages of the new design, but its performance was not as expected. The secondary concentrator, which was affixed to the glass cover, caused thermal bridges. The second stage was carried out at Plataforma Solar de Almería (PSA) where two **ARDISS** receivers were assembled and mounted on a dual-axil tracking system using a LS-1 concentrator. Experimental results were less favorable than those obtained in Madrid. The flaws detected highlighted some weak spots concerning secondary concentrators. It was concluded that future alternatives using them should address some issues like high temperatures reached on secondary concentrators, deterioration of mirror coating and the subsequent increase in the emissivity.

Parallel research activity took place in the Universidad Nacional de México (UNAM) since the 1970s (Almanza and Lentz; 1998). A DSG facility was designed with an evaporator formed by 5 collectors (each 1.2 m long and 2 m wide). It operated in once-through mode producing saturated steam to feed a steam accumulator which

in turns was supplied to a turbine at a pressure up to 0.41 MPa. After upgrading the facility and adding a solar preheater, the overall efficiency of the system was not higher than 3%. Despite not getting outstanding results in terms of system performance, several interesting conclusions about thermal gradients in the absorbers were made in the 1990s. A new concept of composite absorber tube was studied where a copper pipe was attached at the inner face of a steel absorber tube. The high thermal conductivity of copper in conjunction with the steel strength could reduce thermal gradients in the absorber while operating at high pressure.

From the late 1990s to the 2000s several experimental projects were developed at Plataforma Solar de Almería concerning DSG in PTCs (see section 1.5 for further details). The design and construction of the DISS facility as well as the subsequent experimental campaigns provided valuable information and gathered the required know-how for future DSG plants.

Two commercial DSG plants have been constructed up until now. The 5 MW$_e$ plant **Thai Solar One** (TSE-1) is located in Thailand and it has a nominal thermal power of 19 MW$_{th}$ (Khenissi et al.; 2015) whose turbine is fed with superheated steam at 30 bar and 330°C. The solar field is compiled of SL 4600 parabolic-trough collectors with 4.6 m of aperture width and no storage system is used. It operates according to the recirculation mode concept and it started operation in January 2012 but not much information has been released about its performance after some years of operation. **Puerto Errado 2** plant is a 30 MW$_e$ commercial DSG plant located in Calasparra (Murcia, Spain). Unlike TSE-1, it uses Linear Fresnel reflectors[7]. It is formed by 28 parallel rows 940 m long and started production in March 2011. Solar field supplies saturated steam at a nominal turbine pressure of 55 bar (NREL Database; 2016).

All research effort and technological attempts to accomplish commercial deployment of DSG have provided scientific and technical knowledge which highlights the potential advantages of this technology with respect to current commercial systems. However, more research was required in order to address some technical challenges of DSG. This is the reason why the DISS project was launched and accomplished at PSA. All the experimental information gathered after such a long period of operation is of crucial importance for lots of studies, including this thesis.

---

[7]The fact of having fixed absorber, avoids the use of ball joints, in such a way that higher operating pressure can be achieved. It makes this technology a potential alternative to PTCs.

1.5 DISS Facility

After the progress made by previous projects, research had to continue to take advantage of the gained know-how. Europe was the next promoter in the development of DSG. In 1994 a preliminary design of a DSG plant using PTCs was proposed by Müller et al. (1994) and during the next two years subsequent revisions and upgrades were suggested for a future experimental facility. Based on these studies, the first phase of the **DISS** (DIrect Solar Steam) project (Zarza et al.; 1999) started in 1996 with a budget of €5.82 million (of which €2 million was public funding provided by the European Commission). Three public research centers (CIEMAT, DLR and ZSW), three Spanish electric companies alongside several Spanish and German engineering companies took part in this project. In the following 2 years (until November 1998), the definitive design of the **DISS** plant was specified and the facility was installed at Plataforma Solar de Almería.

The original plan consisted of a system formed by two parallel rows of collectors. This could have provided experimental evidence about the interaction between two long parallel ducts with two-phase flow. The difference of irradiance in each row as a consequence of local clouds in future large commercial plants could lead to certain instabilities and control challenges. Due to budget limits, the project was reduced to a single row system with all the auxiliary subsystems. This is the case of the Balance of Plant (BOP) whose main purpose is to act as if a turbine would be installed (see Fig.1.6), including the rest of auxiliary equipment of a standard power block. The superheated steam produced by the solar field feeds a final steam separator (final steam drum in Fig.1.6) whose pressure represents the inlet turbine conditions. Steam phase goes to the equivalent turbine load, which simulates its pressure drop after which an air cooler plays the role of condenser. The feed water tank, which holds and stores all the condensed water, serves as a buffer. Auxiliary systems keep the right fluid conditions in the feed water tank, such as the deaerator, which removes the air generated throughout the whole installation. A preheating system extracts steam from the inlet of the turbine load to increase the temperature of feed water (see feed water preheater in Fig. 1.6). This water preheater allows control of the inlet conditions of the solar field so that varying experimental conditions can be reached (steam cycle with regeneration). The facility was designed to operate in three different operation modes:

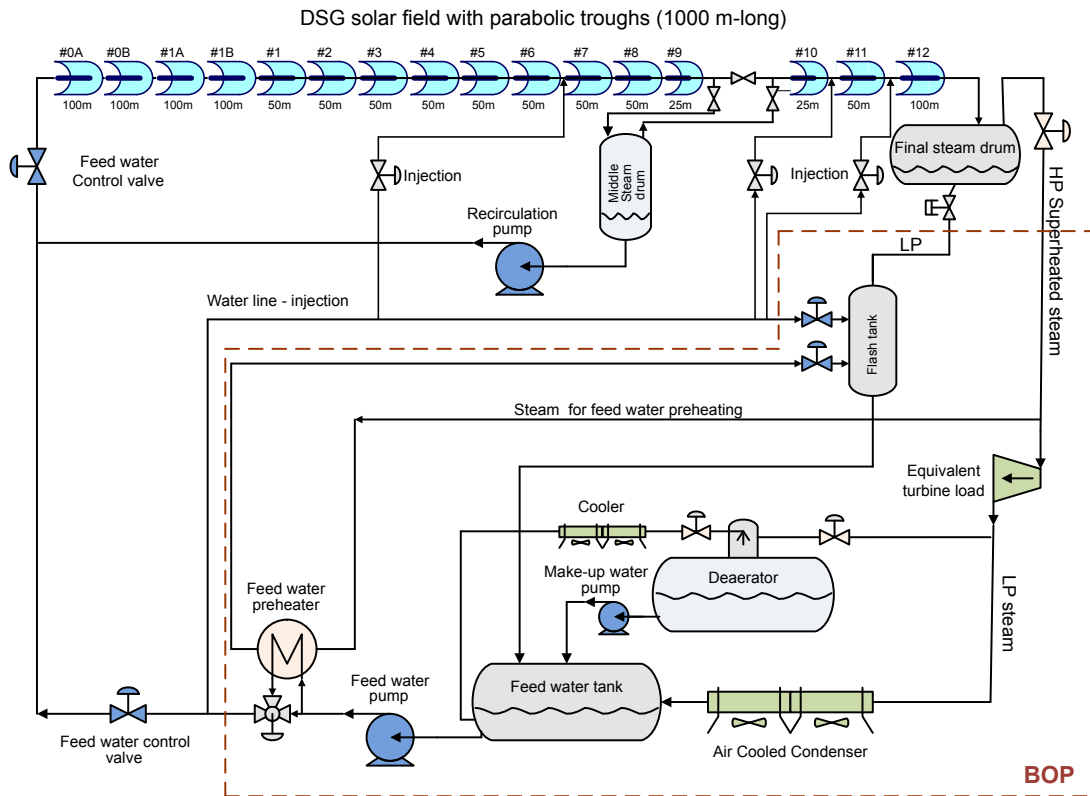- **Once-through** mode: Subcooled water enters into the solar field (collector

Figure 1.6: Diagram of the DISS facility located at Plataforma Solar de Almería.

#0A) where the whole phase change process, as well as water superheating takes place. Superheated steam is produced at the solar field outlet (collector #12). No steam separators are used within the row of collectors so that the mass flow rate of superheated steam produced directly depends on the mass flow rate of feed water. It is the cheapest operation mode in terms of installation costs and system efficiency but implies certain complexity concerning the control strategy of the system. The operation mass flow rate is controlled by the feed water pump along with the feed water control valves.

- **Recirculation** mode: The use of an intermediate steam separator (Middle Steam drum between collectors #9 and #10 in Fig. 1.6) allows an accurate regulation of the two-phase region extension along the solar field. The steam phase is circulated into collector #10 in such a way that single phase flow is guaranteed in the superheating section. The remaining liquid water flows through the recirculation pump to the feed water control valve going into the solar field again. This configuration implies higher costs (an additional pump is required) and penalizes the overall system performance but eases the complexity of control tasks.

Table 1.5: Configuration of collectors in the DISS test facility: Distribution and geometrical characteristics of solar collectors installed in each project.

	Collector tag	PTC Model	Length (m)	$2L_w$ (m)	f_c (m)
DUKE	#0A #0B	SL4600+	8 × 12	4.60	1.20
INDITEP	#1A #1B	ET-100	4 × 25	5.76	1.71
DISS	#1 #2 #3 #4 #5 #6 #7 #8 #9 #10 #11	LS-3	2 × 25 / 1 × 25 / 2 × 25	5.76	1.71
DUKE	#12	SL4600+	8 × 12	4.60	1.2

- **Injection** mode: It is a slightly different version of the once-through mode, where a specific number of injectors add liquid water to the pipeline, so that the length of the two phase flow region can be controlled. An additional circuit fed from the feed water pump supplies liquid water to the injector (e.g. injection between collectors #6 and #7). The **DISS** facility has 9 injectors (only one has been represented for the sake of simplicity). This mode has not been extensively studied yet because of technical limitations concerning systems for void fraction measurement needed to control the degree of opening of injectors.

In the end of 1998, most of the goals of the first phase of the **DISS** project had been accomplished. Not only the design, but the installation and commissioning had been carried out. The solar field was comprised of 11 LS-3 collectors. As listed on table 1.5, the solar field was formed by LS-3 collectors two of which were 25 m long. Unlike the facility designed during the ATS project, DISS collectors were not tilted. Conclusions drawn by previous projects (i.e. **HIPRESS** and **GUDE**) pointed out that absorber tilt was not as critical for two-phase flow stratification as it was thought at first. The absorber used had a thick wall ($R_{si} = 25$ mm and $R_{so} = 35$ mm) made of carbon steel A335 (P22) and they were manufactured by the company Solel Solar Systems. The experimental characterization of the temperature distribution

around the absorber could be made by cross-sectional thermocouples. At specific axial locations a set of 8 thermocouples (Type K class 1) were installed around the pipe in order to know about the absorber wall temperature distribution.

The second phase of the project (Zarza et al.; 2002) lasted until December 2001 with a total budget of €6.06 million (€2.5 million by the European Commission). As reported by Zarza Moya (2004), an ambitious test campaign was performed accumulating 3608 hours of operation where the three operation modes were analyzed. Some aspects of the systems were upgraded. Thermal insulation was improved in the passive sections of the solar field: connections pipes (mineral wool thickness was doubled), steam separators and valves. The algorithm to calculate the sun position for the sun-tracking system was updated and substantial changes in the DAQ system were accomplished. In line with this, additional flow meters, temperature sensors and differential pressure transducer were installed. The facility was operated in both recirculation and once-through mode, including the development and testing of automatic control schemes (Valenzuela et al.; 2005).

The **INDITEP** project carried on with the DISS facility development from 2002 to June 2005 and it was funded with €5.34 million (€2.7 million by the European Commission). Two additional *EuroTrough* (ET-100) collectors were added at the inlet of the DISS facility (collectors #1A and #1B in Fig. 1.6) to perform qualification tests of future commercial plants, so that the nominal power of the upgraded facility resembles to a single row of a commercial plant in terms of nominal power and mass flow rate (INDITEP; 2005). Research on different components required for the operation of DSG plants were performed within the framework of this project. More specifically, new concepts of compact steam separators were tested for improving the system performance in recirculation mode (Malayeri et al.; 2004).

The last upgrade came with the **DUKE** joint project through which DLR, Solarlite GmbH and CIEMAT collaborated from May 2011 to April 2014 (Feldhoff et al.; 2014). Three Solarlite collectors (SL4600+) were added with a lower aperture area (4.6 m of aperture width) than the already-installed collectors. Two of them were installed in the preheating section of the facility (collectors #0A and #0B in Fig. 1.6) whereas a third collector (100 m long) was placed in the superheating section of the facility (collector #12). The current configuration allows reaching higher superheated steam temperatures and pressure (up to 500 °C at 110 bar) and a total thermal power of about 3 MW_{th}. In addition, all the absorbers were replaced by new SCHOTT PTR-70-DSG receivers whose absorber wall is thinner ($R_{si} = 29.5$ mm and $R_{so} = 35$ mm),

and made of stainless steel (AISI 321). New receivers have 6 Type-K thermocouples (Class I) in order to measure temperature distribution around the absorber wall.

1.6 Modeling approaches of DSG in linear focusing systems

Deployment of solar thermal technology relies on simulation capabilities able to prove that new concepts are feasible on a practical basis and form a commercial perspective. The very first step in any development process should be to apply numerical modeling techniques prior to the experimental stage (Rabl; 1985). Numerical results could provide key information about how to plan the experimental research or for making a decision to dismiss it. The simulation of existing CSP systems could also give new insights of how its performance can be improved. As in any CSP system, two main approaches should be addressed: optical and thermal modeling. Optical models simulate how solar radiation is concentrated by means of reflectors (or concentrators) and how refraction (i.e. glass cover of the absorber tube) affects the direction of rays before reaching the absorber surface. The results of the first approach provide the distribution of concentrated solar radiation on the absorber. This information is required to set the boundary conditions in the thermal problem. For the sake of simplicity, both models can be decoupled provided that optical properties of materials (i.e. reflectivity and refraction index) are not strongly dependent on temperature. This approximation lets both models run independently without having to iterate successive approximations to the solution. This aspect is crucial when the computation cost is remarkable and when overall full year's performance of the system is under study. In such case, full year's meteorological data is required in order to assess a representative approximation of the system performance during its lifespan. This meteorological data usually consists of Direct Solar Irradiance (DNI), ambient temperature and wind speed. All this information can be gathered in a Typical Meteorological Year (TMY) by averaging time series for several years (Cebecauer and Suri; 2015)

The knowledge of all the governing equations taking part in the simulated process, gives a deep understanding of the underlying physics. Despite being a powerful tool for research and development, it is worth it to mention that these results are not as conclusive as accurate experimental results. Not all phenomena can be represen-

ted in detail in the model, because their effect on the overall results is negligible in comparison with the complexity and computational cost required to be numerically implemented. Besides, other significant phenomena are not accurately modeled but they can be approximated by experimental correlations. It considerably eases the computation cost and simplifies numerical schemes (e.g. fluid to wall heat transfer and turbulence). In line with this, it is important to know the uncertainty margin associated to these kind of correlations so that a realistic interpretation of results can be completed (Duffie and Beckman; 1980).

1.6.1   Optical modeling

The sun is a spherical massive fusion reactor with a radius of approximately $R_\odot = 696.3 \cdot 10^6$ m (Delache; 1988) whose effective blackbody temperature is 5777 K. The outer layer of the Sun (photosphere) emits most of the energy in a continuous spectrum of radiation. As a result of the eccentric orbit of the Earth, the Sun-Earth distance varies annually following a yearly cycle whose amplitude is about 1.7% and its mean value is $d_{T\odot} = 1.495 \cdot 10^{11}$ m. Based on this mean distance and the Sun radius, it can be easily calculated that the Sun subtends at a semi angle of 4.65 mrad. From the Earth's point of view, the Sun can be seen as a disk (solar disk) whose radial distance from the sun center to the edge is this angle. Besides, the Solar Constant (1367 W/m^2) represents the mean annual power received from the sun per surface unit perpendicular to the propagation direction of radiation before entering the atmosphere (Rabl; 1985). However, the atmosphere has noticeable effects. The value of the DNI measured on the earth surface is sensibly lower than the Solar Constant. The attenuation of sun radiation through the atmosphere cannot be accurately predicted because it depends on varying weather conditions. It explains why DNI is continuously measured by **pyrheliometers**. This experimental information is of crucial importance for working out the real power entering the CSP system and it is an important input variable in any optical model. The solar disk is modified by the atmosphere in the same manner. As indicated by Ballestrín and Marzo (2012), extra-terrestrial solar radiation is attenuated by scattering and absorption by air molecules and solid or liquid aerosols. It makes it necessary to characterize experimentally how the solar power is distributed within the solar disk after passing through the atmosphere, what is also called **sunshape** in the context of solar energy applications. Provided that the center of the sun ($\theta_{ss} = 0$) provides the highest density of power, it decays gradually as sun rays come from sun regions close to the

edge ($\theta_{ss} = 4.65$ mrad). This decay is expressed in terms of relative intensity of radiation as a radial profile. The experimental characterization of this distribution by Neumann et al. (2002) is an excellent reference model of the solar sunshape. It has been obtained after 2300 measurements with a CCD camera from three different locations in Europe since 1997. A later **sunshape** model was published by Buie et al. (2003) after compiling all the available experimental data from Europe and the US. As displayed in Eq. (1.1), the result was the piecewise function, whose transition point is located at $\theta_{ss} = 4.65$ mrad,

$$\phi(\theta_{ss}) = \begin{cases} \frac{\cos(0.326 \cdot \theta_{ss})}{\cos(0.308 \cdot \theta_{ss})} & 0 \leq \theta_{ss} \leq 4.65 \, \text{mrad}, \\ e^{\kappa} \theta_{ss}^{\gamma} & \theta_{ss} > 4.65 \, \text{mrad}, \end{cases} \tag{1.1}$$

and where γ and κ are two parameters which depend on the circumsolar ratio (χ), as detailed in Eq. (1.2):

$$\begin{aligned} \gamma &= 2.2 \ln(0.52\chi)\chi^{0.43} - 0.1, \\ \kappa &= 0.9 \ln(13.5\chi)\chi^{-0.3}. \end{aligned} \tag{1.2}$$

The circumsolar ratio represents the fraction of solar power coming from the circumsolar region (or aureole around the solar disk) respect to the total power emitted by the sun. This free parameter indicates the effects of the atmospheric scattering and dispersion caused on the sunshape. Figure 1.7 depicts a comparison between the experimental characterization obtained by Neumann and the model fitted by Buie for different values of χ. The logarithmic scale makes it possible to observe the effects of χ in the sunshape tail more clearly. The higher χ is, the more fraction of energy is received from the circumsolar region.

The sunshape is a significant input of the optic problem. Note that it strongly affects the maximum concentration ratio and the intercept factor of the concentrator with evident implications on the size adopted for the absorber design.

1.6.1.1 Monte Carlo Ray Tracing method

Among all the available methods to model of the optic problem, Monte Carlo Ray Tracing (MCRT) is a stochastic method suitable for its flexibility to simulate any
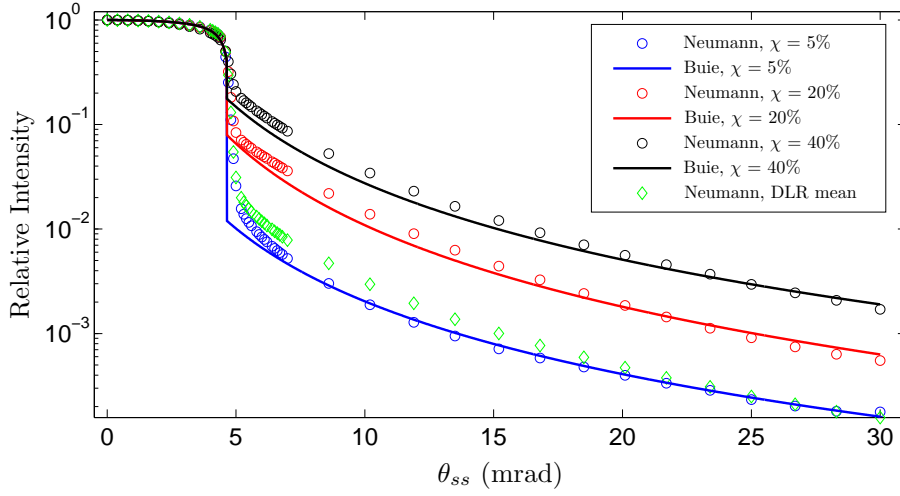
Figure 1.7: Neumann's experimental sunshape in comparison with Buie's model for three values of CSR.

geometry of reflector or absorber. According to this approach, sunlight is modeled as a bundle of discrete rays whose initial direction is obtained from the sun position at a specific moment along with the sunshape distribution. In order to reproduce the pattern of emitting power within the solar disk, the radial angle value (θ_{ss}) associated to each ray follows a particular probability distribution related to the sunshape profile: Evaluating the surface integral of the sunshape profile in spherical coordinates (see θ and φ Fig. 1.8) over the solar disk and the aureole, the cumulative distribution function displayed in Eq. (1.3) and plotted in Fig. 1.9 rules the sequence of radial angles (θ_{ss}) associated to each ray:

$$F_{ss}(\theta_{ss}) = \frac{\int_0^{2\pi} \int_0^{\theta_{ss}} \phi(\theta)\sin(\theta)d\theta d\varphi}{\int_0^{2\pi} \int_0^{\theta_{max}} \phi(\theta)\sin(\theta)d\theta d\varphi}, \tag{1.3}$$

where θ_{max} stands for the radial extent of the sun (i.e. solar disk and the whole sun aureole). As detailed in Eq. (1.4), Monte Carlo methods evaluate the inverse of the cumulative distribution function (F_{ss}^{-1}) from a uniformly distributed random[8] sequence of numbers so that $0 < \hat{\mathbf{X}} < 1$. Provided that the same amount of power is associated to each ray and the sunshape distribution is axial-symmetric, the obtained sequence of angles ($\hat{\theta}_{\mathbf{ss}}$) reproduces the sun sunshape profile. Alternative options use Monte Carlo methods to assign a particular energy to each ray according to the

---

[8]More specifically, $\hat{\mathbf{X}}$ can be generated by a pseudorandom number generator such as the *Mersenne twister* algorithm created by Matsumoto and Nishimura (1998).
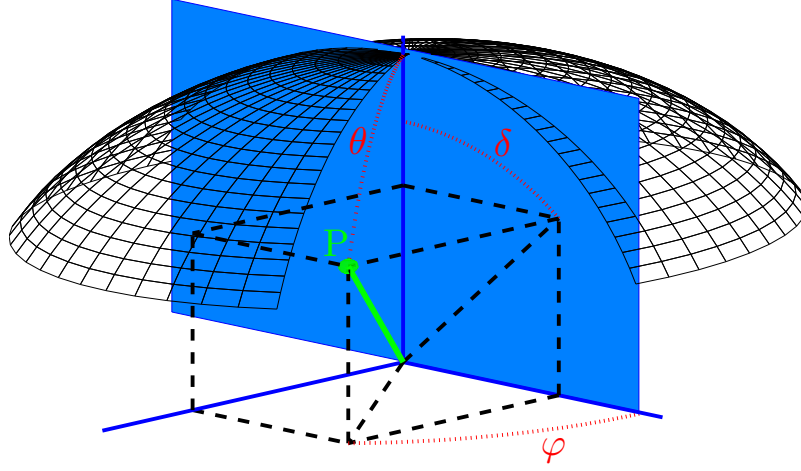
Figure 1.8: Spherical coordinates for surface integration of the sunshape profile. Part of the sphere is removed for the sake of clarity.

sunshape profile whereas the direction of all rays follows a uniform distribution.

$$F_{ss}^{-1}(\hat{\mathbf{X}}) = \hat{\theta}_{\mathbf{ss}}. \tag{1.4}$$

The set of generated rays whose initial direction have been previously calculated require a starting point. Positions are randomly generated following a uniform distribution so that the launched rays depart from points equally distributed throughout a control surface covering the entire solar field. The path of rays is modelled under the approximations assumed by geometrical optics. It means that they propagate in rectilinear direction within the air. Refraction can be applied when rays cross the air-glass interphase (i.e. glass cover of the absorber or glass layer in mirrors) applying the Snell's Law. The specular reflection law is a suitable mathematical relation to describe reflection phenomena taking place in mirrors. As detailed in Eq. (1.5), the normal vector to the mirror surface is $\vec{n}$ whereas $\vec{v}_i$ stands for the unitary vector pointing at the incoming ray direction and $\vec{v}_r$ to the respective direction of the reflected ray.

$$\vec{v}_r = 2\left(\vec{v}_i \cdot \vec{n}\right)\vec{n} - \vec{v}_i. \tag{1.5}$$

However, small-scale slope errors that affect the mirror specularity, alongside miscellaneous errors related to the reflector geometry, penalize the optical performance
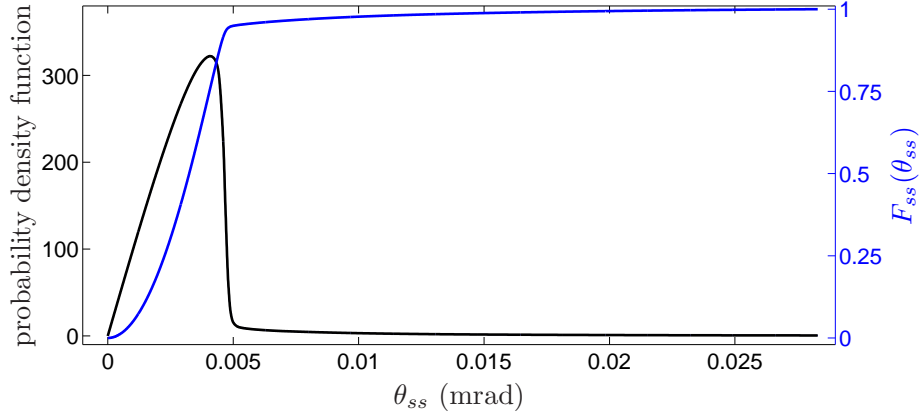
Figure 1.9: Probability density function (black line in the left axis) and cumulative distribution function $F_{ss}(\theta_{ss})$ used to generate the sequence of sun rays from the Neumann's (DLR mean) sunshape.

of the system (Güven and Bannerot; 1986). To model this phenomena the normal vector to the mirror surface can be deviated according to stochastic methods. The most usual approach consists of modeling this deviation according to a gaussian distribution with null mean value ($\mu_{er} = 0$) and a characteristic σ_{er} standard deviation. In line with this, the normal vector can be deviated a radial angle θ_{er}. To get the cumulative distribution function which rules the statistic distribution of θ_{er}, the gaussian density function is integrated in spherical coordinates where it is necessary to assume that $\sin(\theta_{er}) \approx \theta_{er}$ for small values of θ_{er} to get Eq. (1.6):

$$F_{er}(\theta_{er}) = \frac{\int_0^{\theta_{er}} \theta \cdot e^{-\frac{\theta^2}{2\sigma_{er}^2}} d\theta}{\int_0^{\theta_{max,er}} \theta \cdot e^{-\frac{\theta^2}{2\sigma_{er}^2}} d\theta} = 1 - e^{-\frac{\theta_{er}^2}{2\sigma_{er}^2}}, \tag{1.6}$$

in such a way that $\theta_{max,er}$ is the upper limit of the radial angle so that $\theta_{max,er} >> \sigma_{er}$ and where the gaussian function is virtually zero. The analytical solution of the integral makes it possible to easily get Eq. (1.7), from which the sequence of radial deviations applied to each normal vector ($\hat{\theta}_{\mathbf{er}}$) can be calculated directly:

$$\hat{\theta}_{\mathbf{er}} = F_{er}^{-1}(\hat{\mathbf{X}}) = \sqrt{-2\sigma_{er}^2 \ln(1 - \hat{\mathbf{X}})}. \tag{1.7}$$

As previously mentioned, the trajectory of the reflected rays towards the absorber can be simplified as straight lines. The distance followed by them is relevant at the time of evaluating the effects of atmospheric extinction. As reported by Han-

rieder et al. (2017), atmospheric extinction is primarily caused by aerosol particles and water vapor which scatter and absorb solar radiation. Mean distance between the reflector and the absorber strongly conditions this phenomenon. In solar tower systems, where outer heliostats can be more than one kilometre far from the central receiver, atmospheric extinction should be taken into account. On the contrary, the mean distance between the concentrator and the absorber in linear focusing systems does not exceed several meters. As a result, atmospheric extinction can be neglected in this sort of systems. Intersection of reflected beams with the glass cover and the absorber tube can be addressed solving the corresponding system of equations. The model of the cross sectional geometry of the absorber is relevant in terms of algorithm performance. In case of using analytic expressions, the intersections points can be worked out efficiently if the suitable local coordinate system for the absorber is selected. The final concentrated flux profile is obtained after calculating the histogram of the intersection points in the absorber tube surface. Following the already-described MCRT method, an in-house 3D optical model of a LS-3 parabolic-trough collector has been implemented in **paper I**. Based on the Neumann's (DLR mean) sunshape profile and applying a gaussian distribution for modeling non-specular effects on the mirror surface, the concentrated flux profile has been worked out to be used as the boundary condition for the 3D thermal problem. Alternatively, Tonatiuh ray tracing software (Blanco et al.; 2009) has been employed to calculate the flux profile for the thermal-hydraulic problem in **paper IV**.

Most of the issues concerning optical performance in parabolic-trough collectors can be studied by simplified two-dimensional models. It means that rays' path is exclusively traced within the plane perpendicular to absorber axis (i.e. plane showed in Fig. 1.2). This enables faster algorithms suitable for optimization purposes but turning the algorithm into a two-dimensional scenario implies some non-trivial considerations. Besides the evident simplification of the straight line equations which model the ray's trajectory, the integration of the sunshape profile requires some changes. The angle representing the radial dimension of the sunshape (θ) should be projected onto the plane of interest (blue plane in Fig. 1.8) where the ray tracing is performed. In line with this, a new radial angle (δ) is defined onto it (see Fig. 1.8) bounded by $-\theta_{max} \leq \delta \leq \theta_{max}$. The corresponding cumulative distribution function $F_{ss}(\delta_{ss})$ is obtained after applying the change of variable in Eq. (1.8) to Eq. (1.3).

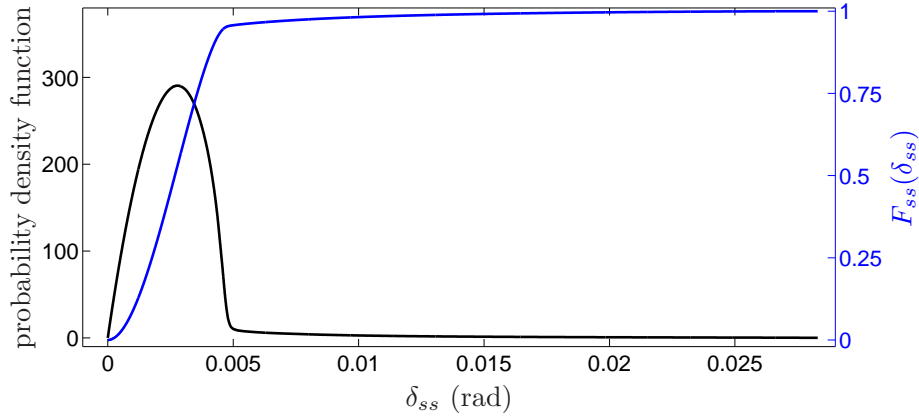$$\delta = \arctan\left[\tan(\theta)\cos(\varphi)\right]. \tag{1.8}$$

Figure 1.10: Probability density function (black line in the left axis) and cumulative distribution function $F_{ss}(\delta_{ss})$ (blue line in the right axis) used to generate the sequence of sun rays from the Neumann's (DLR mean) sunshape in 2D Ray-Tracing algorithm.

As in the 3D case, the value of $F_{ss}(\delta_0)$ stands for the fraction energy emitted by the solar disk which is enclosed within the range $0 < \delta < \delta_0$. The resulting density function and cumulative distribution function are displayed in Fig. 1.10 where some slight differences can be observed with respect to the corresponding distribution in the 3D case. An analogous transformation should be applied for the gaussian distribution ruling the non-specular effects in the reflector surface. All these changes enable to get the concentrated flux profile around the absorber at a representative section provided that the angle of incidence is null. If it is not the case, some additional changes should be applied to take it into account[9]. These results are valid for most of the length of the absorber, with the exception of the edges where the absorber may not receive concentrated radiation.

The 2D MCRT method is the underlying theme to understanding how the inverse MCRT method described in **paper II** and **III** works. The central objective of ray tracing algorithms is to study how solar radiation is concentrated on the absorber. The occurring phenomena is analyzed given predefined solar conditions (specific sun position and atmospheric conditions) as well as the specifications of the elements interacting has to be predefined (i.e. concentrator and absorber geometry). This analytic approach can be replaced by an inverse approach from which the objective of the problem is no longer to calculate the concentrated flux profile, but instead the reflector geometry to get a predefined flux profile.

---

[9]Note that if the angle of incidence is not zero, entering rays are not normal to the aperture plane of the collector and the real trajectory of rays is longer than the one calculated in the 2D plane.

1.6.1.2   Alternative methods

Monte Carlo Ray Tracing is the most widespread method to model the optical performance of CSP systems. Despite its high computing cost, if the algorithm code is implemented efficiently, results can be obtained at an affordable time and computing cost. More specifically, according to the nature of the type of algorithm, it can be fully parallelized enabling scalable codes working in parallel threads regardless of memory limitations. According to that, equivalent problems can be superimposed to increase the results quality. Despite the aforementioned advantages, some alternative tools to MCRT are also available. Analytic approaches are a suitable option when a classic problem is being addressed. This is the case of simple examples of parabolic reflector geometries when some ideal conditions and simplifications are assumed (Hassan and El-Refaie; 1973). This approach was usual in the 1970s and 1980s, when computational resources were limited and rough estimations of intensity peaks in flux profiles on absorbers were necessary. These kind of studies were used to assume uniform radiation intensity on the solar disk along with perfect specular reflection on mirrors. Not only cylindrical absorbers were analyzed but also flat absorbers were studied (Evans; 1977) not to mention other types of concentration systems such as solar furnace (Jose; 1957).

New approaches have recently being published. This is the case of the Finite-Volume ray tracing proposed and described by Craig et al. (2016). However, a previous related study was published by Martinek and Weimer (2013). This technique uses CFD tools to solve the radiative transfer equation by means of the finite volume methods. This enables a perfect coupling of the thermal and optical problem within the same code or software package (e.g. ANSYS Fluent), especially convenient if optical properties are strongly dependent on temperature, like thermal emittance or absorptance. In contrast, the results accuracy may be negatively affected by *false scattering* which consists of a diffusive numerical error related to the spatial discretization used by the Finite-Volume method, requiring a fine mesh. As a results the computing cost associated to this technique make it less cost-effective than MCRT.

1.6.2   Thermal modeling

Conjugate heat transfer process in concentrated solar thermal receivers is the most complex issue addressed when modeling DSG systems. Since it is linear, the

heat equation can be analytically solved without trouble in many cases. However, under some circumstances and some types of boundary conditions, 3D problem is preferably handled numerically for reproducing the temperature distribution in the absorber tube wall. Apart from the usual numerical methods to solve this kind of partial differential equation, such as finite differences or finite elements method, further work is still needed to implement faster ways to ease the computational cost of thermal behaviour in the solid domain. Some semi-analytical approaches may fit for such purpose. On top of that, most of the complexity of the conjugate heat transfer process relies on the heat transfer mechanisms in the fluid domain, in particular for two-phase flow systems. As explained in the introduction of **paper IV**, this issue has major implications on a wide variety of thermal power stations where water is used as heat transfer fluid. Nuclear industry has focused on developing realistic and affordable codes for prediction of system transients and for nuclear safety analysis since the 1950s. Significant progress made in computing power over the last decades of the 20th century has changed the way that numerical models handle heat transfer in two-phase flow. From the 1D Homogeneous Equilibrium Model (HEM) to 3D CFD codes, there are a number of possibilities. The selection of the suitable tool depends on the level of accuracy required to reproduce flow patterns and the computing available time. It is worth it to mention that DSG systems based on linear focus collectors are compiled of kilometres of absorber pipes. It means a vast domain to be solved and therefore, CFD is currently a good option only when studying local phenomena which can be reproduced within a small fraction of fluid domain. For instance, severe slugging can be studied simulating two adjacent collectors including the interconnection pipe between them (see **paper IV** for further details). According to custom concept of DSG plants under study, 1D models are the only feasible option to study the transient behaviour of the whole plant for long periods of time.

1.6.2.1 One-dimensional models: single phase flow

Depending on the operation mode or system configuration, both single phase and two-phase flow may take place along the absorber tube. Despite not representing the most complex aspect of the system modeling, single phase flow is still of research interest in the CSP context. In line with this, **Paper I** presents a new in-house model for calculating the 3D steady-state temperature distribution of the absorber tube wall and the glass cover along with a 1D approach of the single phase fluid flow (see Fig. 1.11). To accomplish that, the fluid spatial description is function of the axial co-
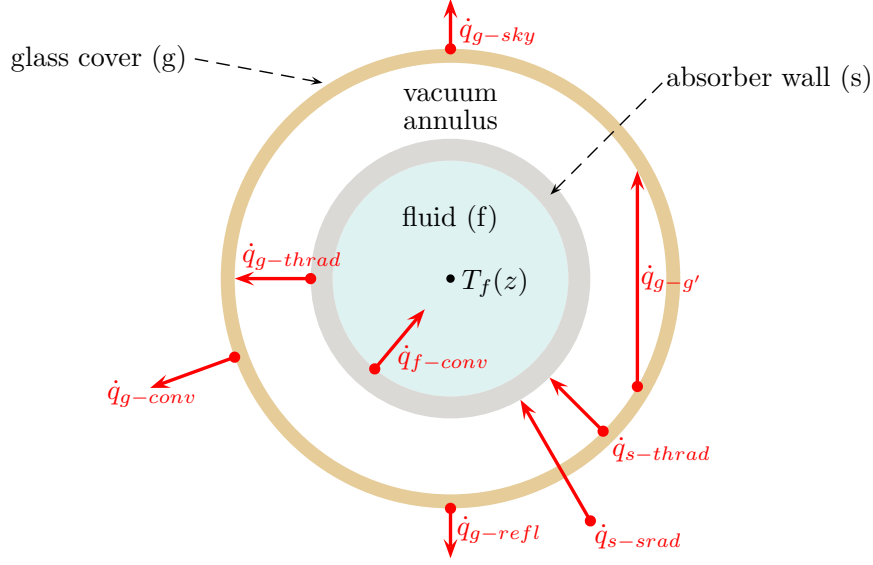
Figure 1.11: Cross-sectional view and representation of the most relevant heat transfer terms in the single phase flow model.

ordinate (z in consistency with **Paper I** notation) so that $T_f(z)$ stands for the average of bulk fluid temperature of the whole cross-sectional area at this axial location. Heat transfer between the absorber tube and the heat transfer fluid is locally-defined for each node of the absorber inner wall ($\dot{q}_{f-conv}$). Mass flow rate at usual operation conditions, guarantee turbulent flow. Otherwise, if laminar flow would take place, the lack of turbulence would significantly reduce refrigeration of the absorber wall increasing considerably its temperature. According to that, *Gnielinski* experimental correlation (Gnielinski; 1976) is used because it is suitable for both transition region ($2300 < Re < 10^4$) as well as for fully developed turbulent regime where the *Pethukov* correlation (Petukhov; 1970) is also valid. Heat transfer correlation is evaluated as a function of the temperature difference between the local temperature of the inner surface of the absorber and the bulk fluid temperature at the same axial location. This approximation makes it possible to couple the 1D approach assumed for the fluid domain with the 3D mesh of the solid domain. The latter, consists of a numerical resolution of the 3D heat equation preferably in cylindrical coordinates on these meshes.

Special attention has to be paid to the radiative heat transfer which takes place through the vacuum annulus. Perfect vacuum is assumed, so convective heat transfer can be neglected. The azimuthal and axial distribution of temperature is taken into account to model the radiative heat transfer from the inner face of the glass cover to the steel absorber ($\dot{q}_{s-thrad}$) and vice versa ($\dot{q}_{g-thrad}$). As a concave surface, ra-

diative exchange between different parts of the inner face of the glass cover has to be included ($\dot{q}_{g-g'}$). The concentrated solar radiation ($\dot{q}_{s-srad}$) passes through the glass cover generating a heat source term to be regarded in the heat equation of the glass cover domain and finally impinges in the outer absorber wall. Similarly, all the heat exchange terms taking place at the glass cover outer boundary are included: convective heat transfer ($\dot{q}_{g-conv}$), and radiative exchange from the glass cover to the sky ($\dot{q}_{g-sky}$) and the reflector surface ($\dot{q}_{g-refl}$).

1.6.2.2 One-dimensional models: two-phase flow

The existence of a significant two-phase flow region in any solar DSG system based on linear focus absorbers, makes its modeling a crucial challenge for the development of this technology. As previously mentioned, the vast fluid domain existing in DSG plants proves the need of fast and reliable codes. According to the current computing resources available, one-dimensional approaches are the only affordable concept to address full scale plant simulations under a wide range of circumstances in transient conditions. The simplest formulation for two-phase flow is the Homogeneous Equilibrium Model (HEM) displayed in Eq. 1.9 for a duct titled an angle θ_{tilt}, where gravitational effects (g) have also been taken into account:

$$\frac{\partial \rho}{\partial t} + \frac{\partial G}{\partial z} = 0, \tag{1.9a}$$

$$\frac{\partial G}{\partial t} + \frac{\partial}{\partial z}\left[\frac{G^2}{\rho_m}\right] + \frac{\partial p_{fric}}{\partial z} + \rho g \sin\left(\theta_{tilt}\right) + \frac{\partial p}{\partial z} = 0, \tag{1.9b}$$

$$\rho \frac{\partial h}{\partial t} + G \frac{\partial h}{\partial z} = Q, \tag{1.9c}$$

$$x = \frac{h - h_l}{h_g - h_l}, \tag{1.9d}$$

$$\alpha = \frac{x}{x + (1-x)\frac{\rho_g}{\rho_l}}, \tag{1.9e}$$

$$\rho = \alpha \rho_g + (1-\alpha)\rho_l. \tag{1.9f}$$

The two-phase flow is assumed as an homogeneous mixture in thermal equilibrium where no relative velocity is considered (drift velocity is zero, $v_l = v_g$) between both

phases. As a consequence, the relation between the void fraction (α) and the two-phase flow mixture (x) is as simple as showed in Eq. (1.9e), where pressure (p) is supposed to be the same for each phase. Flow conditions are presented in terms of mixture quantities. This is the case of the mass flux (G) and mixture enthalpy (h) which are defined in Eq. (1.10) and mixture density (ρ) based on phase quantities:

$$G = \alpha \rho_g v_g + (1 - \alpha)\rho_l v_l, \tag{1.10a}$$

$$h = x h_g + (1 - x)h_l. \tag{1.10b}$$

Phase thermodynamic properties at saturation conditions can be obtained from the corresponding thermodynamic state equations for water, e.g. IAPWS-IF97 formulation by Wagner and Kruse (1998), which depends on pressure: $\rho_g(p)$, $\rho_l(p)$, $h_g(p)$, $h_l(p)$. Term $\partial p_{fric}/\partial z$ comes from the corresponding constitutive relation indicating the frictional pressure drop based on empirical correlations, and ρ_m is defined in Eq. (1.11):

$$\frac{1}{\rho_m} = \frac{x^2}{\rho_g \alpha} + \frac{(1 - x)^2}{\rho_l(1 - \alpha)}. \tag{1.11}$$

The HEM model has been thoroughly applied in the DSG context by means of software packages like Dymola/Modelica (Bonilla et al.; 2012; Feldhoff et al.; 2015) or TRNSYS (Biencinto et al.; 2016) or even using in-house codes. However, as a consequence of some of the simplifications assumed, this model does not accurately reproduce some of the phenomena which characterizes transient thermal hydraulic behaviour of two-phase flow. Models based on drift-flux correlations bring a step forward because relative velocity between both phases is allowed. A semi-empirical correlation based on a linear function between the phase steam velocity (v_g) and the volumetric flux of the two-phase mixture (v) was proposed by Zuber and Findlay (1965), as detailed in Eq. (1.12):

$$v = \alpha\, v_g + (1 - \alpha)\, v_l, \tag{1.12a}$$

$$v_g = C_0\, v + u_{df}. \tag{1.12b}$$

Where C_0 is the distribution parameter whereas u_{df} stands for the drift velocity. They are usually calculated as a function of the void fraction (α) by means of the corresponding semi-empirical correlation which should take into account the pipe tilt, among other factors. This approach was applied to perform nuclear reactor safety analysis (Manera et al.; 2005; Rohde; 1986)[10] based on a wide rage of drift-flux correlations. This assumption implies some modifications and additional terms in the HEM formulation, Eqs. (1.9):

$$\frac{\partial \rho}{\partial t} + \frac{\partial G}{\partial z} = 0, \tag{1.13a}$$

$$\frac{\partial G}{\partial t} + \frac{\partial}{\partial z}\left[\frac{G^2}{\rho_m}\right] + \frac{\partial p_{fric}}{\partial z} + \rho g \sin\left(\theta_{tilt}\right) + \frac{\partial p}{\partial z} = 0, \tag{1.13b}$$

$$\rho \frac{\partial h}{\partial t} + G\frac{\partial h}{\partial z} = Q + \frac{\partial \chi}{\partial t}, \tag{1.13c}$$

$$x = \frac{h - h_l}{h_g - h_l}, \tag{1.13d}$$

$$\alpha = \frac{x}{\left[x + (1-x)\frac{\rho_g}{\rho_l}\right]C_0 + \frac{u_{df}}{G}}, \tag{1.13e}$$

$$\rho = \alpha\rho_g + (1-\alpha)\rho_l. \tag{1.13f}$$

where a source term has been added to the mixture energy balance:

$$\chi = (h_g - h_l)\left[(1-\alpha)x\rho_l - \alpha(1-x)\rho_g\right]. \tag{1.14}$$
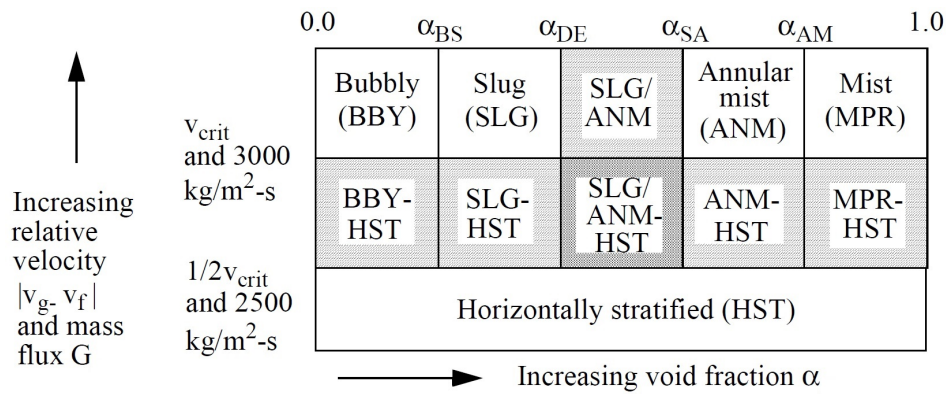
In case that subcooled boiling takes place, an independent steam-phase mass balance should replace Eq. (1.13d), where a new condensation/evaporation rate should be defined by means of a new correlation, e.g. Kelly and Kazimi (1982). The drift-flux correlation approach, has the advantage of giving trustworthy results provided that the drift-flux correlation fits the existing flow conditions. With only three field equations and the corresponding correlations along with constitutive equations, the model can reproduce the thermal-hydraulic behaviour of a DSG plant, where flashing and severe slugging may be reproduced.

---

[10]FLOCAL code was developed to study transients of natural circulation Boiling Water Reactors. This is the case of the AST-500 which was a Soviet design of district reactor. The work published by Manera et al. (2005) used this code to study flashing induced instabilities.

Commercial codes like RELAP5 (RELAP5/MOD3.3; 2001), TRACE, ATHLET or CATHARE (Bestion; 1990), belong to a family of more complex models with 6 field equations: Mass balance, momentum balance and energy balance are considered for each phase. These are two-fluid models where different velocities, densities and temperatures are considered for each phase, with the exception of pressure which keeps being the same for both phases (see section 2 of **paper IV** for further details). This family of codes requires more computational resources than the HEM or drift-flux models. In addition, some numerical issues have to be solved, and quite efficient numerical schemes have been developed in the last decades by the nuclear industry seeking fast codes in custom computers. Unlike in the drift-flux case, where phase movements should be highly correlated (i.e. bubbly and slug flows), two-fluid models can reproduce flow when interaction between phases is less intense, (e.g. stratified flow) where phasic velocities can be fully independent (Morin; 2012). Despite the fact that a drift-flux correlation is no longer required, a set of additional constitutive relations are needed, especially those describing the transfer of mass, momentum and energy through the interfacial surface, e.g. interface friction drag. Wall friction is also regarded for each phase by means of the corresponding phasic correlation, whereas evaporation rate is also modelled by means of empirical functions.

Flow regime maps are a key element to figure out the existing flow regime based on two flow variables: The approach used by RELAP5/MOD3.3 (2001) maps the flow regimes chart through the void fraction (α) and the relative velocity between phases $|v_g - v_f|$ (see Fig. 1.12). The flow regime selected is of significant importance at the time of selecting the appropriate correlation to evaluate the right heat transfer coefficient between the pipe wall and the fluid or other constitutive equations. The distribution of the flow regime map strongly depends on the pipe tilt. As previously noted, RELAP5/MOD3.3 (2001) uses a two-dimensional map for quasi-horizontal ducts ($0° \leq \theta_{tilt} \leq 45°$). However quasi-vertical flow ($45° < \theta_{tilt} \leq 90°$), where buoyancy effects are relevant, requires an additional third variable to map the flow regime chart: void fraction (α), volumetric flux of the two-phase mixture (u instead of $|v_g - v_f|$) and the temperature difference between the steam-phase temperature and saturation temperature ($T_g - T_{sat}$), which describes the boiling regime. Special attention has to be paid to transitions between adjacent flow regimes within the map, where numerical issues may arise if proper smoothing or interpolation techniques are not applied.

0.0	α_{BS}	α_{DE}	α_{SA}	α_{AM}	1.0

v_{crit} and 3000 kg/m²-s

Increasing relative velocity $|v_g\text{-} v_f|$ and mass flux G

1/2v_{crit} and 2500 kg/m²-s

Bubbly (BBY)	Slug (SLG)	SLG/ANM	Annular mist (ANM)	Mist (MPR)
BBY-HST	SLG-HST	SLG/ANM-HST	ANM-HST	MPR-HST
Horizontally stratified (HST)				

Increasing void fraction α

(a) Horizontal flow regime map of RELAP5. Adaptation of map extracted from (RELAP5/MOD3.3; 2001)
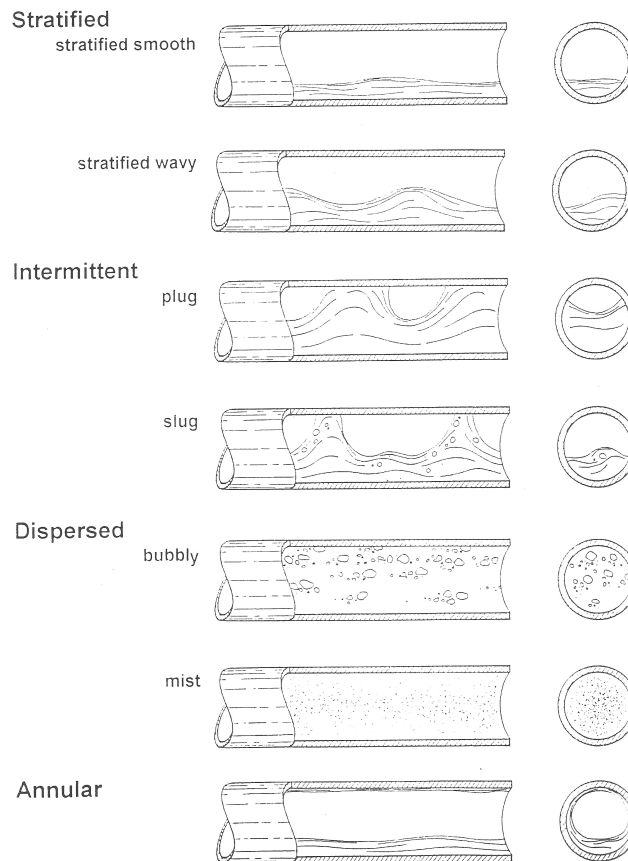
(b) Comon flow patterns in horizontal pipes with two-phase flow. Adaptation of illustration extracted from Müller et al. (1994)

Figure 1.12: Flow regime map for two-phase flow in horizontal pipes.

Table 1.6: Independent unknowns in the CFD model by Hernández-Lobón (2014).

ρ_l	$\rho_l v_{lx}$	$\rho_l v_{ly}$	$\rho_l v_{lz}$	$e\rho_l$		
ρ_g	$\rho_g v_{gx}$	$\rho_g v_{gy}$	$\rho_g v_{gz}$	$e\rho_g$	p	T

1.6.2.3 CFD models applied for solar DSG

There are several examples of use of CFD commercial packages into DSG applications in literature. One of the most representative is the work carried out by Hernández-Lobón (2014) using the commercial software package STAR-CCM+. This 3D model hardly requires empirical correlations because most of terms in the equations are included in the numerical resolution. Reynolds-averaged Navier-Stokes (RANS) approach has been applied to take into account turbulence effects by means of the k-ε model. Only large scale turbulent eddies are simulated by Navier-Stokes equations so that two additional models have to be added in order to include the convection and diffusion of turbulent energy. Thermal equilibrium is assumed in each differential volume for both phases sharing the same value of pressure (p), energy (e) and temperature (T), whereas individual velocities are taken into account for each phase. According to that, 12 independent variables have to be solved (see table 1.6). A total of 10 balance equations are yielded. It means that one additional thermodynamic state equation plus an additional transport equation have to be included. A semi-empirical approach has also been selected to model surface boiling at the inner face of the absorber tube using the Rohsenow (1952) correlation. This correlation has been thoroughly validated, reducing the computing overhead of the system versus other mechanistic models (Lobón et al.; 2014). Despite the fact that the heat equation is solved within the solid domain (absorber tube wall) the thermal insulation by the vacuum annulus and the glass cover has been included through additional heat loss correlations elaborated from experimental data collected at the DISS facility, as well as the concentrated flux distribution is introduced as a fix boundary condition. One of the main contributions of such model is to reproduce flow conditions in the connection pipes, where vertical and horizontal sections are alternatively connected.

2 OBJECTIVES

The main objective of this thesis, is to develop and test new modeling tools for the simulation of solar Direct Steam Generation in linear focus systems as well as the optimization of future designs of Parabolic-Trough Collectors (PTCs). Both thermal and optical models are within the scope of this work. The development and implementation of such models is not the only goal, but also their validation is needed by means of the experimental data obtained from the DISS facility located at Plataforma Solar de Almería. In this context, the chance of arranging experimental campaigns in this facility makes it possible to obtain empirical correlations to evaluate some equation terms that cannot be modeled at an affordable computing cost. A deep understanding of all terms in the governing equations provides a precise knowledge of the underlying physics phenomena taking part in such systems. As a consequence, new strategies and designs can be proposed to improve the overall efficiency and prolong the lifespan of DSG systems. According to the aforementioned general objectives, specific goals of the present thesis are listed:

1. Optical modeling:

   (a) Development of an in-house Monte Carlo Ray Tracing 3D code. Simulation of the LS-3 PTC design (**Paper I**).

   (b) Development of an in-house Monte Carlo Ray Tracing 2D code (**Paper II**).

   (c) Development of a method to design new reflector geometries to homogen-

71

ize the concentrated flux profile around absorber tubes of PTCs (IMCRT method in **Paper II** and **Paper III**).

2. Thermal-hydraulics and thermal modeling:

   (a) Development of an in-house code for DSG purposes where single-phase fluid domain is modeled following one-dimensional approach, whereas heat equation is studied in a three-dimensional domain, including the absorber tube, the glass cover and radiative heat exchange through the vacuum annulus (**Paper I**).

   (b) Implementation of a realistic and detailed model of the DISS facility using a two-fluid model (i.e. RELAP5) to be validated where connection pipes are included. Validation in transient conditions (**Paper IV**).

   (c) Numerical study of the severe slugging phenomena in the connection pipes using RELAP5 (**Paper IV**).

3. Experimental research:

   (a) Plan and performance of a complete test campaign in the DISS facility to validate the proposed thermal models (**Paper I** and **Paper IV**).

   (b) Experimental characterization of the heat losses taking place in the receivers of the DISS facility to evaluate real heat losses after two years and a half of operation of new receiver tubes installed in the system (**Paper IV**).

3 RESULTS OUTLINE

The aim of this chapter is to outline the most relevant results presented in the four papers after the work carried out in this thesis. They are arranged according to the classification of objectives detailed in chapter 2, as well as it is explained how the scope of all papers and their results are related to the main topic of this dissertation.

3.1 Optical modeling results

An in-house 3D Monte Carlo Ray Tracing code has been implemented to calculate the concentrated solar flux distribution onto the absorber in a LS-3 PTC collector by means of Matlab® (see **paper I**). The DLR mean sunshape profile by Neumann et al. (2002) was used alongside a gaussian distribution with a standard deviation of 1 mrad was set to model angular deviation of normal vectors to the reflector surface (non-specular reflection), where temperature-independent optical properties were considered. A new conic eccentricity parameter (ξ) was included to model the bulk reflector deformation due to structural bending, from which the parabola turns into a hyperbola, taking into account a slight aperture of the reflector brackets due to the mirrors weight. Provided that all curves obtained should have the same arc length, the conic eccentricity determines the intensity of such bending (see Fig. 3.1) according to Eq. (3.1). Results provided in this work correspond to a slight deviation of the LS-3 parabola into a hyperbola ($\xi = 1 - 5 \cdot 10^{-5}$), where focal distance is $f_c = 1.71$ m.
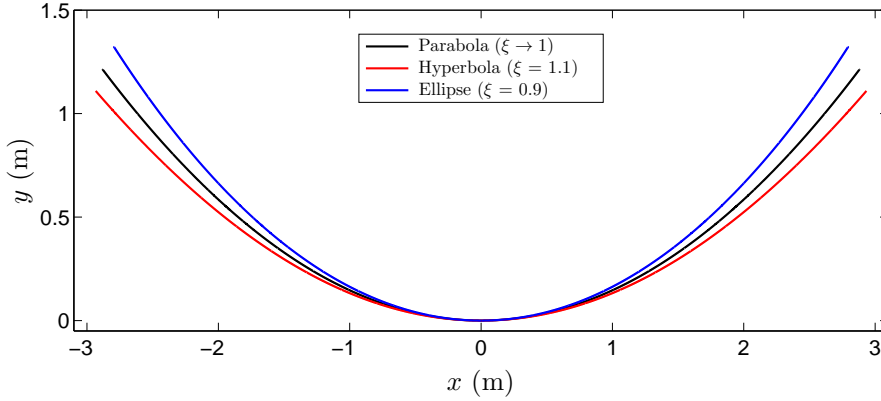
Figure 3.1: Conics to represent (magnified) structural bending of the LS-3 reflector profile from Eq. (3.1) as a function of the conic eccentricity (ξ).

$$y = \frac{\xi}{1 - \xi^2} \left[2f_c - \left(4f_c^2 + x^2 \left(1 - \xi^{-2} \right) \right)^{1/2} \right]. \tag{3.1}$$

Similarly, results also show how thermal bending taking place in the absorber tube affects the flux distribution on it. For that purpose, the longitudinal axis along the absorber is assumed to describe a sinusoidal curve, whose maximum amplitude is a fraction of the gap between the absorber and the glass cover ($\zeta = 0.1$). The reflector surface has not been considered as a continuous surface but gaps between adjacent facets have been included, creating slight shadows in the flux distribution, and besides, gaps between adjacent modules have been taken into account (0.35 m). Results of this MCRT algorithm show the relevance of all the above mentioned factors to work out a realistic distribution of the entire surface of the absorber tube. Special information is provided concerning the radiation shadow at the tube initial edge, as a consequence of gaps between modules when the angle of incidence is positive. It definitely modifies the axial evolution of the fluid temperature at the module inlet. The effects of the absorber thermal bending are described, so that the flux profile broadens just like the maximum flux value decreases in the bended sections since the center of the absorber is displaced from the focal point. It means that thermal bending could have a positive effect smoothing the flux profile around the absorber tube, provided that it does not overtake a certain threshold. Additional conclusions can be drawn in light the computing time required to run the proposed in-house code, where the element-wise arithmetic operations existing in Matlab® enables efficient implementation of ray tracing algorithms.

The execution of 3D ray tracing codes implies the resolution of the trajectory

(a) Pillbox sunshape (max. angle 4.65 mrad) for both cases

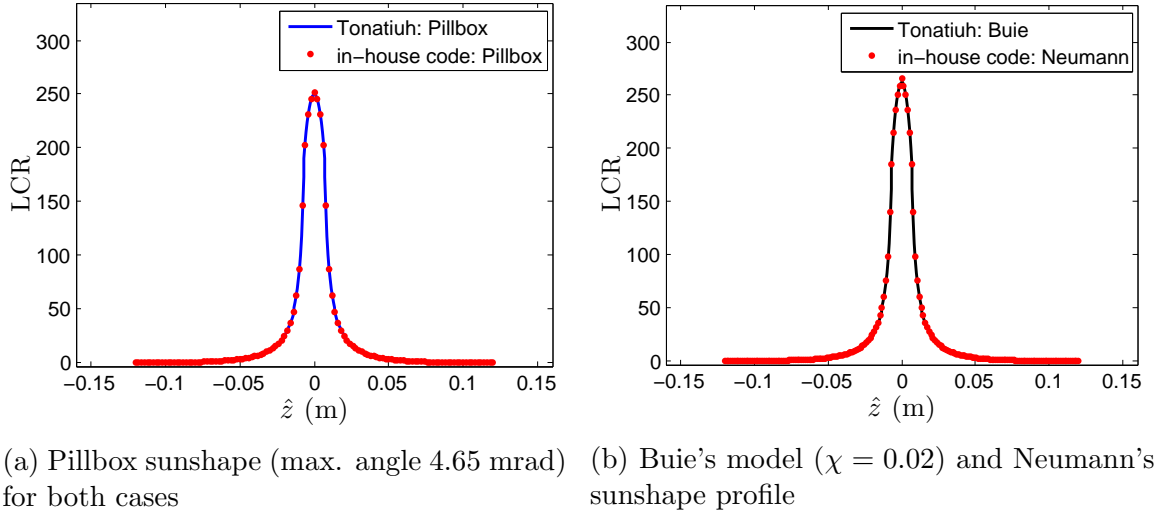(b) Buie's model ($\chi = 0.02$) and Neumann's sunshape profile

Figure 3.2: Validation of the 2D in-house MCRT code with Tonatiuh for a LS-3 reflector concentrating radiation on a flat absorber located at the focal point. Local Concentration Ratio (LCR) vs $\hat{z}$, which stands for the local coordinate laid along the width of the absorber whose origin is in the focal point, i.e. absorber center. Extracted from **paper II**.

of rays entering into the whole aperture plane of the collector, where the axial length is significantly higher than the collector width. The resolution of the full problem is only justified when a detailed description of the axial evolution of the flux profile is needed. Note that most of the length of the absorber is under the same pattern of angular flux distribution and only absorber edges significantly differ from this general pattern. Since the problem is reduced to a specific cross sectional plane, 2D ray tracing models ease considerably the computing cost, from which the general pattern of concentrated flux distribution around the absorber tube is yielded. To implement such 2D code, the concentrated sunshape profile has to be projected onto the cross-sectional plane as explained in section 1.6.1.1. A new in-house 2D MCRT code has also been implemented in Matlab® and validated from the results obtained by Tonatiuh (Blanco et al.; 2009). To check that, a specular parabolic LS-3 reflector is considered with a flat receiver whose center is placed at the focal point of the parabola. This is a suitable geometry to accomplish the validation, because flux intensity peaks are higher respect to other receivers not intercepting rays at the focal point (e.g. absorber tubes). The higher the maximum intensity is, the more evident any difference between the flux profiles is. As depicted in Fig. 3.2, the 2D in-house code accurately reproduces the results supplied by Tonatiuh.

The distribution of concentrated solar radiation on the absorber surface is an

issue of key interest in DSG applications. The existence of two-phase flow may induce several thermal gradients and the subsequent thermal bending in the absorber. Any effort to prevent substantial bends is helpful to avoid receiver failure and to extend lifespan of DSG systems.

The inverse Monte Carlo Ray Tracing method (IMCRT) is a new method proposed and developed within the framework of this thesis. It fundamentally consists of two stages which should be run sequentially with the aim of obtaining a two-dimensional reflector geometry (numerically defined) so that a specific concentrated flux profile (objective profile) can be attained for a given geometry of absorber:

- The IMCRT method is compiled of a first stage which proceeds straightforward solving a sequence of non-linear algebraic systems of equations. The reflector geometry is reduced to a sequence of differential segments defined by a row of points in a two-dimensional space. The solution of each system of equations provides the two-dimensional coordinates of each new point of the sequence defining the reflector geometry. The first stage's solution could be valid in the event that Sun would be a point source, but actually its extent makes that not all rays enter into the mirror surface following the same direction and the real concentrated flux profile achieved is not identical to the objective one. This fact justifies the need of a second stage.

- The second stage in the IMCRT method intends to correct or tweak the reflector geometry provided by the first stage, so that, after considering the sunshape, the real concentrated flux profile is as close as possible to the objective one. In light of results, it can be concluded that the computing cost of the second stage is higher than the first one from afar. Note that the second stage is an iterative algorithm that solves the 2D MCRT problem for each tweak applied to the reflector geometry until the optimum geometry is reached.

The aforementioned 2D in-house MCRT code is used to validate which is the final concentrated flux profile obtained from the new reflector geometry. The IMCRT method is initially proposed and tested for flat absorbers in a parabolic specular mirror (**paper II**). The simplicity of this geometry allows a first approach to show and explain how this method works and the advantages and limitations it has. Two models of objective profile have been studied: Constant and triangular concentrated flux profiles, which are characterized by their half width on the flat absorber surface
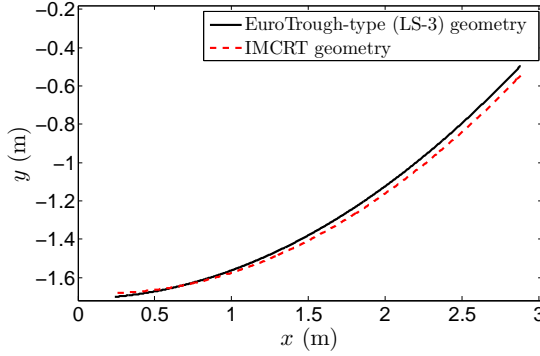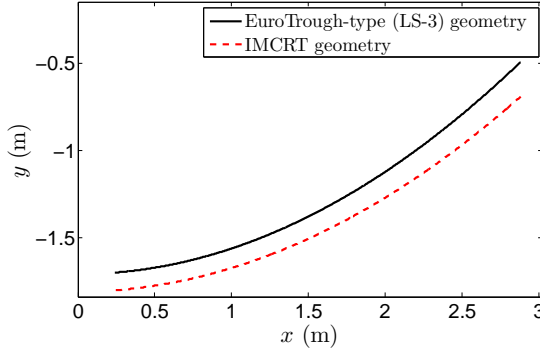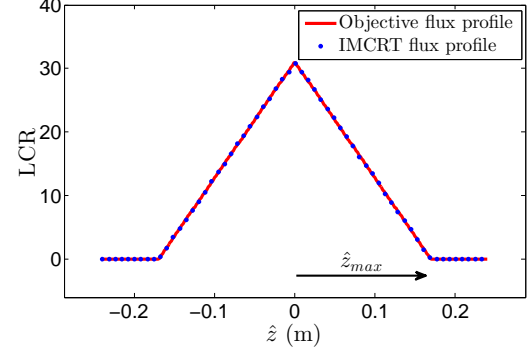
(a) Comparison of reflector geometries for constant flux profile
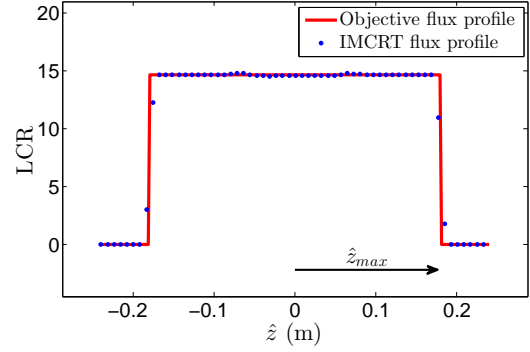
(b) Final flux profile provided by the IM-CRT method for constant objective profile ($\hat{z}_{max} = 0.18$ m)

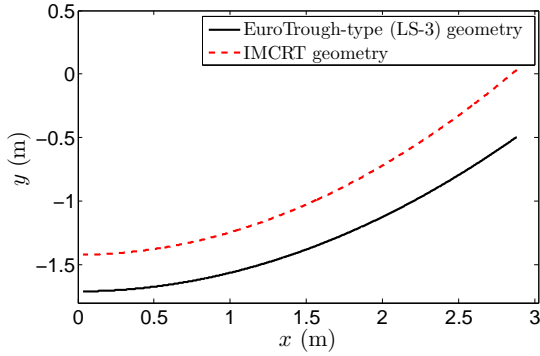(c) Comparison of reflector geometries for triangular flux profile

(d) Final flux profile provided by the IM-CRT method for triangular objective profile ($\hat{z}_{max} = 0.17$ m)

Figure 3.3: Results of the IMCRT method for the flat absorber case (**paper II**).

$(\hat{z}_{max})$[1]. The first one is a good example to check the IMCRT method limitations to obtain final radiation profiles with sharp edges and slopes [see Figs. 3.3(a) and (b)]. It compares the LS-3 reflector geometry with the modified geometry provided by the IMCRT method to obtain a quasi-planar concentrated flux profile showed in Fig. 3.3(b), where it can be observed that the plateau region is virtually constant, but the "tail" of the flux profile slightly differs from the objective profile. Meanwhile, Fig. 3.3(c) compares the LS-3 reflector with the geometry calculated by the IMCRT method for a triangular objective profile with a half width of $\hat{z}_{max}$ [red curve in Fig. 3.3(d)]. In this case, the obtained concentrated flux profile by means of the IMCRT method, accurately reproduces the objective one.

**Paper III** applies the IMCRT method to cylindrical tubes (or round absorber

---

[1]Note that the hat symbol has been put above $\hat{z}$ to avoid confusion with variable z representing the axial coordinate in the thermal model.
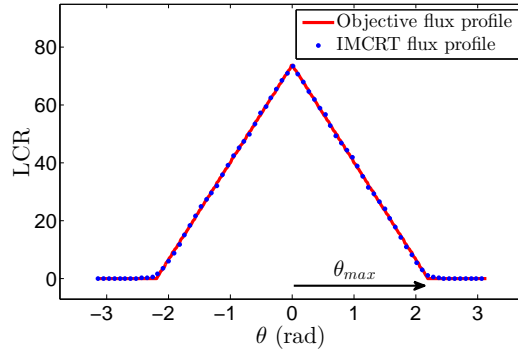
(a) Comparison of reflector geometries for constant flux profile
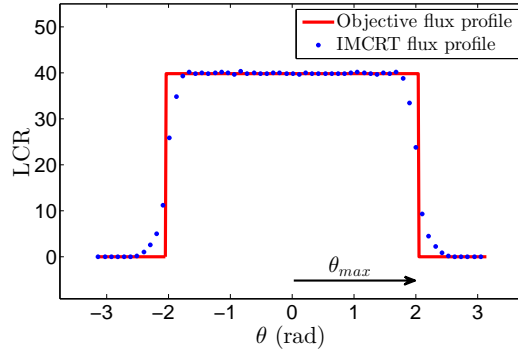
(b) Final flux profile provided by the IMCRT method for constant objective profile ($\theta_{max} = 0.65\pi$)
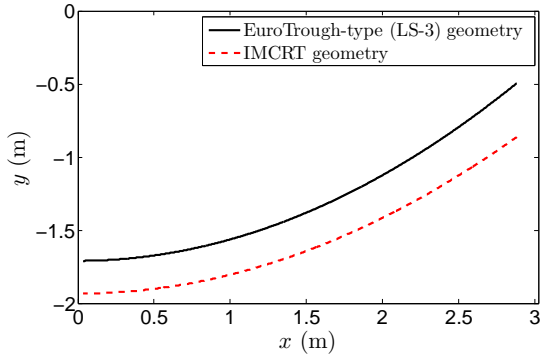
(c) Comparison of reflector geometries for triangular flux profile

(d) Final flux profile provided by the IMCRT method for triangular objective profile ($\theta_{max} = 0.7\pi$)

Figure 3.4: Results of the IMCRT method for the round absorber case (**paper III**).

tubes), which are the most common type of absorbers in linear-focus systems. Consequently, it is of practical interest. In order to show the IMCRT capability to achieve a wide variety of concentrated flux profiles on the absorber, like showed in the flat absorber case, two models of objective profile are used: constant and triangular flux profiles. The variable that circles the absorber cross section is θ, so both models are defined in terms of the angular half width (θ_{max}). As depicted in Fig. 3.4(a) and (c), the LS-3 geometry is compared with the reflector geometry calculated for each objective profile. As previously mentioned, the IMCRT method is not able to reproduce flux profiles with sharp edges (i.e. constant profile), where profile tails significantly differ from the objective one [see Fig. 3.4(b)], whereas the triangular profile is perfectly reproduced by the new geometry provided by the IMCRT method [see Fig. 3.4(d)].

It is worth mentioning that there exist multiple solutions for each problem.

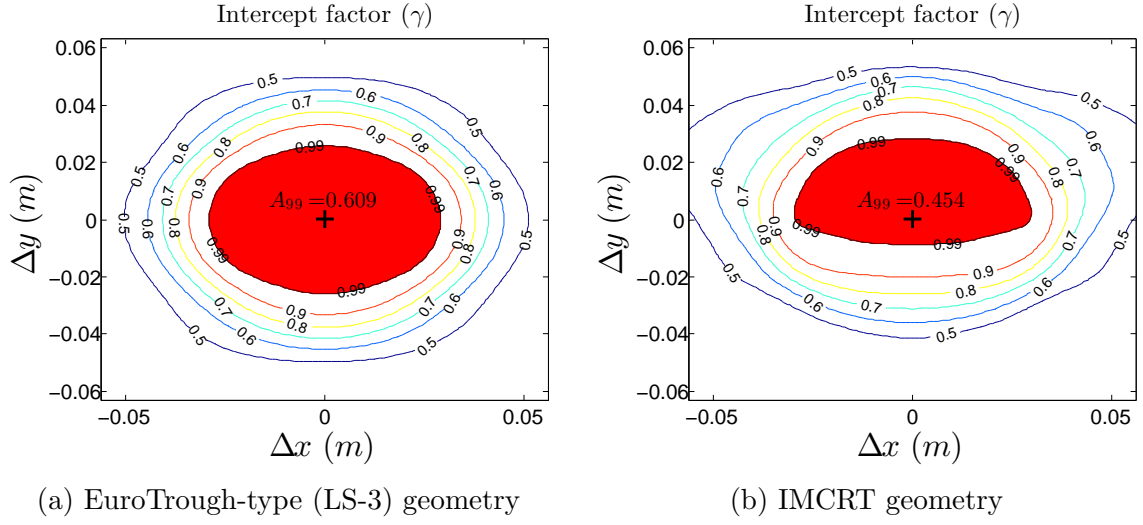(a) EuroTrough-type (LS-3) geometry

(b) IMCRT geometry

Figure 3.5: Comparison between the defocusing performance charts of the LS-3 and the IMCRT reflector geometries. They correspond to the constant objective profile case in absorber tubes (round absorbers) [i.e. reflector geometries depicted in Fig. 3.4 (a)].

Given a specific reflector width (e.g. 5.76 m for the LS-3 geometry), there are two free parameters: Ψ (an angle directly related to the rim angle) and the objective profile half width ($\hat{z}_{max}$ or θ_{max} depending on the absorber geometry). However, the second stage is basically a non-linear optimization algorithm which may lead to different solutions, depending on the optimization strategy.

Not only the determination of some examples of modified geometries, but also the optical performance of such geometries has been assessed. In line with this, the *defocusing performance chart* is proposed. It evaluates the intercept factor of a specific reflector geometry vs two-dimensional displacements of the absorber tube center ($\Delta x, \Delta y$). It is an illustrative way of showing how vulnerable a specific reflector is to any accidental displacements of the absorber tube. As an example, Fig. 3.5 compares the defocusing performance chart of the LS-3 geometry with the corresponding to the new geometry proposed by the IMCRT method for the constant objective profile case in absorber tubes. In light of the information displayed, the modified geometry is more vulnerable to downwards displacements of the absorber, in agreement with the parameter A_{99}. It indicates the non-dimnensionalised area of the chart where the intercept factor remains $\gamma > 0.99$.

3.2 Thermal modeling results

3.2.1 Single-phase flow model

A new steady-state thermal model is presented in **paper I** where the solid domain (i.e. absorber tube wall and glass cover) is modelled in 3D, whereas the fluid domain is simulated following a 1D approach for single-phase flow. A detailed thermal analysis of a single absorber tube (4.06 m long) is performed when superheated steam flows along it, where the cross-sectional distribution of temperature in the absorber wall is studied. The heat transfer coefficient between the fluid and the absorber tube is calculated by means of the corresponding correlation. The evaluation of this term depends, among other factors, on the relative roughness ϵ/D of the pipe inner wall, which also conditions pressure drop along it. For this reason, the surface roughness has been experimentally characterized by means of confocal and interferometry techniques (3D microscope Leica DCM3D) from which a 3D surface map has been produced (see Fig. 3.6). The average maximum height of a particular linear profile along the 3D map has been experimentally determined ($R_z = 13.65$ μm) according to the ISO 4287. The calculated value of such parameter can be associated with the classical definition of ϵ used in the model.

Radiation absorption through the glass cover has also been considered. In order to evaluate the source term in the heat equation within the glass domain, the spectral-averaged attenuation coefficient ($\bar{\beta}$) has been calculated from the spectral transmittance and reflectivity using a Perkin Elmer spectrophotometer along with the ASTM G173-03 Reference Solar Spectra from a 3-mm-thick borosilicate sample.
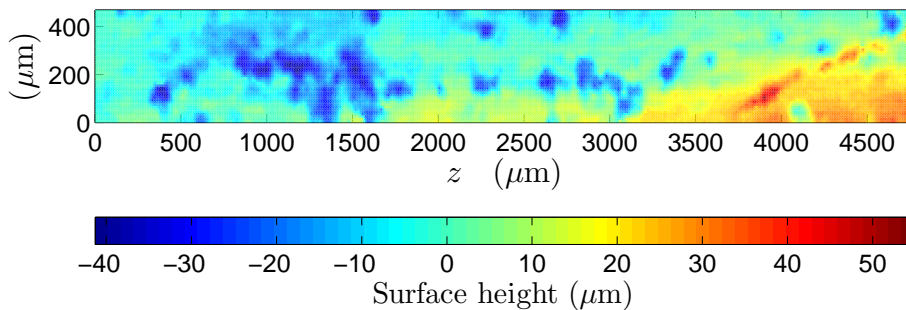

Figure 3.6: Map of the inner surface of the absorber tube obtained from a sample of the DISS text facility along the axial coordinate (z).

Table 3.1: Steady-state operating conditions of the experimental cases tested: model inputs.

Case	DNI (W/m^2)	Angle of incidence (deg)	Reflectance (-)	T_{in} (K)	P_{in} (MPa)	$\dot{m}$ (kg/s)	T_∞ (K)
1	921	14.7	0.86	560.0	6.188	0.64	303.3
2	804	14.8	0.85	551.6	6.125	0.53	307.2
3	771	12.7	0.85	532.8	3.237	0.52	309.6
4	790	17.3	0.85	527.8	3.223	0.50	307.9
5	853	20.4	0.75	616.5	10.085	0.58	307.0
6	823	11.9	0.90	585.5	6.113	0.53	305.6
7	910	13.7	0.87	576.0	5.854	0.64	299.0
8	804	14.6	0.87	551.7	3.161	0.53	301.8

Experimental data obtained from the DISS facility in the superheated steam region (from collector 9 to 11) is used to validate the model. It was collected before the modifications made in the DISS test facility for the DUKE project. It means that the absorber tubes were those made of carbon steel and manufactured by the company Solel. Readings of fluid pressure and temperature have been acquired (see table 3.1) as well as cross-sectional temperature distributions by means of 8 Type-K thermocouples installed in the facility prior to the last upgrade. The specific set of thermocouples used in this validation are located at 35 cm from the pipe outlet edge. Stable irradiance conditions (DNI), ambient temperature (T_∞), sun fix sun position (angle of incidence), as well as constant inlet fluid conditions are assumed: mass flow rate ($\dot{m}$), inlet temperature (T_{in}) and inlet pressure (P_{in}). Meanwhile, the specular reflectance of mirrors was measured at 660 nm with a portable reflectometer. The study covers 3 operation pressure ranges: 3, 6 and 10 MPa. As shown in table 3.1, flow rates are within the range of 0.5 - 0.64 (kg/s), that is usual in real operation conditions at the aforementioned experimental loop.

Eight experimental cases have been solved numerically in order to validate the model in steady-state conditions. Outlet fluid temperature, pressure drop along the 4.06-m-long absorber as well as absorber wall temperature distribution have been compared (see table 3.2). The maximum temperature measured by the Cross-sectional thermocouples (CS max. Temp.) and the maximum gradient between these thermocouples (CS thermal grad.) is contrasted with the temperature calculated by the model at the corresponding position of the cross-sectional thermocouples. Both, the experimental and the numerical global efficiency (η_{exp} and η_{mod}) are compared.

In light of results listed in table 3.2, disagreements between model and experimental values are within the experimental uncertainty range most of the times. Be-

Table 3.2: Model results in comparison with experimental measurements.

Case	Experimental data					Model results				
	Outlet Temp. (K)	Press. drop (MPa)	CS max. Temp. (K)	CS thermal grad. (K)	η_{exp}	Outlet Temp. (K)	Press. drop (MPa)	CS max. Temp. (K)	CS thermal grad. (K)	η_{mod}
1	565.0	0.0024	594.0	28.3	0.64	565.4	0.0022	595.0	28.6	0.69
2	556.5	0.0017	583.2	24.5	0.65	556.6	0.0015	583.6	25.9	0.67
3	539.9	0.0031	576.9	33.1	0.62	540.6	0.0030	574.0	30.9	0.67
4	535.1	0.0029	567.1	28.9	0.64	535.6	0.0028	569.4	31.1	0.68
5	620.4	0.0015	641.3	24.3	0.52	620.8	0.0012	643.9	22.6	0.57
6	592.1	0.0017	628.6	37.8	0.62	593.1	0.0017	627.8	32.8	0.71
7	581.4	0.0027	613.3	32.6	0.58	582.5	0.0026	614.8	31.0	0.69
8	559.2	0.0035	598.9	37.9	0.60	560.4	0.0034	596.9	33.7	0.69

sides, the pressure drop comparison shows that the 1-D approach accurately reproduces the HTF axial evolution of pressure. The experimental global efficiency η_{exp} is generally lower than the corresponding numerical one η_{mod}. Such difference can be explained owing to several factors: The first one is related to the perfect vacuum consideration. Vacuum leak is responsible for the gradual vacuum level decay in time, a fact not considered by the model. Additionally, a slight loss is due to free-molecular diffusion, which has not been included in the model. Finally, some parameter values have been taken from manufacturers data sheet, corresponding to brand-new conditions of the receiver. As an example, the temperature distribution of the absorber outlet section corresponding to the case # 1 is depicted in Fig. 3.7. Due to the vacuum annulus, it can be observed that temperature on the glass cover is noticeably lower than in the absorber tube domain. In case that vacuum would be partially or totally lost, the glass cover temperature would be sensibly higher. It means that the proposed model is an adequate tool to set reference temperatures of the outer surface of the glass cover to detect damaged receivers.

3.2.2 Thermal-hydraulic model for two-phase flow

As explained in section 3.2.1, the goal of **paper I** was to model the existing heat transfer mechanisms between solid parts of the receiver and the single-phase flow domain. For DSG purposes it is essential to model the two-phase flow region. In this case, not an in-house code has been implemented, but a commercial code for nuclear reactor safety analysis has been applied to perform transient simulations of the whole DISS facility (**paper IV**). Standard capabilities of RELAP5 have been used to model subcooled water, two-phase flow and superheated steam regions of the
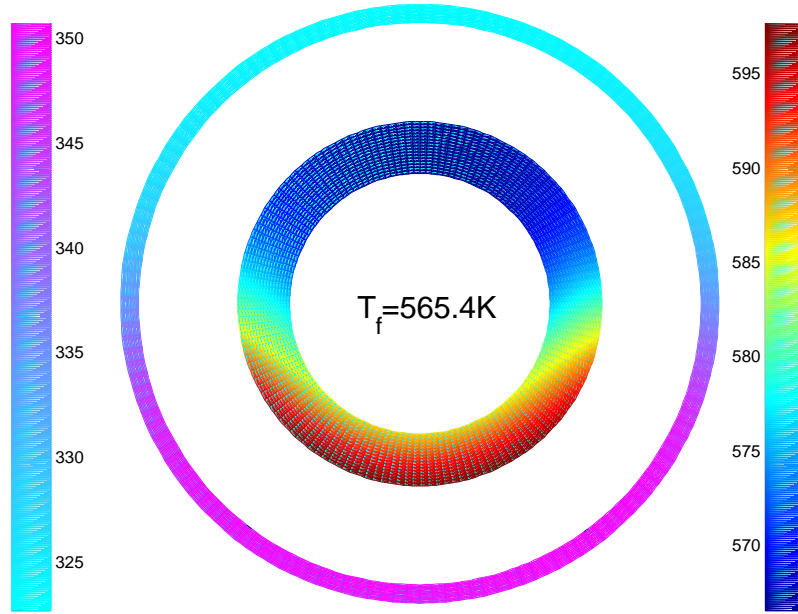
Figure 3.7: Case #1 temperature (K) distribution at the absorber outlet section ($z = 4.06$ m). Glass envelope temperature distribution is shown in the left bar and steel absorber temperature distribution in the right one. HTF outlet temperature T_f is displayed in the center.

DISS loop, operating in once-through mode.

The receiver has not been modeled in detail but the stainless-steel absorber tube[2] has only been taken into account. According to the limitations of the code, a 3D model of the absorber tube wall is not allowed. Some simplifications have been applied instead. It means that heat diffusion is modelled applying a two-dimensional approach where the angular distribution around the absorber is partially neglected. Instead of a continuous domain, a set of 6 slabs wraps the fluid domain around. Only radial and axial discretization is addressed within the same solid slab, whereas the angular distribution is approximated with the 6 temperature values of the slabs distributed around. The main limitation of this approach consists on the fact that no heat exchange is allowed between adjacent slabs in the angular direction. As a 1D two-fluid model, the heat transfer between the inner tube wall and the fluid is calculated in terms of bulk fluid properties at each axial location. In other words, no local heat transfer phenomena in the fluid are studied like in CFD models. As previously mentioned, neither the glass cover domain nor the vacuum annulus have been modeled. An experimental correlation to approximate real heat losses has been

---

[2]This new type of tubes (manufactured by Schott) replaced the former carbon steel absorbers in the DUKE project.

used instead (see section 3.2.3).

The azimuthal distribution of concentrated solar radiation around the absorber is calculated by means of an optical model performed by Monte Carlo Ray Tracing method implemented in Tonatiuh. A gaussian distribution has been used to model the reflector surface slope error (σ_{er}=2 mrad). Since no angular discretization around the solid domain is allowed, only constant distribution of concentrated radiation flux can be set for each slab. The model takes also into account connection pipes between adjacent collectors, where vertical and horizontal sections have been included, issue that conditions the system transient behaviour. Each collector module has been discretized into 14 nodes, and each connection pipe, according to its characteristics, has its own nodalization scheme.

Table 3.3: Operation conditions of the simulated cases

Case #	DNI_{max} (W m^{-2})	$\dot{m}$ range (kg s^{-1})	$\overline{P}_{out}$ (MPa)	$\overline{T}_{out}$ (K)
1	810	[0.8 - 1.2]	3.07	536.9
2	966	[0.9 - 1.2]	3.28	552.1
3	920	[0.8 - 2.0]	1.17	440.0
4	972	[1.0 - 1.2]	5.55	587.0
5	957	[1.0 - 1.3]	3.17	549.2
6	947	[1.0 - 1.2]	3.11	568.6

A total of six experimental cases have been simulated in order to validate the transient thermal hydraulic model. Experimental data correspond to full day tests (including the start up and turn off procedures) carried out in the DISS test facility during the year 2016, where operation pressure up to 6 MPa have been reached for a wide range of mass flow rates (see table 3.3). Such tests represent common working conditions or events likely to happen like clouds shadow, changes in the mass flow rate or sudden defocusing of any collector. A detailed comparison between the model results and the experimental time series is depicted in Fig. 3.8. The axial evolution of pressure is compared for two instants of time where good agreement can be observed. Since no experimental characterization of void fraction is possible, numerical void fraction evolution is also displayed alone in Figs. 3.8 (a)-(b). The experimental and numerical time series of the outlet fluid temperature (T_{out}) as well as the the whole loop pressure drop (ΔP) are compared in Fig. 3.8 (c). Maximum temperature difference (ΔT_{CS}) between different slabs around the fluid (absorber pipe) is shown in Fig. 3.8 (d) at a specific axial location ($x = 868.5$ m). According to that, the existing approach followed by RELAP5 to model the absorber wall provides descriptive results of the thermal gradients on it.
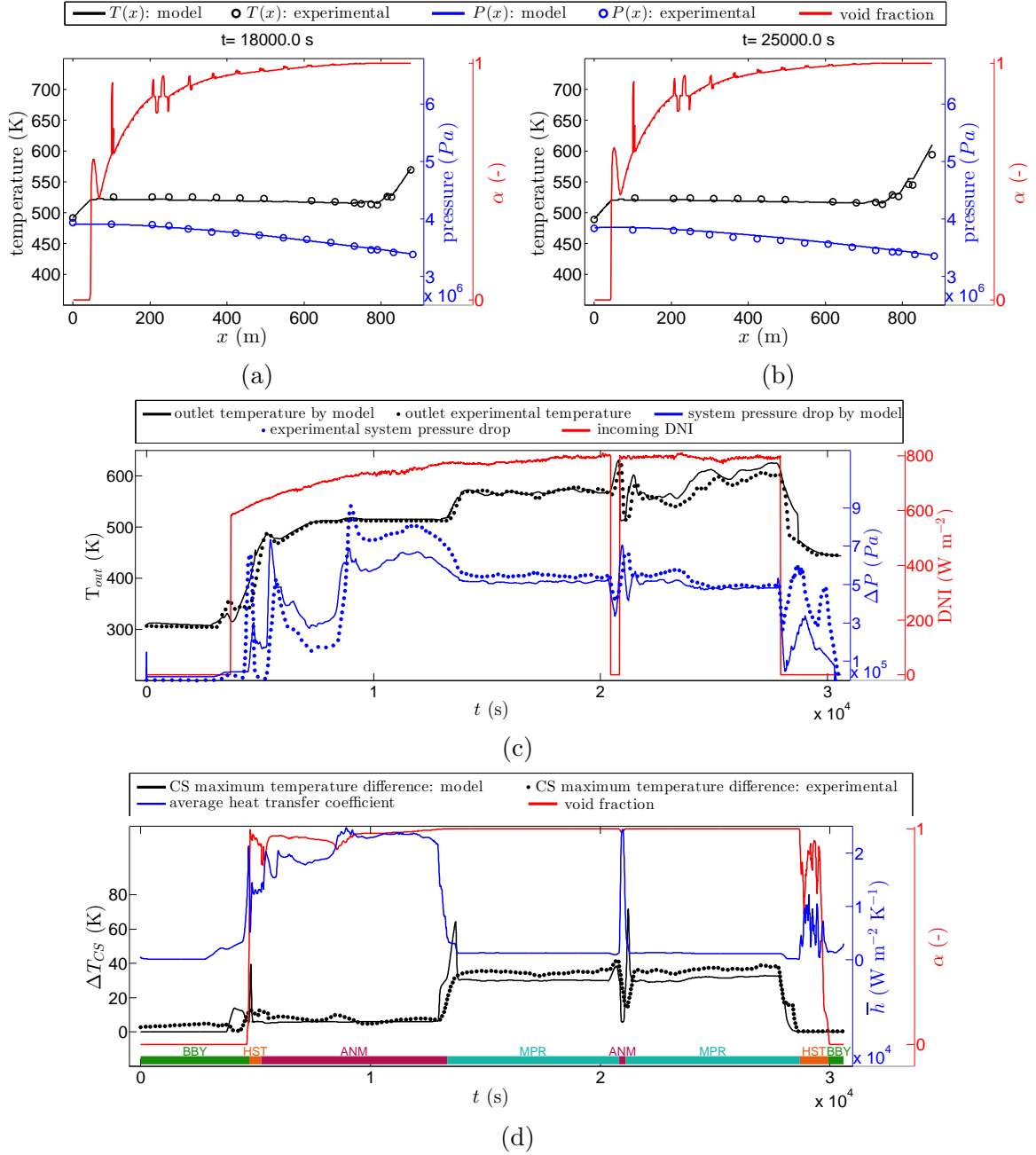
84

Figure 3.8: Case #1 validation. (a)-(b) Axial evaluation at two different times of numerical void fraction alongside experimental and numerical values of fluid temperature and pressure. (c) Numerical fluid temperature at the outlet along with system pressure drop vs. experimental data, where the incoming DNI is also included. (d) Time evolution at collector #11 ($x = 868.5$ m): numerical vs. experimental temperature difference in the absorber tube wall; average heat transfer coefficient ($\bar{h}$) alongside void fraction; and at the bottom, colour bar displaying the type of flow regime at this axial location (see **paper IV** for further details).

Taking the system outlet temperature as the reference variable, difference between numerical and experimental results have been assessed for the six cases solved. Root-mean-square error (RMSE) and mean absolute error (MAE) as well as their respective normalized errors (NRMSE and NMAE) have been listed in table 3.4. The MAE is suitable to describe model errors which are uniformly distributed, whereas RMSE is a better metric to describe errors having a normal distribution rather than a uniform distribution. The maximum NRMSE is 6.9 % and the maximum NMAE is 5.2%, both values correspond to case #3. According to these errors, RELAP5 provides results in good agreement with the experiments, with the exception of predictions of pressure drop. The experimental uncertainty of the pressure transmitters in the DISS facility, which is above 1.5%, could explain this discrepancy. Special attention has been paid to the transients, checking that the model reproduces accurately the dynamic of the system.

Table 3.4: Table of errors based on the fluid temperature at the system outlet

Case #	RMSE (K)	NRMSE (%)	MAE (K)	NMAE (%)
1	16.7	5.2	9.8	3.0
2	14.1	3.9	7.7	2.1
3	13.4	6.9	10.1	5.2
4	9.7	2.6	6.7	1.8
5	16.0	4.2	10.1	2.7
6	17.2	4.4	9.2	2.4

An additional numerical study has been carried out with RELAP5 concerning a specific transient phenomena (named severe slugging) which may take place in connection pipes (**paper IV**). Despite having steady conditions at the inlet, oscillations in the mass flow rate at the outlet of the connection pipe may take place under some specific conditions of pressure and steam quality. Due to gravitational forces, slugging phenomenon is the result of cyclical accumulation of liquid water in the riser (note that the connection pipe is formed by vertical sections). This cyclical pattern can be characterized by analyzing the amplitude of the mean void fraction ($< \alpha >$) in the last three sections of the connection pipe (riser). To study this issue, two adjacent collectors linked by a connection pipe have been simulated at a nominal pressure of 0.5 MPa. Based on 374 tests, slugging phenomenon has been reported for low values of inlet mass flow rate and low quality in the entering two-phase mixture. As displayed in Figure 3.9, numerical results have been compiled so as to get an amplitude chart to point out the most critical region, where $\dot{m}_{in}$ stands for the inlet mass flow rate at the first collector inlet and $\hat{x}_{in}$ represent the steam quality a this point. The region
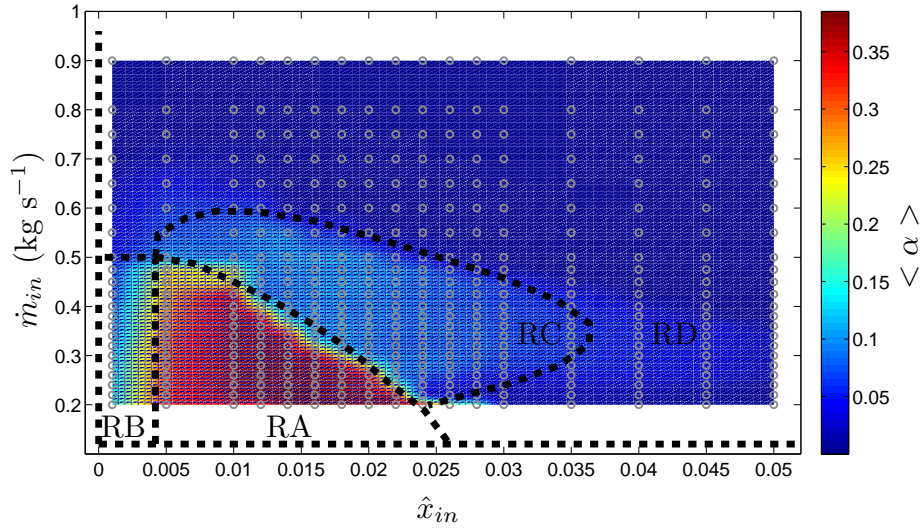
Figure 3.9: Characteristic amplitude ($< \alpha >$) of the average void fraction oscillations in the connection riser between two adjacent solar collectors at constant outlet pressure ($P_{out} = 5 \cdot 10^5$ Pa). Amplitude as a function of total mass flow rate ($\dot{m}_{in}$) and quality ($\hat{x}_{in}$) of the saturated two-phase flow mixture at the inlet.

A (RA in Fig. 3.9) has been found to show the highest amplitude of oscillations. It means that at low operating pressure, slugging may take place at the beginning of the two-phase flow region, given that severe slugging have been reported for low values of $\hat{x}_{in}$.

3.2.3 Experimental characterization of heat losses

Most of the available models of PTCs do not simulate the glass cover and the vacuum annulus. The absorber tube is modelled alone instead, whereas thermal exchange between the absorber and the glass cover and with the ambient is simplified by means of a heat loss correlation. It is determined experimentally and it is usually expressed in terms of the polynomial regression detailed in Eq. 3.2:

$$q_{HL}\left(\Delta T\right) = a\Delta T + b\Delta T^4 \qquad \left(\text{W m}^{-1}\right). \tag{3.2}$$

Unlike other experimental characterizations, which have been carried out in test bed: Dreyer et al. (2010); Feldhoff et al. (2014), the experimental data required for the polynomial fitting has been obtained from a set of steady-state tests carried out in the DISS facility. Schott PTR-70-DSG absorbers, installed during renovation accom-
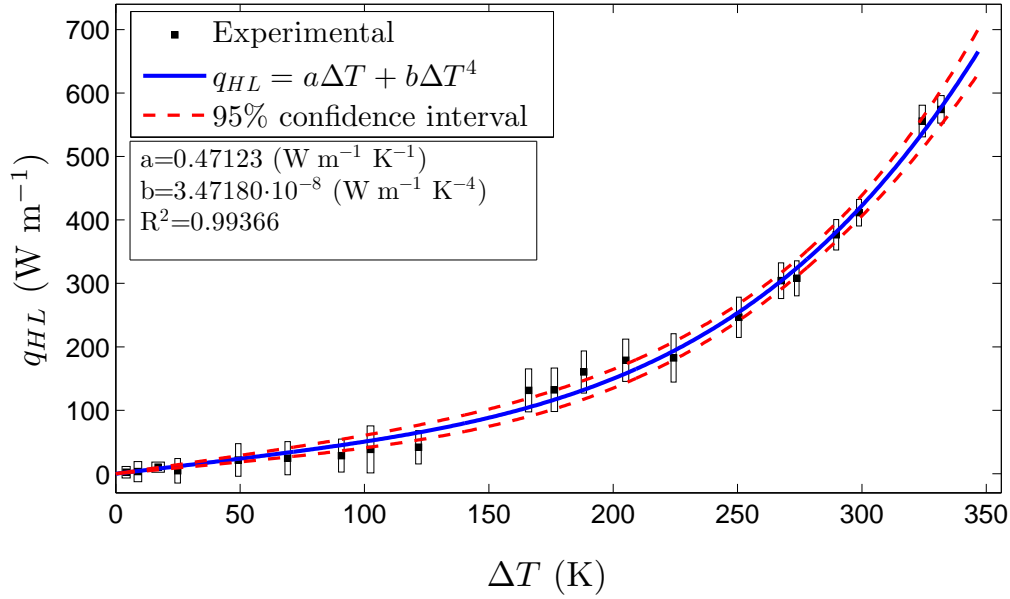
Figure 3.10: Heat losses obtained by curve fitting with the adopted model $q_{HL}(\Delta T)$ from experimental measurements at the DISS test facility.

plished in 2013, have been tested 2 years and a half later. Heat losses predicted by the present correlation are higher than those estimated by the existing correlations. The fact that tests have been carried out on already-installed receivers, provides a more realistic estimation of such heat losses taking place on the solar field.

Since it is not possible to measure the steam quality along the DISS loop, single phase flow conditions have been set to measure sensible heat changes between the inlet and the solar collector outlet while the tested collector is defocused, i.e. non-tracking the sun. This correlation is useful to model the whole collector in real working conditions in the solar field. It also includes several heat losses associated to absorber junctions and brackets. The absorber wall temperature has been measured by means of the thermocouples installed on them. Heat losses (q_{HL}) have been related to the difference between the ambient and the average temperature of the absorber wall (ΔT) in Fig. 3.10. This correlation is applied as the outer boundary condition of the solid domain (outer absorber wall). The bounding box in each experimental point represents the experimental uncertainty associated to the heat loss (q_{HL}) and temperature (ΔT) through the measures of mass flow rate, pressure and temperature.

4 CONCLUSIONS

Different methods to simulate Direct Steam Generation (DSG) systems based on Parabolic-Trough Collectors have been studied in this thesis. However, some of the results and conclusions drawn can also be extended to other linear-focusing solar systems. Different approaches have been tested and validated from experimental data collected from the DISS facility located at Plataforma Solar de Almería. The implementation of some in-house codes both for optical and thermal modeling has enabled a thorough understanding of the underlying physics, which in turns makes it possible to propose new methods to optimize geometry of reflectors and other elements in these systems. The execution of such codes, and the computing resources required, give an idea of how future models to simulate full scale solar fields have to be arranged as well as the type of assumptions that have to be taken in order to simulate them at an affordable computing cost without penalizing the results accuracy. Main conclusion are classified as follows:

1. Optical modeling:

   (a) In light of the results provided by the in-house 3D Monte Carlo Ray Tracing code implemented in Matlab$^{®}$ (**paper I**), it can be confirmed that the element-wise arithmetic operations existing in this software, speeds-up significantly the resolution of the algorithm. Code parallelization are also possible without significant changes in the structure of the code.

   (b) The reduction of the ray tracing algorithm to the cross-sectional plane (2D

Monte Carlo Ray Tracing algorithm) reproduces the characteristic distribution of concentrated solar radiation around the absorber tube. Both the sunshape profile as well as the statistical distributions modeling non-specular reflection on mirrors, have to be projected onto the cross-sectional plane. It is worth mentioning that additional changes are needed in the algorithm if the angle of incidence is not zero.

(c) A new method called Inverse Monte Carlo Ray Tracing (IMCRT) is proposed to design reflector geometries, when a specific objective profile is required on a predefined absorber. This method has been tested for flat absorbers (**paper II**) and round absorbers (**paper III**). Results show that those objective profiles consisting of smooth functions can be easily reproduced. However, some limitations concerning objective profiles with sharp tails exist (i.e. quasi-constant objective profile). This method is proved to be a potential tool to design ad-hoc linear-focus reflectors for specific applications, including concentrated photovoltaic systems.

(d) It can be affirmed that new commercial reflector geometries can be designed to get more homogeneous concentrated flux distribution on absorber tubes than the existing ones (parabolic reflectors) to prevent thermal bending. It can be attained without penalizing significantly the intercept factor or increasing the reflector cost.

2. Thermal-hydraulics and thermal modeling:

(a) It is feasible to couple a full 3D model of the solid parts of linear receivers to get the 3D temperature field, with a 1D description of the fluid domain by means of the corresponding convective heat transfer correlation (**paper I**). Experimental results collected from the DISS facility have been used to validate this type of model.

(b) When modeling heat transfer by means of thermal radiation through the vacuum annulus of receivers (**paper I**), the fact of considering the axial evolution of temperature accounts for a representative fraction of the computing cost. The implementation of future codes for full scale solar fields should address simpler ways to handle that (e.g. crossed-string method).

(c) Transient simulations have been performed using RELAP5 to model a single-loop DSG system based on PTCs. Results show that RELAP5 is a

quite efficient tool to model such thermal-hydraulic problem (**paper IV**) in this context. However, standard capabilities of this code do not allow an accurate modeling of the absorber tube wall. Further changes are required to solve the heat equation in three-dimensions to take into account the angular distribution of temperature in that wall.

3. Experimental research:

   (a) A new correlation for heat losses has been obtained from a test campaign carried out at the DISS facility (2016). It has been shown that heat losses can be evaluated experimentally on already-installed receivers on a DSG system at a wide range of temperatures.

According to the aforementioned conclusions, some **future research** can be highlighted. Regarding the optical modeling, it is relevant to test the IMCRT method taking into account some additional factors. This is the case of the angle of incidence (single-axis tracking collectors), which may cause some difficulties in the second stage when some specific objective profiles are imposed. At the same time, it is interesting to check what is the influence of this angle on the final profile achieved. In addition, future studies to check the application of the IMCRT method to point focus reflectors are of interest as well.

Future research lines for the implementation of models for Direct Steam Generation purposes, require to develop fast thermal-hydraulic codes. The 1D drift-flux formulation used by the nuclear industry is a potential alternative along with an analytic solution for the heat diffusion in the absorber tube wall. However, some issues have to be checked. Firstly, it has to be verified that the available drift-flux correlations accurately predict the drift velocity within the connection pipes. Secondly, when a detailed modeling of boundary conditions is needed for the heat equation in the absorber tube wall, it is not still clear whether a 3D semianalytic solution will be the most efficient way in comparison with a pure numerical approach.

Bibliography

AENOR (2013). Centrales termosolares, Terminología (norma UNE 206009:2013).

Ajona, J. I. and González, L. (1996). ARDISS Project, 2nd Draft, *Technical Report 42C11-PSA-02*, EU JOULE II Programme.

Ajona, J. I., Herrmann, U., Sperduto, F. and Mendes, J. F. (1997). ARDISS Project, 4th Semestrial report, *Technical Report JOU2-CT94-0311*, EU JOULE II Programme.

Ajona, J. and Zarza, E. (1994). Benefits Potential of Electricity Production with direct Steam Generation in Parabolic Troughs, *in* O. Popel, S. Fris and E. Shchedrova (eds), *Proceeding of the 7th International Symposium on Solar Thermal Concentrating Technologies*, Institute for High Temperature of Russian Academy of Science (IVTAN), Moscow Rusia (September 1994), pp. 300–314. ISBN: 5-201-09540-2.

Almanza, R. and Lentz, A. (1998). Electricity production at low powers by direct steam generation with parabolic troughs, *Solar Energy* **64**(13): 115 – 120.

Baharoon, D. A., Rahman, H. A., Omar, W. Z. W. and Fadhl, S. O. (2015). Historical development of concentrating solar power technologies to generate clean electricity efficiently a review, *Renewable and Sustainable Energy Reviews* **41**: 996 – 1027.

Ballestrín, J. and Marzo, A. (2012). Solar radiation attenuation in solar tower plants, *Solar Energy* **86**(1): 388 – 392.

Barnea, D. (1987). A unified model for predicting flow-pattern transitions for the whole range of pipe inclinations, *International Journal of Multiphase Flow* **13**(1): 1– 12.

Bestion, D. (1990). The physical closure laws in the CATHARE code, *Nuclear Engineering and Design* **124**(3): 229 – 245.

Biencinto, M., González, L. and Valenzuela, L. (2016). A quasi-dynamic simulation model for direct steam generation in parabolic troughs using TRNSYS, *Applied Energy* **161**: 133 – 142.

Blanco, M., Mutuberria, A., García, P., Gastesi, R. and Martín, V. (2009). Preliminary validation of Tonatiuh. In: (Ed.), Symposium Solar PACES Conference (September 2009).

Bonilla, J., Yebra, L. J., Dormido, S. and Zarza, E. (2012). Parabolic-trough solar thermal power plant simulation scheme, multi-objective genetic algorithm calibration and validation, *Solar Energy* **86**(1): 531 – 540.

Bosetti, V., Catenacci, M., Fiorese, G. and Verdolini, E. (2012). The future prospect of PV and CSP solar technologies: An expert elicitation survey, *Energy Policy* **49**: 308 – 317. Special Section: Fuel Poverty Comes of Age: Commemorating 21 Years of Research and Policy.

Buie, D., Monger, A. and Dey, C. (2003). Sunshape distributions for terrestrial solar simulations, *Solar Energy* **74**(2): 113 – 122.

Caldés, N., Varela, M., Santamaría, M. and Sáez, R. (2009). Economic impact of solar thermal electricity deployment in spain, *Energy Policy* **37**(5): 1628 – 1636.

Çetin, M. and Eğrican, N. (2011). Employment impacts of solar energy in Turkey, *Energy Policy* **39**(11): 7184 – 7190. Asian Energy Security.

Cebecauer, T. and Suri, M. (2015). Typical Meteorological Year Data: SolarGIS Approach, *Energy Procedia* **69**: 1958 – 1969.

Chaanaoui, M., Vaudreuil, S. and Bounahmidi, T. (2016). Benchmark of Concentrating Solar Power Plants: Historical, Current and Future Technical and Economic

Development, *Procedia Computer Science* **83**: 782 – 789. The 7th International Conference on Ambient Systems, Networks and Technologies (ANT 2016) / The 6th International Conference on Sustainable Energy Information Technology (SEIT-2016) / Affiliated Workshops.

Coady, D., Parry, I., Sears, L. and Shang, B. (2017). How large are global fossil fuel subsidies?, *World Development* **91**: 11 – 27.

Cohen, G. E., Kearney, D. W. and Kolb, G. J. (1999). Final report on the operation and maintenance improvement program for concentrating solar power plants, *Technical Report SAND99-1290*, Sandia National Laboratories, Albuquerque, New Mexico.

Cohen, G. and Frier, S. (n.d.). Ten years of solar power plant operation in the Mojave desert, *Proceedings of Solar 97*, the 1997 ASES Annual Conference, Washington DC (April 1997).

Collares-Pereira, M., Gordon, J., Rabl, A. and Winston, R. (1991). High concentration two-stage optics for parabolic trough solar collectors with tubular absorber and large rim angle, *Solar Energy* **47**(6): 457 – 466.

Craig, K., Moghimi, M., Rungasamy, A., Marsberg, J. and Meyer, J. (2016). Finite-volume ray tracing using Computational Fluid Dynamics in linear focus CSP applications, *Applied Energy* **183**: 241 – 256.

CSP Today (2017). CSP Today Global Tracker. [Online].
URL: *http://tracker.newenergyupdate.com/tracker/projects*

CSP World (2017). CSP World Map. [Online].
URL: *http://cspworld.org/cspworldmap*

Dagan, E., Müller, M. and Lippke, F. (1992). Direct Solar Steam Generation in Parabolic Trough Collectors, *Technical Report (Internal)*, CIEMAT & DLR, Plataforma Solar de Almería.

Delache, P. (1988). Variability of the solar diameter, *Advances in Space Research* **8**(7): 119 – 128.

DoE initiative aims to advance US solar industry (2014). *Renewable Energy Focus* **15**(3): 4 – 4.

Dreyer, S., Eichel, P. and Gnaedig, T. (2010). Heat loss measurements on parabolic trough receivers, *16th SolarPACES, 2010, Perpignon (France)* .

Duffie, J. A. and Beckman, W. A. (1980). *Solar Engineering of Thermal Processes*, Wiley, New York.

ESTELA (2012). European Solar Thermal Electricity Association. Solar Thermal Electricity. Strategic Research Agenda 2020 – 2025. [Online; Last access online 26-Jan-2017].
URL: *http://www.estelasolar.org/wp-content/uploads/2015/11/2012-ESTELA -Strategic-Reseach-Agenda-2020-2025_Summary.pdf*

European Comission (1997). Energy for the Future: Renewable Sources of Energy. White Paper for a Community Strategy and Action Plan. COM(97) 599 final.

Evans, D. (1977). On the performance of cylindrical parabolic solar concentrators with flat absorbers, *Solar Energy* **19**(4): 379 – 385.

Feldhoff, J. F., Eickhoff, M., Keller, L., Alonso, J. L., Meyer-Grünefeldt, M., Valenzuela, L., Pernpeintner, J. and Hirsch, T. (2014). Status and first results of the DUKE project component qualification of new receivers and collectors, *Energy Procedia* **49**: 1766 – 1776. Proceedings of the SolarPACES 2013 International Conference.

Feldhoff, J. F., Hirsch, T., Pitz-Paal, R. and Valenzuela, L. (2015). Transient Models and Characteristics of Once-through Line Focus Systems, *Energy Procedia* **69**: 626 – 637.

Fernández-García, A., Zarza, E., Valenzuela, L. and Pérez, M. (2010). Parabolic-trough solar collectors and their applications, *Renewable and Sustainable Energy Reviews* **14**(7): 1695 – 1721.

Fernández, S. and Acuñas, A. (2012). New Optimized Solar Collector: SENERtrough-2. 18th SolarPACES Conference, September 2012, Marrakech, Morocco.

Gnielinski, V. (1976). New equations for heat and mass transfer in turbulent pipe and channel flow, *Int. Chem. Eng* **16**(2): 359–368.

Grágeda, M., Escudero, M., Alavia, W., Ushak, S. and Fthenakis, V. (2016). Review and multi-criteria assessment of solar energy projects in Chile, *Renewable and Sustainable Energy Reviews* **59**: 583 – 596.

Güven, H. M. and Bannerot, R. B. (1986). Determination of error tolerances for the optical design of parabolic troughs for developing countries, *Solar Energy* **36**(6): 535 – 550.

Haer, T., Kalnay, E., Kearney, M. and Moll, H. (2013). Relative sea-level rise and the conterminous united states: Consequences of potential land inundation in terms of population at risk and GDP loss, *Global Environmental Change* **23**(6): 1627 – 1636.

Hanrieder, N., Wilbert, S., Mancera-Guevara, D., Buck, R., Giuliano, S. and Pitz-Paal, R. (2017). Atmospheric extinction in solar tower plants A review, *Solar Energy* . DOI: 10.1016/j.solener.2017.01.013.

Hassan, K.-E. and El-Refaie, M. F. (1973). Theoretical performance of cylindrical parabolic solar concentrators, *Solar Energy* **15**(3): 219 – 244.

Hernández-Lobón, D. (2014). *Contribución al modelado Termo-hidráulico de Captadores Solares Cilindroparabólicos para la Generación Directa de Vapor.*, PhD thesis, Universidad de Almería. Departamento de Química y Física.

Ho, C., Mehos, M., Turchi, C. and Wagner, M. (2014). Probabilistic analysis of power tower systems to achieve sunshot goals, *Energy Procedia* **49**: 1410 – 1419.

Ho, C., Sims, C. and Christian, J. (2015). Evaluation of Glare at the Ivanpah Solar Electric Generating System, *Energy Procedia* **69**: 1296 – 1305. International Conference on Concentrating Solar Power and Chemical Energy Systems, SolarPACES 2014.

INDITEP (2005). Integration of DSG technology for electricity production - (INDITEP). European Commission Project ID: ENK5-CT-2001-00540 [Online; Last access online 09-Feb-2017].
URL: *http://cordis.europa.eu/project/rcn/70234_en.html*

Jose, P. D. (1957). The flux through the focal spot of a solar furnace, *Solar Energy* **1**(4): 19 – 22.

Kelly, J. and Kazimi, M. (1982). Interfacial Exchange Relations for Two-Fluid Vapor-Liquid Flow: A Simplified Regime-Map Approach, *Nuclear Science and Engineering* **81**(3): 305 – 318.

Khenissi, A., Krüger, D., Hirsch, T. and Hennecke, K. (2015). Return of Experience on Transient Behavior at the DSG Solar Thermal Power Plant in Kanchanaburi, Thailand, *Energy Procedia* **69**: 1603 – 1612.

Kost, C., Engelken, M. and Schlegl, T. (2012). Value generation of future CSP projects in north africa, *Energy Policy* **46**: 88 – 99.

Law 661/2012 of 27 December (2012). BOE no. 312, Dec 28, 2012 (88081 - 88096). [Online; Last access online 20-Jan-2017].
URL: *https://www.boe.es/diario_boe/txt.php?id=BOE-A-2012-15649*

Lobón, D. H., Baglietto, E., Valenzuela, L. and Zarza, E. (2014). Modeling direct steam generation in solar collectors with multiphase CFD, *Applied Energy* **113**: 1338 – 1348.

Malayeri, M., Zunft, S. and Eck, M. (2004). Compact field separators for the direct steam generation in parabolic trough collectors: An investigation of models, *Energy* **29**(56): 653 – 663. SolarPACES 2002.

Manera, A., Rohde, U., Prasser, H.-M. and van der Hagen, T. (2005). Modeling of flashing-induced instabilities in the start-up phase of natural-circulation BWRs using the two-phase flow code FLOCAL, *Nuclear Engineering and Design* **235**(14): 1517 – 1535.

Martín, H., de la Hoz, J., Velasco, G., Castilla, M. and de Vicua, J. L. G. (2015). Promotion of concentrating solar thermal power (CSP) in Spain: Performance analysis of the period 1998-2013, *Renewable and Sustainable Energy Reviews* **50**: 1052 – 1068.

Martinek, J. and Weimer, A. W. (2013). Evaluation of finite volume solutions for radiative heat transfer in a closed cavity solar receiver for high temperature solar thermal processes, *International Journal of Heat and Mass Transfer* **58**(12): 585 – 596.

Matsumoto, M. and Nishimura, T. (1998). Mersenne Twister: A 623-dimensionally Equidistributed Uniform Pseudo-random Number Generator, *ACM Trans. Model. Comput. Simul.* **8**(1): 3–30.

Mehos, M., Turchi, C., Vidal, J., Wagner, M. and Ma, Z. (2017). Concentrating Solar Power Gen3 Demonstration Roadmap, *Technical Report NREL/TP-5500-67464*, National Renewable Energy Laboratory (NREL), Golden, Colorado.

Morin, A. (2012). *Mathematical modelling and numerical simulation of two-phase multi-component flows of CO_2 mixtures in pipes*, PhD thesis, Norwegian University of Science and Technology. Faculty of Engineering Science and Technology.

Müller, M., Lippke, F., Zarza, E., Hansen, J. and Ajona, J. (1994). *Direct Solar Steam in Parabolic Trough Collectors (DISS). Pre-Design of a Flexible PSA-Based Test Facility*, ISBN: 84-605-1479-X, Almeía, Plataforma Solar de Almería.

Murphy, L. and May, E. K. (1982). Steam Generation in Line-Focus Solar Collect-
ors: A Comparative Assessment of Thermal Performance, Operating Stability, and
Cost Issues, *Technical Report SERI/TR-632-1311*, Solar Energy Research Institute
(SERI), Golden, Colorado 80401 (US).

Nakumuryango, A. and Inglesi-Lotz, R. (2016). South Africa's performance on re-
newable energy and its relative position against the OECD countries and the rest
of Africa, *Renewable and Sustainable Energy Reviews* **56**: 999 – 1007.

Neumann, A., Witzke, A., Jones, S. and Schmitt, G. (2002). Representative terrestrial
solar brightness profiles, *J. Sol. Energ-T ASME* **124**(2): 198–204.

NREL (2015). Andasol–1: Main characteristics. [Online; Status date 16-Nov-2015].
URL: *https://www.nrel.gov/csp/solarpaces/project_detail.cfm/projectID=3*

NREL Database (2016). Concentrating Solar Power Projects. [Online].
URL: *https://www.nrel.gov/csp/solarpaces/index.cfm*

Petukhov, B. (1970). Heat Transfer and Friction in Turbulent Pipe Flow with Variable
Physical Properties, Vol. 6 of *Advances in Heat Transfer*, Elsevier, pp. 503 – 564.

Pollet, B. G., Staffell, I. and Adamson, K.-A. (2015). Current energy landscape in the
Republic of South Africa, *International Journal of Hydrogen Energy* **40**(46): 16685
– 16701.

Price, H. and Kearney, D. (2003). Reducing the Cost of Energy from Parabolic Trough
Solar Power Plants, *Technical Report NREL/CP-550-33208*, National Renewable
Energy Laboratory (NREL), Golden, Colorado.

Protermosolar (2017). Mapa de proyectos en España. Asociación española de la In-
dustria Termoeléctrica. [Online].
URL: *http://www.protermosolar.com/proyectostermosolares/mapadeproyectosen-
espana/*

Pytilinski, J. (1978). Solar energy installations for pumping irrigation water, *Solar
Energy* **21**(4): 255 – 262.

Rabl, A. (1985). *Active Solar Collectors and Their Applications*, Oxford University
Press. ISBN: 9780195035469.

RD 436/2004 of 12 March (2004). BOE no. 75, March 27, 2004 (13217 - 13238).
[Online; published 23-March-2004].
URL: *https://www.boe.es/diario_boe/txt.php?id=BOE-A-2004-5562*

RD 661/2007 of 25 May (2007). BOE no. 126, May 26, 2007 (). [Online; Last modification published 13-Jul-2013].
URL: *https://www.boe.es/buscar/act.php?id=BOE-A-2007-10556*

RD 9/2013 of 12 July (2013). BOE no. 167, Jul 13, 2013 (52106 - 52147). [Online; Last access online 20-Jan-2017].
URL: *https://www.boe.es/diario_boe/txt.php?id=BOE-A-2013-7705*

RELAP5/MOD3.3 (2001). *Code Manual*, NUREG/CR-5535 edn, Information Systems Laboratories, Inc.

Renewables 2016 Global Status Report (2016). *Technical Report ISBN 978-3-9818107-0-7*, Renewable Energy Policy Network for 21st century, REN21 Secretariat, Paris, France.

Rohde, U. (1986). *Ein teoretisches Modell fur Zweiphasen-stromungen wasser-gekulthen Kernreaktoren und seine Anwendung zur Analyse des Naturumlaufs im Heizreaktor AST-500*, PhD thesis, Akademie der Wissenschaften der DDR. Zentralinstitut für Kernforschung Rossendorf bei Dresden.

Rohsenow, W. (1952). A Method for Correlating Heat-Transfer Data for Surface Boiling of Liquids, *Transactions of ASME* **74**: 969 – 976.

Sarzynski, A., Larrieu, J. and Shrimali, G. (2012). The impact of state financial incentives on market deployment of solar technology, *Energy Policy* **46**: 550 – 557.

Skumanich, A. (2011). CSP at a crossroads: The first solar electric power plants are still proving their worth after three decades, so why aren't we seeing more CSP reach the development stage?, *Renewable Energy Focus* **12**(1): 52 – 55.

Soria, R., Portugal-Pereira, J., Szklo, A., Milani, R. and Schaeffer, R. (2015). Hybrid concentrated solar power (CSP)-biomass plants in a semiarid region: A strategy for CSP deployment in brazil, *Energy Policy* **86**: 57 – 72.

Starke, A. R., Cardemil, J. M., Escobar, R. A. and Colle, S. (2016). Assessing the performance of hybrid CSP + PV plants in northern Chile, *Solar Energy* **138**: 88 – 97.

Taitel, Y. and Dukler, A. E. (1976). A model for predicting flow regime transitions in horizontal and near horizontal gas-liquid flow, *AIChE Journal* **22**(1): 47–55.

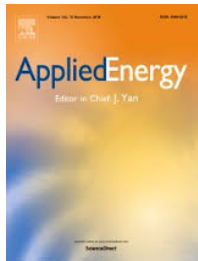The Deseret News (1946). Mirror Gives Steam Power, **341**(73): 3. Salt Lake City, Utah, US.

Valenzuela, L., Zarza, E., Berenguel, M. and Camacho, E. F. (2005). Control concepts for direct steam generation in parabolic troughs, *Solar Energy* **78**(2): 301 – 311. ISES Solar World Congress 2003.

Vallentin, D. and Viebahn, P. (2010). Economic opportunities resulting from a global deployment of concentrated solar power (CSP) technologies – The example of German technology providers, *Energy Policy* **38**(8): 4467 – 4478.

Vieira-de-Souza, L. E. and Gilmanova Cavalcante, A. M. (2016). Concentrated Solar Power deployment in emerging economies: The cases of China and Brazil, *Renewable and Sustainable Energy Reviews* . DOI: 10.1016/j.rser.2016.10.027.

VijayaVenkataRaman, S., Iniyan, S. and Goic, R. (2012). A review of climate change, mitigation and adaptation, *Renewable and Sustainable Energy Reviews* **16**(1): 878 – 897.

Wagner, W. and Kruse, A. (1998). *IAPWS Industrial Formulation 1997 for the Thermodynamic Properties of Water and Steam*, Springer Berlin Heidelberg, Berlin, Heidelberg, pp. 7–37.

Wang, Q. and Li, R. (2015). Cheaper oil: A turning point in paris climate talk?, *Renewable and Sustainable Energy Reviews* **52**: 1186 – 1192.

Williams, N. (2007). Climate change rises on the 2007 agenda, *Current Biology* **17**(2): R38 – R39.

Wu, C. (2016). Chinas 13th Five-Year Plan for Electric Power Cut CSP Projects by Half to 5GW. [Online; published 7-November-2016].
URL: *http://en.cspplaza.com/chinas-13th-five-year-plan-for-electric-power-cut-csp-projects-by-half-to-5gw-by-2020.html*

Zarza, E., Hennecke, K., Hermann, U., Langenkamp, J., Goebel, O., Eck, M., Rheinländer, J., Ruiz, M., Valenzuela, L., Zunft, S. and Weyers, D. (1999). *DISS-phase I PROJECT: Final Project Report.* Document: DISS-MQ-QA-27. Contract: JOR3-CT95-0058. Editorial CIEMAT (Madrid). ISBN: 84-7834-358-x.

Zarza, E., Morales, A., Rojas, E., Valenzuela, L., León, J., Eickhoff, D. W. M., Eck, M., Hennecke, K., Rheinländer, J., Langenkamp, J. and González, S. (2002). *DISS-phase II PROJECT: Final Project Report.* Document: DISS-MQ-QA-48. Contract: JOR3-CT98-0277. Editorial CIEMAT (Madrid). ISBN: 84-7834-427-6.

Zarza Moya, E. (2004). *Generación directa de vapor con colectores solares cilindro parabólicos : Proyecto DIrect Solar Steam (DISS)*, PhD thesis, Universidad de Sevilla.

Zarza-Moya, E. (2017). 5 - Innovative working fluids for parabolic trough collectors, *in* M. J. Blanco and L. R. Santigosa (eds), *Advances in Concentrating Solar Thermal Research and Technology*, Woodhead Publishing Series in Energy, Woodhead Publishing, pp. 75 – 106.

Zhang, S., Andrews-Speed, P., Zhao, X. and He, Y. (2013). Interactions between renewable energy policy and renewable energy industrial policy: A critical analysis of china's policy approach to renewable energies, *Energy Policy* **62**: 342 – 353.

Zuber, N. and Findlay, J. (1965). Average Volumetric Concentration in Two-Phase Flow Systems, *ASME. Journal of Heat Transfer* **87**(4): 453 – 468.

PAPER I

Abstract:

Parabolic-trough collectors (PTC) solar systems are one of the most promising of a wide range of the available solar technologies. Continuous breakthroughs are being achieved. Mainly due to the considerable amount of solar PTC plants that are being under operation in different countries. Within this continuous improvement effort, Direct Steam Generation (DSG) has been under development. DSG will lead to cheaper systems, not only for electricity generation but for heat process requirements. Working with superheated steam as thermal fluid, implies thicker pipe walls. Current numerical models neglect the radial dimension. In this context, simulating DSG absorbers implies considering radial domain discretization. A single phase model has been developed in order to work the 3D temperature field out on the solid parts, including the glass cover. Vacuum annulus has been assumed between stainless steel absorber and the glass envelope. The thermal radiative interaction between those parts has been considered without constant temperature assumption over the glass envelope. Finally, unidimensional approximation has been applied to the fluid domain. The whole code has been developed from the elemental (PDEs) governing equations and has been implemented in Matlab. The numerical model has been validated from experimental results. These results have been gathered from an experimental DSG test facility with parabolic-troughs.

II PAPER II

Abstract:

A new method called Inverse Monte Carlo Ray Tracing (IMCRT) is proposed to calculate the numerical description of line-focus concentrator geometries. This paper describes the method application to flat absorbers. The aim of this method is to calculate the reflector geometry so that the resulting concentrated flux profile is as close as possible to some required distribution on the predefined absorber geometry. Parabolic trough collectors (PTC) concentrate radiation onto the absorber inducing thermal gradients around it. The IMCRT method provides the chance to redefine the reflector geometry in order to get homogeneously distributed radiation onto the absorber without secondary reflectors. This method is useful to define continuous linear reflectors for concentrated photovoltaic (CPV) purposes, where a quasi-planar concentrated flux distribution is required onto flat absorbers. The reflector geometries obtained by the IMCRT method for the covered examples have been validated with a 2D in-house ray tracing code.

PAPER III

Abstract:

The application of the Inverse Monte Carlo Ray Tracing (IMCRT) method to define the concentrator geometry of solar collectors with round absorbers is presented. Such absorber geometry is the most common in current commercial systems. Parabolic trough collectors (PTC) concentrate radiation onto the absorber tube generating a non-homogeneous flux distribution, which may cause thermal stress problems; especially the case in direct steam generation systems. The proposed methodology is applied to calculate new reflector geometries considering two different objective flux profiles. The results have been obtained regarding the solar sunshape and the glass cover refraction. The geometries obtained have been validated with a 2D in-house ray tracing code.

PAPER IV

Abstract:

Direct steam generation in parabolic-trough solar collector requires reliable and efficient two-phase flow modelling tools. One-dimensional models based on 6 equations are a suitable approach. The present article aims to show that RELAP5 is able to simulate a single-loop system including transients caused by sudden events like solar collector defocusing or fast changes in direct solar irradiance. The numerical results have been validated with experimental data from the DISS facility located at Plataforma Solar de Almería. Six operation days have been compared using a new heat loss correlation, which has been measured on the same facility. The implemented model considers connection pipes, elbows, change of height, thermal insulation in the passive sections, collectors slope and absorbers. The numerical results are in good agreement with the experiments and it proves that RELAP5 can reproduce the underlying thermo-hydraulic phenomena. An additional numerical study of severe slugging in the connection pipes has been done, where two adjacent collectors linked by a connection pipe have been simulated at a pressure of 5 bar. Based on 374 tests, slugging phenomenon has been reported for low values of inlet mass flow rate and low quality in the entering two-phase mixture.